Aus der Universitätsklinik für Zahn-, Mund- und Kieferheilkunde
Abteilung für zahnärztliche Prothetik
Albert-Ludwigs-Universität Freiburg i.Br.

Reliability and failure modes of anterior zirconium-oxide crowns dependent on coping design

I N A U G U R A L - D I S S E R T A T I O N
zur
Erlangung des Zahnmedizinischen Doktorgrades
der Medizinischen Fakultät
der Albert-Ludwigs-Universität
Freiburg i.Br.

Vorgelegt 2013
von Magdalena Kimmich
geboren in Stuttgart

Dekan: Prof. Dr. Dr. h.c. mult. H. E. Blum
1. Gutachter: Prof. Dr. C. F. Stappert
2. Gutachter: Prof. Dr. P. Hahn
Jahr der Promotion: 2013

CONTENTS

1   INTRODUCTION

The development of all-ceramic dental restorations is at the forefront of research in dental material science. Currently, the increasing demand for aesthetically pleasing and biocompatible dental restorations has inevitably led the interest away from metal-based to all-ceramic restorations.[1-11] However, the limited strength of ceramic materials is a major drawback of all-ceramic restorations.[12-15] Due to these limitations, ceramic materials have been primarily employed in combination with a stable metal framework, allowing the restoration to withstand the high mechanical stresses in the masticatory system. With the introduction of yttria stabilized zirconium dioxide (Y-TZP) as a high-strength dental ceramic material, the use of all-ceramic restorations has become possible. Due to a mechanism called "transformation toughening", the Y-TZP shows exceptionally high tensile strength compared to other ceramic materials.[1, 15-17] The Y-TZP is white because it reflects light diffusely, and as such its optical properties far surpass that of even the most advanced metal materials.[8, 18] This becomes particularly important in the restoration of anterior teeth. However, the remaining opacity of the Y-TZP has aesthetic drawbacks, and thus, the present use is limited to frameworks, copings, abutments and implants.[19, 20]

The main concern raised about zirconia-based restorations is the high rate of veneering porcelain chipping. While bulk fractures, which are observed in all other all-ceramic systems[21-24], are rare in zirconia-based systems[21, 25, 26], chipping has been reported as the most frequent failure mode in the majority of clinical and laboratory studies on zirconia.[21, 24, 27-35] In contrast to delamination and bulk fracture, chipping occurs as a cohesive fracture within the veneering porcelain, as the strong framework material shifts the system's fracture mode from the core to the veneer layer. However, as the chipping rates for metal-based restorations are usually lower than for zirconia-based restorations, especially for fixed dental prostheses (FDPs)[21], chipping seems to be a problem specific to zirconia. Various reasons for this phenomenon have been previously discussed, yet without decisive resolution. Among these, the low thermal conductivity of the zirconia[36], the surface property changes of the zirconia induced by the veneering porcelain[37] and a mismatch of the coefficient of thermal expansion between the zirconia and the veneering porcelain[38] have been at the center of discussion.

While these manufacturing problems remain, one solution which may enable better use of the material with minimal chipping occurrence might be to increase the thickness of the core coping in the interproximal and incisal portion of the crown (anatomical design). The rationale behind this idea is that the increased coping thickness will maintain a constant layer thickness of the veneering porcelain and, as a result, might be more favorable in regard to the stress distribution inside the veneering material.[39-41] Therefore, this forms the basis of the research project herein.

Previous works indicate that posterior zirconia crowns with improved veneering porcelain support show higher fatigue resistance than crowns with a constant layer thickness of the zirconia.[39, 42-44] The objective of the study within this thesis is an in vitro comparison of two different zirconia coping designs. The effect of an anatomical coping design on the fatigue behavior of the veneering porcelain is investigated using mouth motion step-stress accelerated life testing.

2   LITERATURE REVIEW

2.1   DENTAL CERAMIC MATERIALS

The word ceramic is derived from the Greek word "keramos", meaning "potter" or "pottery". By definition, it includes "solid materials which are nonmetallic and inorganic with a crystalline structure".[45]

Ceramic materials are used in all fields of life with a wide range from cooking supplies to missile cone noses.[46] In comparison to the high-strength ceramics used in the industry, which are most commonly based on zirconia, dental ceramics should be strong and aesthetically pleasing at the same time. In order to achieve these aesthetic results in dentistry, the material needs a certain degree of translucency. Therefore dental ceramics are structurally located between industrial ceramics and glass.

2.1.1   TWO BASIC STRUCTURES

In order to understand the complex structure of modern dental ceramics, it helps to consider them a composite, meaning a composition of two or more entities. As we know the term composite usually from particle-filled resins, its meaning can be transferred to ceramics. Ceramics consist of a matrix and fillers.[47] According to the atomic structure of the matrix, ceramic materials are divided into two main composition categories: Silicate ceramics and oxide ceramics.

In spite of the differences in composition, the fact that they are basically cohered by covalent and ionic bonds is valid for all kinds of ceramic materials. This is important in order to understand the most problematic issue of these materials: their brittleness.[48]

2.1.1.1   SILICATE CERAMICS

A silicate is a chemical compound containing a center silicon anion (Si^{4+}). Silicates are the major minerals of the earth's crust, where feldspar is the most common mineral followed by quartz.[49] To understand the structure of silicate ceramics better, one should look at the structure of pure quartz. The dental silicate ceramics can be seen as a modification of

this structure and will be explained later in this chapter. Table 1 shows a selection of current dental silicate ceramic materials and their applications.

The basic anatomic module of quartz is SiO_4^{4-}, which is the conjugate base of silicic acid ($Si(OH)_4$) and has tetrahedron geometry.[50] In quartz, the SiO_4^{4-}-tetrahedron exists as a three-dimensional network called silica or silicon dioxide (SiO_2). Every silicon anion is connected to another four silicon anions by four oxygen bridges.

If silica is melted, the atomic bonds are broken. If the melt cools down, it either becomes crystalline or amorphous depending on the speed of cooling. If it is cooling down fast, atoms do not have time to form a proper lattice. As a result, the formed substance is amorphous. Amorphous means that, even if there are covalent and ionic bonds (short order range), a long order range does not exist. Therefore it is highly translucent and comparatively more susceptible to fracture. This is what we call quartz glass – or simply glass. It appears as a "frozen melt".[8] If the melt is cooling down slowly, a proper lattice forms. The formed substance is crystalline which means a short and a long order range exist. This substance is called quartz. It is more opaque and less susceptible to fracture.

Pure quartz glass is not suitable for dental application because of its high sintering temperature, its high transparency and its high susceptibility to fracture. In order to create a clinically applicable dental ceramic material, the pure quartz glass is modified by adding impurities:

1) Network former and network modifier which lower the sintering temperature by loosening the strict silica network:

    a) Network formers (Al_2O_3 and B_2O_3) are molecules that are able to form a network. According to this definition silica is also a network former. Unlike the silicon anion, boron and aluminum anions are charged 3+. Being covalently bonded to the silica network, there is no possibility for silica to form a strict network because of the negative electric charge which is inserted in the network and the fact that in some places oxygen bridges are missing. For example:

$$O = Al - O - Al = O \; + \; O - Si - O_3 \; \rightarrow \; O = Al - O - Al - O - Si - O_3$$
$$| $$
$$O^-$$
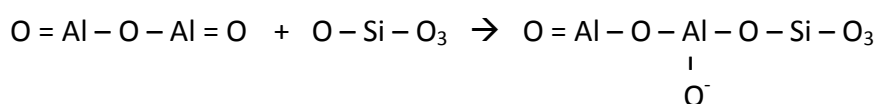
b) Network modifying alkali-salts (Na_2O and K_2O) split up Si-O-Si bonds by becoming ionic binding partners to silica during cooling. Potassium and sodium have a bigger atomic radius than silicon, thus the bond strengths inside the network decrease. For example:

$$Na_2O \ + \ O_3-Si-O-Si-O_3 \ \rightarrow \ O_3-Si-O^- \ + \ {}^-O-Si-O_3 \ + \ 2\,Na^+$$
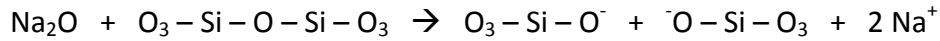
Besides its effect on the sintering temperature, the decrease of bond strength inside the network increases the coefficient of thermal expansion (CTE).[2, 8, 51]

If network formers and network modifiers are added to pure silica, the product results in the chemical formula of feldspar (($Na_2O \cdot Al_2O_3 \cdot 6\,SiO_2$) or ($K_2O \cdot Al_2O_3 \cdot 6\,SiO_2$)). Therefore, all kinds of silicate ceramics which contain a matrix of this composition are called feldspathic ceramic.[46]

2) Filler particles which hinder crack propagation and diffuse light:

These fillers are usually crystalline but can also be particles of high melting glasses that are stable at the sintering temperature of the ceramic. The resulting ceramic is called glass-ceramic if the fillers are not added mechanically as powder during manufacturing, but precipitated within the starting melt by special nucleation and growth heat treatments.[8, 51-56] The crystals act as a "roadblock" to cracks. A crack propagating in the amorphous phase will sooner or later strike a crystal. It must go through or around it, which diverts energy from the propagating crack and may also stop it entirely.[14, 46, 57] It is also possible to control the transparency of the porcelain by adding a special amount of crystals of a special size. Transparency is generally a result of extremely fine crystallite size, much smaller than the wavelength of visible light and the refractive indices of the matrix and the filler.[58] There are three more reasons why crystals are added to the glassy matrix: First, the fact that crystals have a high CTE compared to glasses makes it possible to alter the CTE of the ceramic by adding more or less of these fillers.[8, 59, 60] Second, depending on their size, crystals also have influence on the abrasion resistance of the material.[46] Third, crystals etch faster or slower than the matrix. This leads to a microretentive surface which can be utilized for adhesive bonding.[8] However, all improvements effected by embedding fillers in a glassy matrix depend on the size of those. The smaller and the more uniform

crystals are distributed, the higher the flexural strength, translucency and abrasion resistance of the emerging material.[46, 58, 61-63]

The two main filler categories for dental glass-ceramic materials are leucite and lithium disilicate:

a) Leucite ($K_2O \cdot Al_2O_3 \cdot 4\ SiO_2$) is a crystal, whose structure resembles feldspar.[64] It is created in an aluminosilicate glass by increasing its K_2O content, adding nucleating agents and using special heat treatments.[65-68] During cooling, a change in the lattice symmetry of the crystal occurs below 605-625°C. Cubic leucite crystals become tetragonal leucite crystals accompanied by a 1.2% increase in volume.[59, 69, 70] On the one hand, this increase in volume will create tangential compressive stress in the glassy matrix around the crystals helping to counteract the flexural stress of a propagating crack.[71] On the other hand, a high difference in the CTE of the matrix and the fillers generates radial tensile stress that can end up in signs of microcracking and, thus, weakens the material.[65, 72, 73] This effect is compensated by choosing a very small crystal size.[63, 74] Another reason why leucite was chosen as filler is that its index of refraction is close to that of feldspathic glasses. This is an important factor concerning the maintenance of some translucency.[8, 58, 75] Besides that, leucite crystals etch faster than the matrix, creating microretentive sites for adhesive cementation.[76-78]

b) Lithium disilicate crystals ($Li_2Si_2O_5$) are grown out of a $SiO_2 \cdot Li_2O \cdot Al_2O_3 \cdot K_2O \cdot ZnO$ basic glass by adding P_2O_5 as a nucleating agent and using special heat treatments.[53, 79, 80] The process of nucleation is much more complex because of the presence of nanosized crystal phases.[81, 82] There are two different microstructures existing during processing: Firstly, the intermediate lithium metasilicate crystals which are smaller and distributed at a lower concentration throughout the glassy matrix. In this so-called "blue" stage it is easy to mill the ceramic. Later, the final-stage microstructure arises. Crystals are larger and highly concentrated, resulting in higher strength.[79, 83-87] The very low refractive index of lithium disilicate crystals and their matrix allows embedding a higher number of crystals of a larger size in the matrix which makes the glass-ceramic reflect light very naturally while it is also providing improved flexural strength.[46] Additionally, so as already observed in leucite glass-ceramics, tangential compressive stresses are generated around

Matrix	Filler	Percentage of filler	Uses	Process	Trade name (Company)
Felspathic glass	High-melting glasses	~40%	Inlays, Onlays, Veneers, Veneers for ceramic copings	CAD/CAM	Mark II (Vita), Triluxe (Vita), Celay (Vita)
				Layering	VM 7/9/13/15 (Vita), AllCeram (Degudent)
	Leucite	~20%	Inlays, Onlays, Veneers, Veneers for metal copings	Layering	VMK-95 (Vita), Omega 900 (Vita), Response (Vita), Ceramico 3 (Dentsply), IPS d.sign (Ivoclar), Reflex (Wieland)
		30-50%	Inlays, Onlays, Veneers, Single-unit crowns	CAD/CAM	IPS Empress CAD (Ivoclar), Paradigm C (3M ESPE)
				Heat-pressing	IPS Empress Esthetic (Ivoclar), OPC (Pentron Ceramics)
				Layering	Cerinate (DenMat), Fortress (Mirage), Finesse AllCeramic (Dentsply)
Special silicate glass (containing Fluorine)	Fluorapatite	~20%	Veneers for ceramic copings	Layering	IPS e.max Ceram (Ivoclar)
				Heat-pressing	IPS e.max ZirPress (Ivoclar)
Special silicate glass (containing Lithium)	Lithium Disilicate	70%	Monolithic: Single-unit crowns, anterior three-unit FDPs	CAD/CAM	IPS e.max CAD (Ivoclar)
				Heat-pressing	IPS e.max press (Ivoclar), 3G (Pentron ceramics)

(Table 1) A selection of current dental silicate ceramic materials and their applications. Material properties are not included but will be presented in chapter 2.1.3. Companies: Vita Zahnfabrik, Bad Säckingen, Germany; Degudent, Hanau, Germany; Dentsply, York, PA, USA; Ivoclar Vivadent, Schaan, Liechtenstein; Wieland, Pforzheim, Germany; 3M ESPE, St. Paul, MN, USA; Pentron Ceramics, Somerset, NJ, USA; DenMat, Santa Maria, CA, USA; Mirage, Kansas City, KS, USA.

the crystals due to a mismatch in thermal expansion of the crystals and the matrix. By contrast, lithium disilicate ceramics show no microcracking induced by this mismatch.[88] Lithium disilicate crystals have a layered structure and a needle-like morphology which makes them interlock at a high degree. This improved material compound is another important reason for the significantly higher fracture toughness of lithium disilicate ceramics compared to other glass-ceramics.[79, 82, 89] In contrast to leucite glass-ceramics, the application of hydrofluoric acid etches the glassy matrix first.[78, 90]

With regard to the materials used in this study, a third filler category – fluorapatite – should be mentioned. Nanofluorapatite ceramics contain a crystalline phase exclusively composed of fluorapatite crystals ($Ca_5(PO_4)_3F$), embedded in a matrix of a fluorine-containing glassy matrix. Due to the analogy of the fluorapatite crystals to the hydroxylapatite of the enamel they are supposed to improve the optical effects of the restoration.[91, 92]

2.1.1.2 OXIDE CERAMICS

The basic units of oxide ceramics contain a center metal anion, which is either aluminum (Al^{3+}) or zirconium (Zr^{4+}), surrounded by a certain amount of oxygen cations. The difference between silicon (Si^{4+}) and aluminum and zirconium, respectively, is the fact that silicon is a metalloid while the other two are base metals. The bond between base metals and oxygen is much stronger because of their high oxidation potential.[71] This results in a strictly regular lattice structure and a highly dense configuration of the oxide ceramic crystals. Hence, the ceramic is stronger but at the same time more opaque. The resulting formulas are Al_2O_3 (aluminum oxide or alumina) and ZrO_2 (zirconium dioxide or zirconia). Naturally, they occur as corundum (Al_2O_3) and baddeleyite (ZrO_2).[49] Zircon ($Zr(SiO_4)$), a modification of ZrO_2, is commonly used in the jewelry industry as a translucent or colored gemstone.[93] The dense and strong-bonded structure as well as the absence or small concentration of silicon atoms makes it impossible to etch oxide ceramics in dental clinical application.[78]

Matrix	Dopant	Percentage of dopant	Uses	Process	Trade name (Company)
Special silicate glass (containing lanthanum) — 30%	70% { Spinell		Framework or coping	CAD/CAM, slip-casting	In-Ceram Spinell (Vita)
	Alumina — Magnesium	3%			In-Ceram Alumina (Vita)
	Alumina-Zirconia — Ceria	12%			In-Ceram Zirconia (Vita)
Alumina	Magnesium	3%	Framework or coping	CAD/CAM, dry-pressing	Procera Alumina (Nobel Biocare)
				CAD/CAM	In-Ceram AL (Vita)
Zirconia	Yttria	3-5%	Framework or coping	CAD/CAM (hard machining)	DC-Zirkon (DCS), Denzir (Decim), Everest ZS (KaVo)
				CAD/CAM (soft machining)	Procera Zirconia (Nobel Biocare), Lava Zirconia (3M ESPE), In-ceram YZ (Vita), Cercon Zirconia (Dentsply), IPS e.max ZirCAD (Ivoclar), Katana Zirkonia (Noritake), Zenostar Zr (Wieland), Zerion (Straumann), Everest ZS (KaVo)

(Table 2) A selection of current dental oxide ceramic materials and their applications. Material properties are not included but will be presented in chapter 2.1.3. Companies: Vita Zahnfabrik, Bad Säckingen, Germany; Nobel Biocare, Gothenburg, Sweden; DCS, Allschwil, Switzerland; Decim, Dentronic AB, Skelleftea, Sweden; KaVo, Biberach, Germany; 3M ESPE, St. Paul, MN, USA; Dentsply, York, PA, USA; Ivoclar Vivadent, Schaan, Liechtenstein; Noritake, Fair Lawn, NJ, USA; Wieland, Pforzheim, Germany; Straumann, Basel, Switzerland.

In dentistry, oxide ceramics are used in two different ways: As interpenetrating phase ceramics consisting of a continuous network of an oxide ceramic network interpenetrating a second continuous glass-based network, or as polycrystalline solids without fillers. A selection of oxide ceramic materials in current dental use is shown in table 2.

1. Interpenetrating phase ceramics:

Interpenetrating phase ceramics are a mixture of oxide and glassy ceramics combining the advantages of both systems. A scaffold made of a porous sintered oxide ceramic is produced by slip-casting. Consequently, this infrastructure contains small hollows in which a melted low-viscosity lanthanum glass is inserted subsequently.[94-96] It may help to imagine the oxide scaffold to be a sponge soaking up the fluid glass using capillary action. In contrast to particle-filled glass-ceramics, either phases are continuous throughout the ceramic and neither representing an isolated filler.[97] In the dental clinic, this method of infiltrating a porous skeleton with melt glass has been described as the In-Ceram® method.[98]

The oxide ceramics used for interpenetrating phase ceramics can either be spinel, alumina or zirconia-alumina. Spinel ($MgAl_2O_4$) is the magnesium aluminum member of the larger spinel group of minerals.[49] It is more translucent but weaker than pure alumina.[19] Lanthanum was added to the infiltrating glass because it decreases its viscosity and increases its index of refraction.[99]

By reason of the large oxide ceramic content and their highly dense, less porous structure, these kinds of ceramics are stronger than any glassy ceramic. Furthermore, the two-phase morphology makes it hard for cracks to propagate through the material. Cracks will stop at the interface or be deflected similar to the mechanisms in particle-filled glass-ceramics.[100] Since the glassy matrix is reduced to less than 30%vol it is not possible to etch interpenetrating phase ceramics with hydrofluoric acid in order to create a microretentive surface.[101, 102]

2. Polycrystalline solids:

Polycrystalline ceramics are single-phase materials and, therefore, they do not contain glassy components. As mentioned above, all atoms are densely packed into regular arrays due to the tight bonds of anions and cations. This results in higher strength and opacity compared to silicate ceramics. In dentistry, alumina and zirconia can therefore only be

used as a coping veneered with a more translucent porcelain. Additionally, polycrystalline ceramics are more difficult to process into complex shapes. With that said, well-fitting copings were not practical before the availability of computer-aided manufacturing (CAM).[8] Zirconium dioxide can also be used for other medical applications such as total hip replacements (THR);[103, 104] enabled by its excellent mechanical properties.

Zirconia holds a unique place amongst oxide ceramics. In regards to the material properties, a peculiar relation can be seen between alumina and zirconia. While alumina is harder than zirconia, the fracture toughness of zirconia is higher. This is the result of a zirconia-specific mechanism called transformation toughening which will be explained in the following:

From a material science point of view, pure zirconia (ZrO_2) cannot be used because it expands during cooling. This provokes spontaneous cracks and finally fragments the material.[71] Historically, the most dramatic increase in its industrial applicability has been brought about by the discovery that this expansion can be controlled,[16, 17, 105, 106] turning an adversity into an advantageous property.

The reason for the expansion of pure zirconia induced by cooling is that the geometry of the lattice depends on the temperature. At room temperature and pressure the crystals are monoclinic (m). The monoclinic state is the most stable form of zirconia with the lowest internal energy. With increasing temperature the crystals transform to a tetragonal (t), by approximately 950-1170°C, and then to a cubic structure (c) starting at about 2370°C with melting by 2716°C. These transformations are reversible and accompanied by a considerable change in volume which is approximately +2.3% (c→t) and +4.5% (t→m), respectively. Since the sintering temperature of pure zirconia is approximately 1300-1500°C, the material in its dental use underlies an expansion of 4.5%vol during cooling, changing from a tetragonal to a monoclinic structure.[37, 107-112]

In order to stabilize the tetragonal state, oxides called "dopants" are added to zirconia. As opposed to the particle-shaped "fillers" in silicate ceramics and interpenetrating phase ceramics, the term dopant describes modifying atoms.[47] It includes yttria (Y_2O_3), ceria (CeO_2), calcia (CaO) or magnesia (MgO). All of these anions are charged 3+ and thus, are less valent than zirconium. They substitute on Zr^{4+} sites and leave a fraction of oxygen sites vacant in order to retain charge neutrality.[113] As the m phase is strained, it is disfavored whereas the more symmetric c* and t* lattice structures are favored.[114]

The resulting c* and t* lattice structures are analogous to those in pure zirconia but metastable (metastable is represented by "*").[107] Metastable means that if a certain amount of activation energy is impinged on the structure it will revert in a state of lower energy. For zirconia, at room temperature, this state of lower energy is the monoclinic state and the activation energy is the tensile stress at a crack tip. Once a crack is propagating in a stabilized zirconia ceramic material, the energy at its tip will enforce the metastable t*- and c*-phases surrounding the tip to transform into the m phase with an associated 4.5%vol localized expansion. The volume increase creates compressive stresses at the crack tip and the energy associated with crack propagation is dissipated both in the t→m transformation and in overcoming the compressive stresses arising from the volume expansion.[1, 16, 17, 115-117] This characteristic results in a material with extraordinarily high flexural strength.

The t→m lattice transformation is sometimes called martensitic transformation because it is of the same nature as the martensitic transformation occurring in steel and can be compared to it.[118, 119] Martensitic transformations are characterized by being diffusionless, occurring athermally and involving shape deformation.[107, 116, 120] That is the reason why the first article published about transformation toughening in zirconia was titled: "Ceramic steel?"[16]

Random transformation of the t*-grains is prevented by the compressive stresses applied on them by the surrounding matrix. Regarding this, an interesting characteristic of transformation toughened zirconia is the generation of compressive layers on the surface of the material by surface t*-grains which are not constrained by the matrix. Therefore, they can spontaneously transform to the monoclinic state.[1, 121]

Depending on the volume fraction of the metastable t*-phase and the way it is dispersed in the fabricated body, three zirconia systems are available for dental use: DZC, PSZ and TZP. The simplest of these systems are the dispersed zirconia ceramics (DZC). The term comprises a material in which intergranular t*-ZrO_2 is dispersed in a matrix made of another ceramic material, with ZTA (zirconia toughened alumina) being the most commercially developed DZC system.[17, 122-124]

In partially stabilized zirconia (PSZ), t*-ZrO_2 intragranular precipitates exist within a matrix of stabilized c*-ZrO_2. This is achieved by adding a lower concentration of oxides than it is required for full c*-ZrO_2 stabilization.[16, 107, 118, 125] Further investigations on PSZ showed

that the mechanical properties of zirconium dioxide increased linear with the content of remaining t*-phase. As a result of this, a zirconia material made of a 100% small t*-grains was developed. This material is called tetragonal zirconia polycrystals (TZP) or 3Y-TZP, respectively, when doped by 3%mol Y_2O_3.[17, 126-128] In dentistry, zirconium dioxide ceramics are used almost exclusively as 3Y-TZP. Its mechanical properties strongly depend on the grain size of the zirconia crystals. Above a critical size (>0.3 µm) the crystals tend to spontaneous t→m transformations whereas below a certain grain size (~0.2 µm) the transformation is not possible. Consequently the processing has a strong impact on the stability and mechanical properties of 3Y-TZP ceramics.[37, 116, 126, 129-131]

A possible problem with 3Y-TZP appears its susceptibility to aging, which is also known as low temperature degradation (LTD). The slow surface transformation to the stable monoclinic phase in the presence of water or vapor leads to microcracks. This further leads to a cascade of events cleaving a way down into the specimen. The process is suspected to account for severe fractures of the material in total hip replacements (THR).[132, 133] However, presently, there is no proof of correlation between LTD and the failure probability of dental ceramic materials. Problems with the use of zirconia in dentistry point more towards its compatibility with veneering porcelains and its high opacity.

2.1.2 MANUFACTURING OF DENTAL CERAMICS

Today, many different dental ceramic systems are available. As described in the latter chapters they are sophisticated and can hardly be generalized. In order to generate these complex structures and their advanced properties, they need to be processed in a certain way. So as there are many different kinds of dental ceramics, there are different ways to process each of them. The manufacturing process has a strong impact on the clinical outcome of all-ceramic restorations compared to other dental materials. Ceramic materials are more sensitive to flaws implemented during the manufacturing process and – due to the sensitivity of the work flow – there is a higher chance of creating flaws during manufacturing.

In general, ceramic materials are created by the application of heat which breaks up covalent and ionic bonds. These bonds are rearranged subsequently during cooling, according to the desired shape. Breaking up bonds can be achieved by either sintering or melting

the ceramic powder. While melting includes a complete change of state from solid to liquid, sintering means to compress a porous structure bypassing the liquid state.[45] The sintering process can be described as "a complex sequence of high-temperature reactions occurring above the softening point of the porcelain and leading to partial melting of the ceramic matrix, with coalescence of the powder particles".[72, 134, 135] It results in a densification of the ceramic. In both cases of sintering and melting, the ceramic shrinks, though to different extents. Thermal shrinkage occurs in both cases whereas contraction shrinkage only occurs during sintering.[71]

The four most important processing techniques, using either sintering or melting, are presented in the following.

2.1.2.1 LAYERING

The layering technique is the traditional way to process dental ceramic materials. The materials used are a powder consisting of a synthetically compounded ceramic raw mixture, and distilled water including binders. Both are hand-mixed and the slurry is built up by hand on a die or a framework. Afterward, the material is sintered in a vacuum to remove the water including the binder and to compact the ceramic. This procedure can be repeated several times using different shades of ceramic powder. The final layer is called glazing; it is supposed to produce a smooth, shiny and impervious outer layer.[136, 137]

Given the fact that different shades of ceramic powder are available for one process, this technique is typically used for aesthetically challenging purposes such as anterior veneer restorations and veneering porcelains on metal and ceramic copings and frameworks.[46] The disadvantage is that air voids are often present; resulting in a rough surface and a weaker material, as these voids initiate crack formation.[138-140] Additionally, the high sintering shrinkage (~20%) has to be calculated and glass-ceramic materials cannot be used with this technique because they require special heat treatments.

2.1.2.2 HEAT-PRESSING

To overcome the creation of inhomogeneity and porosities during manufacturing, this technique has been developed using presintered materials in the form of ingots. The in-

gots are heated in a special automatic press furnace. In a malleable state, the material flows under pressure into a refractory mold formed using the lost-wax technique as it is generally known from the casting of dental alloys.[46, 71, 102, 141] The heat-pressing technique is used to either produce monolithic restorations or to over-press an oxide ceramic coping with a glass-ceramic veneering porcelain.

The materials used to produce the ingots are glass-ceramics that have already undergone special nucleation and heat treatments.[80] Therefore they contain crystals and feature a high density which reduces the shrinkage during the pressing procedure. The heat-pressing step conduces to the shaping of the restoration and further disperses the crystals. If additional firings are carried out on the pressed material, the dispersion of crystals can be approved even further. Moreover, beneficial tangential compressive stresses can be arisen by a CTE mismatch between the crystals and the matrix.[72]

A higher number of crystals, a better crystal distribution, compressive stresses around the crystals and a reduction of pores are assumed to be responsible for the increased flexural strength of the restorations fabricated by this technique in comparison to the traditional layering technique.[62, 140, 142-146] It should be remarked, however, that there is still a remaining porosity of about 9%vol in the final restoration and, interestingly, compressive stresses around the crystals have also been suspected to cause microcracking. This decreases the mechanical properties of the glass-ceramic.[101, 147] Another disadvantage of this technique is that, inherently, the pressed restoration is monochrome and has to be stained or veneered subsequently in order to enhance its aesthetic appearance.

2.1.2.3 SLIP-CASTING

As mentioned above, interpenetrating phase ceramics are traditionally produced by this technique. The "slip" is a homogenous dispersion of ceramic powder in a special water solution. It is applied on a plaster die forming the desired shape whereby the water is removed via capillary action. Consequently, a dimensionally stable network is created which is slightly sintered to a porous interconnected network afterwards, and then infiltrated with molten lanthanum glass.[46, 101] Slip-casted blanks of the In-Ceram® system are also available for CAD/CAM production.

2.1.2.4 MACHINING

Industrial processing of materials by a machine is usually aided by computer. This is how the term Computer Aided Manufacturing (CAM) in dental technology was educed. The master piece for the final dental restoration produced by the CAM unit can either be manually manufactured and analogically copied or virtually designed. The first procession technique is called copy milling; the latter is called CAD/CAM, whereby CAD stands for Computer Aided Design.[148]

The invention of CAD/CAM systems has been crucial in the development of all-ceramic restorations. Well-fitting prostheses made of high-strength ceramic cores were not previously available due to the high sintering temperatures and the high shrinkage of those materials. Nevertheless, almost every ceramic material can be processed by the CAD/CAM technology and thus the desired restorative material can be chosen only by the indication set. Further advantages of those systems are the achievement of industrial standards for dental restorations, including the homogeneity of those, and the higher efficiency of fabrication. This higher efficiency, in its maximum realization, led to the chairside production of dental restorations.[149, 150] However, the aesthetic outcome in the ceramic can only be monochromatic.

All CAD/CAM systems consist of three components:

1. A digitalization tool/scanner that transforms tangible geometry into digital data.

2. Software that processes data, and depending on the application, produces a data set for the product to be fabricated.

3. A production technology that transforms the data set into the desired product.[151]

Even though other fabrication methods such as laser sintering and electrophoretic dispersion can be applied as production technology, CAD/CAM is commonly associated with milling. In CAD/CAM systems, milling means shaping a ceramic restoration out of a ceramic ingot. Resin, wax and even metallic ingots for provisional, diagnostic or restorative purposes are available as well.[152]

Depending on the ceramic material chosen for the restoration, the milling procedure can take place in two different states of the material.[153] On the one hand, ingots can be milled in a state in which the ceramic material is fully sintered. This procedure is called hard machining and was the original intention when CAD/CAM technologies were invent-

ed in the early 70's.[81, 154, 155] On the other hand, ingots can be shaped in a state where the ceramic material is softer but also in need of further sintering. This idea is called soft shaping and is considerably new seeing as it was invented in 2001.[156, 157]

1. Hard machining:

Early materials that were suitable to be milled in a fully sintered stage were feldspathic ceramics and glass-ceramics.[158] Still these materials are available for chairside production of inlays, onlays and anterior all-ceramic crowns. The term chairside implies that no treatment by a dental technician has to be carried out on the material subsequently. The recommended treatment after milling is polishing. Polishing is crucial since it reduces the surface roughness. Machining of fully sintered ceramics typically creates surface flaws that could, in the long-term, be detrimental to the in vivo performance of the ceramic restoration.[81, 159-161]

Lithium disilicate ceramics cannot be used without involvement of a dental laboratory, even if they can be shaped by means of the CAD/CAM technology in the dental laboratory. The reason is that they are milled in a partially crystallized state, the so-called "blue state", in which the crystals are not yet fully developed. In this state the ceramic is easy to mill because it is softer. However, it already contains moderate strength because sintering has been completed. Subsequent heat treatments are necessary for full crystallization in order to achieve the high strength of these materials.[83]

Last but not least, even oxide ceramics can be milled in a fully sintered state. In the case of zirconia, this state is generated by hot isostatic pressing (HIP).[1, 37, 162] Even though a further sintering shrinkage does not have to be considered in this case, the density of the material makes it hard to mill. Higher wear of the cutters, longer milling times and remaining questions about the surface state after grinding makes hard machining of zirconia unattractive to dental technology.[15, 151, 163-167] Up to now, the only application for hard milled zirconia is the production of large frameworks due to the high accuracy that can be achieved.[168]

2. Soft machining:

Soft machining is mainly applied with respect to oxide ceramics. In the past, the fit of ceramics milled in a presintered state was often unsatisfactory because of non-optimized

machining parameters and limited accuracy of the chemical composition of the starting powders. The result was an inhomogeneous and unpredictable shrinkage during sintering.[157] New techniques have led to the availability of highly controlled starting powders and the consequent possibility to consider the shrinkage during milling. Thus, the CAD/CAM unit compensates the following sintering shrinkage by first milling an enlarged version of the restoration.[169]

The blanks are produced by cold isostatic pressing resulting in a "green-state" ceramic. Afterwards, the green blanks are presintered to "white-state" blanks; ensuring stability during their transportation and the milling process.[15, 151, 157] After milling, the sinterization is completed at high temperatures at which the material acquires its final mechanical properties. In the case of zirconia, the sintering shrinkage of presintered white blocks remains approximately 25% up to the desired 99% density of the final restoration.[156] As sintering conditions also affect the grain size and the amount of cubic phase in 3Y-TZP, a careful handling of the sintering process by the dental technician is essential.[170, 171]

Despite the high sensitivity of the work flow, soft machined zirconia has performed excellently.[172-175] This might be due to the fact that a more consistent final state of the ceramic material is created, providing that the machined restoration remains intact after sintering.[37]

For this reason the technique was extended to alumina, which was originally manufactured by CAD/CAM supported dry-pressing in the Procera® system.[176, 177, 178] Furthermore, this concept is now used to produce the oxide ceramic scaffold for interpenetrating phase ceramics out of a prefabricated blank which is in a second step infiltrated with lanthanum glass.[98] Both materials have shown good results with this technique.[179, 180]

2.1.3 PROPERTIES OF CERAMIC MATERIALS

The major gains of ceramic materials are their excellent optical and biological properties whereas the major failing is their mechanical properties due to the material brittleness. Generally, the properties of a material derive from its microstructure. As distinguished to metallic bonds in metallic materials, porcelain is characterized by more stable covalent and ionic bonds. On the one hand, the linked, high bond energy allows for reducing the density. As a result, it increases the translucency of the material which is best seen in

feldspathic ceramics. The strong bond also prevents atoms from exchanges with the surrounding medium which results in biological inertness. On the other hand, the atoms in the lattice can only have fixed binding partners. Therefore, flowing of the atoms inside the lattice structure and sliding of the lattice planes against each other is not possible. Once these bonds are broken, a great amount of energy is needed to rearrange them. The result is an incapability of plastic deformation, also known as brittleness.

2.1.3.1 OPTICAL PROPERTIES

In order to create a natural looking dental restoration, the optical behavior of the restorative material should be similar to that of the natural tooth which absorbs, scatters and transmits light. The amount of transmitted light was reported 70% for enamel and 30% for dentine.[9, 181, 182] Metal only reflects the light whereas, depending on the composition, ceramic materials transmit and scatter light.

Light transmission and partial scattering in dental porcelain is enabled by the amorphous glassy phase. The crystalline phase mainly scatters and diffusely reflects the light.[19] This leads to the dilemma that a strong ceramic material is more opaque as it transmits less light, or vice versa. The amount of reflected and scattered light does not only depend on the amount of the crystalline phase but also on the thickness of the material and the size of the crystals in comparison to the wavelength of the light.[183] Furthermore, the chemical nature of the crystals is important since the refractive index determines the light absorption and the relative refractive index of the crystal to the matrix affects the light scattering.[58] From a clinical point of view, the underlying tooth structure seems to be important, while the color of the luting agent has been found to be a minor factor in the optical outcome of an all-ceramic restoration.[184-186]

The following provides some examples of relative translucency of various ceramic materials in decreasing order: feldspathic ceramic > In-Ceram spinell > glass-ceramic > In-Ceram alumina > In-Ceram zirconia and metal alloy (control).[19, 20] This data shows that the translucency of the zirconia is comparable to metal. Yet, the amount of translucency of the zirconia can be increased to a certain degree by a reduction of the material thickness. The main difference between those two core materials is that the zirconia reflects light diffusely, resulting in a white color. This is more favorable to dental restorations be-

cause it avoids the grayish discoloration of the adjacent tissue. When properly veneered, colored zirconia frameworks could produce clinically acceptable color match and have the capacity to mask a dark background such as a dark tooth or core buildup material.[18]

2.1.3.2 CHEMICAL PROPERTIES

There is less known about chemical reactions of oxide ceramics occurring in the oral cavity, meaning under low temperatures and normal pressure. This might be due to the outstanding bond strengths in these materials. However, there are two important chemical phenomena when it comes to the clinical application of dental silicate ceramics: Etching and leaching.

Leaching of silicate ceramics takes place in aqueous environments such as the oral cavity. With water penetrating, nonbridging oxygen atoms of the silica react with hydroxyl ions of the water. These ions diffuse outwards with the alkali cations, thereby maintaining electrical neutrality. Leaching can result in material weakening, surface roughening and in an increased abrasion potential against contacting surfaces. In lithium disilicate containing ceramics this becomes even more important due to the potential release of toxic Li^+ ions. However, the Li^+ release has been found to be less than the daily limit from food sources.[187]

Etching of dental silicate ceramics can only be achieved by the application of hydrofluoric acid (HF) since it is the only acid that is able to dissolve bonds in silicate substances ($4\ HF + SiO_2 \rightarrow SiF_4 + 2\ H_2O$). The same happens when small amounts of HF get in contact with human bone; moreover, HF interferes in the nervous system and, therefore, it should be handled very carefully. Because it is reabsorbed by the skin immediately, a cauterization of the size of a palm (40% HF) can be lethal.[188]

Oxide ceramics contain only a very small amount or no silicate at all making it impossible to etch these materials. In order to etch a dental ceramic material, its silica content should be at least 15%vol.[78] Hydrofluoric etching is critical for the adhesive cementation of feldspathic and glass-ceramics.[189] A selective dissolution of the different components within these materials creates microretentive etching patterns whereby the acid preferentially attacks the amorphous glassy phase.[90] In leucite reinforced glass-ceramics the crystals are dissolved preferentially since the amorphous phase is stabilized by boron.[77]

Additionally, etching activates the surface generating unsaturated oxygen bonds that serve as binding partners for the silane applied subsequently in order to create a chemical bond to the hydrophobic resin cement.[190] Acid etching was reported to have no influence on the strength of the material itself.[76]

2.1.3.3 COEFFICIENT OF THERMAL EXPANSION (CTE)

The manufacturing process of dental ceramics requires the application of heat. Heating leads to an expansion of the material since atoms start to move faster and thus usually occupy a greater space. The coefficient of thermal expansion specifies to which amount, relatively to the initial length, a material expands by the application of 1 Kelvin heat. It is given in $10^{-6}K^{-1}$.

Regarding dental ceramic materials, the CTE becomes more important during cooling as a mismatch of different components in a linked ceramic system leads to internal stresses which can initiate cracks.[191] This applies either to crystals with respect to their matrix, to ceramic bilayers or to porcelain-fused-to-metal (PFM).

It is generally accepted that a CTE slightly below (~10%) the metal or ceramic framework is desired for the veneer in order to generate compressive stresses in the veneering porcelain. If the CTE of the veneer is significantly higher than the CTE of the framework, tensile stresses are created. These tensile stresses are tolerated far less than compressive stresses, resulting in possible veneer delamination.[191-193] Matching veneering porcelains for different framework materials are usually provided by the manufacturer. CTE values of selected ceramic materials are shown in table 3.

2.1.3.4 MECHANICAL PROPERTIES AND TESTING METHODS

Unlike optical properties, mechanical properties can be objectified by special testing methods. As mentioned above, the brittleness of dental ceramic materials is the most problematic property of those. When used in materials science, brittleness describes materials that break without significant deformation when subjected to stress. Generally, these materials fail in tension and shear rather than in compression.

Cracks causing failure usually originate from surface microcracks induced by processing. Tensile stresses in the material lead to tensile stress spikes at the crack tip exceeding the bond strength of the atoms.[194] As a result of this, the crack propagates down into the material. Existing voids and prestresses in the material and the presence of water surrounding the material can trigger crack propagation. Surface microcracks, voids and prestresses are usually a result of the manufacturing process. Microcracks unavoidably arise from grinding when subsequent polishing or glazing is missing. Voids are created by the application of the layering or heat-pressing technique whereas prestresses can have various causes such as a mismatch in CTE, high cooling speed or improper insertion of the restoration. Voids and prestresses lead to a reduced fracture resistance of the material. Water, as a major part of the oral environment, assists crack propagation as it undergoes a chemical reaction with the material at the crack tip in which bonds are broken. The resulting hydroxyl ions imply the release of alkali ions from the porcelain and thus, lead to a local decrease in fracture resistance.[195, 196]

Moreover, the amount, size and nature of crystals contained in the glassy matrix of silicate ceramics can decelerate crack propagation since they act as a "roadblock to cracks".[46] Further factors that have an impact on the mechanical properties of dental ceramic materials are the cementation method (cement modulus and thickness), the preparation design, the dimensions of the core and the veneer, the underlying (tooth-) structure and the loading position, direction and magnitude.[197]

2.1.3.4.1 HARDNESS

Hardness is defined as the resistance that a material opposes a penetrating object. It is usually given in GPa, the unit for mechanical pressure and tension (1 Pa = 1 N/m^2). The most common hardness testing method in engineering with dental ceramic materials is the Vickers microindentation test. This is a test where a small diamond indenter in the shape of pyramid with square base (point angle = 136°) is loaded and pressed smoothly, without impact, into the ceramic material and held in place for 10-15 seconds. The deeper the indenter sinks into the material (for a given load), the softer it is.[198] After the load is removed, the impression diagonals are measured and the Vickers hardness (HV) is calculated (HV = 1854.4 L / d^2 (L=load in grams-force; d=diagonal in μm)).[199]

The hardness values of selected ceramic materials are shown in table 3. Even though alumina is harder than zirconia, the strength of zirconia is higher due to the transformation toughening mechanism. This shows that the hardness of a material is not necessarily decisive for the evaluation of its strength.

2.1.3.4.2 YOUNG'S MODULUS (ELASTIC MODULUS)

The elastic modulus (E) is a measure of the resistance a material opposes an elastic deformation and actually states how strong the material constituents are bound together. According to the Hooke's law, it describes the linear correlation between stress and strain ($E = \sigma/\varepsilon$ = const. (σ=stress in GPa, ε=strain in %)) given in GPa. The Young's modulus can be measured using tensile testing in which a sample is subjected to uniaxial tension until failure. The measurements are recorded plotting stress against strain resulting in a stress-strain curve. In the stress-strain curve, the Young's modulus is represented by the slope of the elastic (linear) portion of the curve. The higher the tolerated stress, the higher the slope, the higher the Young's modulus and the stiffer the material.[71]

The stiffness is important in how forces are distributed and redistributed before failure. In brittle materials, the elastic modulus is usually higher than in ductile materials such as metals.

The Young's modulus values of selected ceramic materials are given in table 3. Although the Young's modulus depends on other material properties such as hardness or tensile strength, there is no strict correlation between those. However, the elastic modulus and the hardness of materials usually behave proportionally.

2.1.3.4.3 FRACTURE TOUGHNESS

The fracture toughness (K_{IC}) is the resistance a material opposes crack propagation at the vicinity of the crack tip. Unlike strength, it is an intrinsic characterization of material response because it is not sensitive to size and density of surface flaws.[14] Hence, this property does not depend on the condition of the material and can be used to compare different materials.

The fracture toughness is measured using either the biaxial or the three point bending test. In order to avoid the measurement of random surface flaws and thus, the tensile strength of the material, a notch is sawn on the bottom side of the material. Depending on the force required and the measured remaining cross section, the fracture toughness can be calculated and is given in MPa√m.

The relative fracture toughness values of selected ceramic materials are shown in table 3. The table clearly shows that zirconia is superior to all other ceramic systems regarding the resistance opposed to a propagating crack.

Fracture toughness, hardness and elastic modulus are measures of brittleness (B). The brittleness parameter B can be calculated on a theoretical basis as a ratio of deformation/fracture energy $(B = (H_v * E)/K_{IC}$; H_v=Vickers Hardness, E=elastic modulus, K_{IC}=fracture toughness).[200]

2.1.3.4.4   TENSILE STRENGTH AND ULTIMATE STRENGTH

The term strength (σ) describes the stress limit of a material whereby stress (given in MPa) means the tension or pressure that the material is able to bear. For ceramic materials, the strength is similar to the tensile strength as compression is tolerated far more than tension. Stress is caused by load (given in N) subjected to constant material properties such as hardness, elastic modulus and fracture toughness and the surface condition of the material. Therefore, strength is a conditional material property. Tensile strength and fracture toughness are the most important properties in engineering with dental ceramic materials since they characterize the structural performance.[201, 202]

The tensile strength is measured applying an increasing, defined amount of load on a standardized sample causing tensile stress. The tensile strength σ is calculated referring the load at failure to the surface area of the sample ($σ = F/A^2$; F=force, A=area). Three different testing methods can be applied: The biaxial bending test, the three point bending test and the four point bending test. Whereas the three point bending test is easy to comprehend, the advantage of the four point bending test is that the surface of the tensile zone is larger avoiding that random surface flaws located just below the indenter do not have too much influence on the results. In order to avoid stress peaks on the sharp edges of the discs used in the three and four point bending test, the biaxial bending test

can be applied. In this test, a round disc is centrally loaded. The values of each testing method have to be considered separately since they show different results.

Furthermore, the results depend on various other factors such as the speed of loading, the surrounding medium and of course the geometry and surface quality of the specimen. It has to be noticed as well, that values of flexural strength are usually raised on new materials and therefore, only describe the initial strength. They do not consider the degradation of the material under constant load and environmental influences. The decrease in strength has been reported to be up to 40% when constant load is applied to the specimens.[203]

Typical values of the initial bending strength of selected ceramic materials are shown in table 3. According to the standard ISO 6872 and 9693, a flexural strength of at least 100 MPa is required for ceramic coping materials and 50 MPa for veneering porcelains, respectively.[204, 205] In metals, the tensile strength is much higher since they are susceptible to plastic deformation. The limit of elastic deformation for metals is given as 0.2% yield strength.

In contrast to tensile strength, the ultimate strength is determined using samples that resemble the shape of the manufactured piece as in our case dental crowns and bridges. It is measured using the single load to failure test in which a dental restoration is loaded until failure. In complex structures it is not possible to measure the surface area of the specimen and hence, the load at failure is given in N.

2.1.3.4.5 WEIBULL MODULUS

As the failure probability of ceramic materials strongly depends on surface flaws and voids caused by the manufacturing process, the strength values for specimens of a similar geometry and material composition are subjected to comparatively high scattering. Furthermore, the frequency of failure in a group of specimens increases slowly and decreases rapidly after the peak is reached. Therefore, they can hardly be specified by the arithmetic average for which the values should correspond to the Gaussian distribution.

The Weibull strength ($\sigma_{63.3}$ or σ_0), in correlation to the median strength, indicates the stress at which 63.3% of the specimens fail. In correlation to the standard deviation, the Weibull modulus (m) describes the scattering of values in relation to the Weibull strength.

Consequently, the Weibull modulus is the measure of the structural reliability of a group of ceramic specimens as it gives evidence to the homogeneity of its flaw distribution.[206]

In Weibull analysis, the double natural logarithm of failure probability is plotted against the measured strength for each specimen of a group. The calculation of the failure probability is elaborate and will not be described further. By means of the Weibull graph, the Weibull modulus m can be estimated as the slope of the line regressed through the data.[207] The higher the Weibull modulus, the closer the values, and the more reliable the ceramic material.

Weibull moduli of ceramic materials used in dentistry usually range from 5.2 - 23.6.[149, 195] As the Weibull modulus strongly depends on the manufacturing process of the material, it does not make sense to describe typical values for different material compounds but for different processing methods. In general, CAD/CAM processed, prefabricated ceramic materials show extraordinarily high Weibull moduli (18.4 - 23.6) since flaws and voids inside the material are reduced to a minimum and the manufacturing process is standardized for all specimens of a group.[149] Additionally, there is no correlation between the flexural strength and the Weibull modulus m of a ceramic material. For example, CAD/CAM fabricated feldspathic porcelain shows higher m-values than zirconia but lower flexural strength.[149, 166, 208] It has to be noted, that the Weibull modulus m is a parameter used in classical mechanical engineering. The Weibull analysis used in fatigue testing of dental restorations includes the β-value (Weibull shape factor). Both, the m- and the β-value describe the slope of the curve in the Weibull plot. They can, however, not be compared to each other, since the Weibull plots are not the same.

2.2   CLINICAL FAILURE MODES OF ALL-CERAMIC RESTORATIONS

There are various causes which lead to failure of all-ceramic restorations. On the one hand, biological complications, such as caries, periodontitis, loss of vitality and abutment/tooth fracture, involve the replacement of a restoration. On the other hand, there are technical complications which compromise the longevity of all-ceramic crowns and FDPs.[21, 217] These can be marginal gaps, loss of retention or material-specific mechanical fractures. In all-ceramic restorations, there are three main mechanical failure modes: Bulk fracture, delamination and chipping. The term bulk fracture describes the fracture of the

	CTE [10^{-6} K^{-1}]	Vickers hardness [GPa]	Young's modulus [GPa]	Fracture toughness [MPa√m]	Tensile strength [MPa]
Materials used in this study					
e.max Ceram (nanofluorapatite glass-ceramic)	9.50 ± 0.25	5.4 ± 0.2	65	-	90 ± 10
Procera Zirconia (zirconium dioxide)	10.4	14	210	6	1200
Other materials					
e.max CAD (lithium disilicate glass-ceramic)	10.45 ± 0.25	5.8 ± 0.1	95 ± 5	2 – 2.5	360 ± 60
e.max Press (lithium disilicate glass-ceramic)	10.2 – 10.5	5.8	95	2.75	400
Alumina	7.6	14.9	390	3.1 – 4	695
Metal alloy	14 – 15	1.7 – 3.5	65 – 205	60 – 100	-
Enamel	17	3 – 4	75 – 100	0.6 – 1.5	20
Dentine	11	0.6	13 – 15	3.2	80

(Table 3) CTE (Coefficient of thermal expansion) and mechanical properties of selected dental ceramic materials in comparison to casting alloys and calcified tooth structure.[12, 48, 71, 91, 209-216] - = not available.

entire crown or FDP, including all layers. Delamination and chipping only involve the fracture of the veneering porcelain, excluding the coping. Whereas delamination includes the complete detachment of the veneering porcelain from the coping, chipping describes a cohesive fracture within the veneering porcelain.

Unfortunately, long-term clinical data on zirconia-based all-ceramic restorations is not yet available. There are also very few long-term clinical studies on other all-ceramic restorations at present. One study investigates the long-term survival of alumina-based all-ceramic crowns (Procera AllCeram, Nobel Biocare, Gothenburg, Sweden). It reports a success rate of 92.2% after 10 years.[218] The long-term clinical success of leucite reinforced glass-ceramic crowns (IPS Empress I, Ivoclar Vivadent, Schaan, Liechtenstein) has been confirmed by one study. This study found a mean survival rate of 95.2% after 11 years. More precisely, the mean survival rate of the crowns in this study is 98.9% for anterior crowns and 84.4% for posterior crowns.[219] Existing five-year data on all-ceramic single

crowns is promising since it shows survival rates close to PFM single crowns (4.4% cumulative failure rate for PFM crowns / 6.7% cumulative failure rate for all-ceramic crowns).[217] This review did not include zirconia-based crowns. A five-year retrospective clinical trial on zirconia-based crowns reported a cumulative failure rate of 9%, which is higher compared to the other all-ceramic materials investigated in this study.[220] A significantly higher failure rate can be observed for all-ceramic FPDs – including zirconia-based FDPs – when compared to metal-based FPDs (after 5 years: 11.4% cumulative failure rate for all-ceramic FDPs / 5.6% cumulative failure rate for PFM FDPs).[21] Furthermore, clinical data on implant-supported all-ceramic restorations, especially FDPs, are not sufficient to provide a convenient level of evidence as only a very small amount of studies are existing yet.[27-29]

The clinical studies also show that the fracture modes of all-ceramic restorations have changed decisively since the availability of zirconia as a strong substructure material. While bulk fractures have been the main reason for loss of monolithic glass-ceramic or bilayer In-Ceram and alumina-based restorations[21-24], cohesive fractures of the veneering porcelain appear to be a zirconia-specific problem shifting the systems fracture mode from the core to the veneer layer. Framework fractures have only been reported in a few studies on zirconia, most of them on FPDs and inlay-retained FPDs.[21, 25, 26] On the contrary, chipping of the veneering porcelain has been reported by the majority of studies on zirconia as the most frequent complication.[21, 24, 27-35] With respect to the differences in failure evaluation, follow-up period and materials used in those studies, it is hard to give general evidence. Thus, the chipping rates of FDPs with zirconia frameworks range from 0 to 54% after one, two, or three years of observation. In any case, the occurrence of chipping in metal-ceramic FDPs was significantly lower showing an average rate of 2.9% after a five-year observation period.[21] For zirconia-based crowns, chipping rates were lower ranging from 0 to 9% after two or three years of observation. These results are close to the results shown for PFM crowns (5.7% after 5 years).[217, 221-223]

2.2.1 CHIPPING IN ZIRCONIA-BASED ALL-CERAMIC RESTORATIONS

In the literature, various possible causes for the chipping phenomenon have been discussed. Given the fact that chipping during function signals the presence of tensile stress-

es likely associated with the zirconia-porcelain interface, a mismatch in thermal expansion of the two materials is often suspected to be accountable.[38] This is a well-known matter in material science; therefore most manufacturers provide veneering porcelains adjusted to the CTE of zirconia. Yet, the same principle is used for metal-ceramic systems as well.[37] Therefore, another idea came up suspecting surface property changes to be the origin of the tensile stresses. The dissolution of stabilizing dopants (e.g. yttria or ceria) of surface zirconia crystals in the silicate network of the veneering porcelain might conceivably lead to local changes in the tetragonal configuration of the zirconia crystals. As a result of this, the transformation toughening effect occurs on the surface of the core material. At the porcelain-zirconia interface and in absence of cracks, it will lead to tensile stresses on the bottom side of the veneering porcelain. This results in probable starting points for cracks. Another origin of the phase transformation of surface zirconia crystals has been discussed suspecting liquid silicate penetration of zirconia grain boundaries to be responsible. This might occur analogous to the water penetration of Y-TZP at moderately elevated temper-atures which is known as LTD.[37]

Further factors that might influence chipping are the design of the framework and the manufacturing method of the veneering porcelain. Several ideas have been suggested regarding the design of the coping. Anatomically designed copings with increased incisal and interproximal thickness, thus providing a constant layer thickness of the veneering porcelain, are considered to be more favorable concerning the stress distribution inside the material compared to copings of a constant layer thickness.[39-41] Unfortunately, little scientific evidence confirms this assumption. Only four laboratory studies show better results for anatomically designed copings on molar crowns or abutments, whereby none of them includes SSALT (step-stress accelerated life testing, described in chapter 2.3.2).[39, 42-44] This observation is supported by two short-term clinical studies in which an increased zirconia coping thickness is recommended.[32, 35] Another way to design zirconia copings for all-ceramic restorations improving the support of the veneering porcelain was suggested by Bonfante et al.[224] It is relating to the design of PFM restora-tions as it includes a partial cervical zirconia collar reaching from the oral to the interprox-imal areas. Again, only a small number of laboratory studies are existing, resulting in am-bivalent outcomes.[225, 226] Clinically, this anatomical coping modification is used with good outcome but yet, long-term studies are missing.[227, 228]

Besides this, further research is required on which is the best way to manufacture the veneering porcelain for zirconia copings or frameworks. Laboratory studies point out differing results for the hand-layering and the over-pressing technique. Three laboratory studies show similar results for both veneering techniques but none uses SSALT on crowns or FDPs. Whereas two studies on dental molar crowns either use a single load to failure test or a simple cyclic loading[150, 229], the third one assays ceramic trilayers under SSALT.[230] One study, performed using SSALT on zirconia-based molar FDPs, found better results for the hand-layered veneering porcelain.[231] So as compared to these studies, clinical studies point out similar results. They show either good results for the over-pressing technique[22, 25], little chipping for hand-veneered copings and frameworks[32, 35] or notice no difference between both techniques.[232]

In summary, current scientific data supports neither one way to process the veneering porcelain nor the other. This might be due to the fact that the manufacturing process of both methods cannot be standardized and, therefore, is strongly influenced by the skills of the dental technician. Recently, a new fabrication mode has been introduced by Beuer et al.[150] who suggested to sinter a CAD/CAM fabricated glass-ceramic veneering porcelain to the zirconia coping. In this first study, remarkable results are shown for molar crowns under single load to failure testing compared to molar crowns veneered by the over-pressing or hand-layering technique.

A further explanation for the high chipping rates of zirconia closely connected to the manufacturing process is the exceptionally low thermal conductivity of zirconia and silicate ceramics compared to alumina or metal alloys. As described by Swain[36], residual stresses arise in the veneering porcelain during cooling because of a temperature gradient between the cool outer surface and the comparably hot inner surface adjoining the coping. This results in compressive stresses on the surface of the material increasing its apparent strength while at the same time it leads to compensating tensile stresses in the depth which accelerate crack propagation. The faster the cooling and the lower the thermal conductivity of the core material, the higher is the temperature difference inside the veneering porcelain and the higher are the residual stresses. This becomes even worse when the layer thickness is increased, as in the case for the over-pressing compared to the hand-layering technique[233], or if the layer thickness within one material varies strongly.

2.3 LABORATORY TESTING OF ALL-CERAMIC RESTORATIONS

In order to justify the clinical application of any dental material, clinical studies are unfailingly the most telling arguments. The main disadvantage of clinical studies is, however, the long term which is needed to conduct them being at least 3-5 years.[234] Besides that, clinical studies are very costly. Sometimes it is difficult to give general evidence of a standardized model, as patients participating in the study and inserted restorations are individual.

By contrast, laboratory studies enable researchers to investigate and compare standardized dental materials and restorations in a time and cost effective way predicting failure modes and lifetimes. The mechanical testing of ceramic materials is usually realized by two types of in vitro testing methods: static loading tests and cyclic loading tests.

2.3.1 STATIC LOADING TESTS

As mentioned in chapter 2.1.3.4.4, the application of a static load until failure results in the measurement of the initial strength of the material which can either be the initial bending strength or the initial ultimate strength, depending on the specimen's geometry. Both usually result in load values which are higher than expected in the clinical situation. It is assumed that the mean masticatory forces in the anterior dentition range from 140-200 N. In the posterior region, stresses of 300 N are expected, but they can increase up to 500-900 N during grinding.[235]

Unfortunately, the high load values obtained from static loading tests do not reflect the clinical situation. These tests do not reproduce the chemical, thermal and mechanical loading conditions existing in the oral cavity. In the clinical situation, restorations have to withstand a high number of low loading cycles in the presence of water. While water accelerates crack propagation, a phenomenon which is called slow crack growth (as described in chapter 2.1.3.4.), the application of a constant low, cyclic load causes microscopic damage accumulation.[236-239] It has been shown that even after 1000 loading cycles, the strength of some ceramic materials might decrease to 60% of their initial strength.[203] Hence, crack propagation clinically develops in a different way as it does when static load

is applied until failure.[240, 241] As a result of this, not only failure loads but also failure modes in single load to failure tests do not resemble the clinical situation.

2.3.2 FATIGUE TESTING

The progressive and localized structural damage of a material caused by cyclic loading is called fatigue.[242] It comprises the processes of crack initiation, crack propagation and final fracture of the tested material.[243] Fatigue is affected by many variables, such as temperature, moisture and loading magnitude and direction.

A recently developed mouth-motion fatigue model called SSALT (step-stress accelerated life testing) has been reported to be able to reproduce clinical failure modes and thus, to predict the clinical reliability of a restoration.[244, 245] In this model, the damage of the material is accumulated in a relatively short time, as the load is increased step by step from low to high values until failure occurs whereby the amount of loading cycles decreases. The load values and the amount of cycles follow three different protocols, namely a mild, a moderate and an aggressive profile. The ratio of specimens used with each profile is 8:4:2.[246, 247] The profiles resemble three kinds of masticatory function and the ratio has been chosen according to the frequency of its clinical occurrence. Furthermore, the distribution of samples across the three profiles results in an efficient use of specimens and machine time. The most important profile is the mild profile as it applies the lowest load for the highest amount of cycles. As a result, it is the profile in which failure is affected by fatigue the most.

Furthermore, SSALT includes a sliding contact at a defined angle of 30° in water and the usage of a sphere indenter with a defined diameter (d = 6.25 mm) imitating blunt antagonizing cusps.[248] The sliding of the indenter during loading is important to reproduce the chewing motion. This motion is guided by the cusp inclines of posterior teeth or the incisal edges of the anterior teeth, respectively, where sliding contacts occur at various rates and magnitudes. The sliding component has been reported to be highly detrimental to the material as it leads to the extension of the stress field below the indenter (see chapter 2.4.2). The 30°-angle of the specimen to the axis of the indenter reproduces the average clinical tooth inclination. Moreover, the presence of water during indentation is

critical since we are dealing with restorations in the oral cavity. As mentioned above, water is an important factor assisting slow crack growth (chapter 2.3.1 and 2.1.3.4).

The specimens used for SSALT can either have a flat-layered geometry or an anatomically correct shape. The first model is standardized and used to analyze the fatigue behavior and fracture modes of a material before more complex, anatomically correct structures are used.[230, 241, 249-251]

2.4 FRACTOGRAPHY

According to the ASTM standard C1322-05b, the objective of fractography is "to provide an efficient and consistent methodology to locate and characterize fracture origins in advanced ceramics".[252] In contrast to metal, brittle materials fail catastrophically with no preceding plastic deformation. This makes the fractured surface of those materials a structural map of the mechanical processes leading to failure. These mechanical processes are crack initiation and propagation. Cracks propagate in response to stress and strains. Finding the origin of a crack and understanding the direction and manner a crack propagated through the material gives information about its causes - and thus the source of failure.[253]

The tools used for the examination of the fractured surface are most importantly the stereomicroscope and the scanning electron microscope (SEM). The stereomicroscope offers a three-dimensional view on the surface of the specimen allowing the evaluation and detection of cracks by color and reflectivity. However, higher magnifications are needed to see distinctive features of a crack. This can only be achieved using the SEM.[253, 254]

2.4.1 CRACK PATTERNS OF THE FRACTURED SURFACE

Basically, fractography is pattern recognition as propagating cracks leave determined fracture patterns. In the following chapters, the most important fracture patterns found in dental ceramic restorations are described mainly corresponding to George Quinn;[253] based on a nomenclature introduced by Van Fréchette.[255]

2.4.1.1 FRACTURE MIRROR

The fracture mirror is the most important feature as it represents the origin of a crack. However, it can hardly be found in fractured dental ceramics. It is a "relatively smooth region surrounding the fracture origin".[252, 256] The fracture mirror is the area where the crack radiates outwards from a flaw and, in a short distance, accelerates in velocity from almost zero up to 1800 m/s in microseconds. As the velocity increases, the crack starts to tilt and twist out of the main fracture plane in response to the stress field in front of it. This does not proceed for very long since creating new surfaces requires a lot of energy. The tiny deviations, if they have become large enough, can be perceived under the stereomicroscope as a belt surrounding the fracture origin. This fracture pattern is called mist zone.[253]

The size of the fracture mirror gives an idea of the stress inside the material at the moment of fracture. Large stresses cause small mirrors and vice versa.[253] This might explain the low incidence of fracture mirrors in dental crowns. The loads applied to test dental ceramic restorations are comparatively small. Thus, the fracture mirrors might become so large that they cover the whole fractured surface. Another fact which might explain the low frequency of fracture mirrors in dental restorations is the larger grain size of crystals in dental ceramic materials compared to glass.[254]

2.4.1.2 HACKLE

Hackle is defined as "a line on the surface running in the local direction of cracking, separating parallel, but noncoplanar portions of the crack surface".[255] Tracing those lines backwards is an effective method to localize the fracture origin.[257, 258] Although several different hackle lines are defined by Quinn[253], wake hackle and twist hackle are the ones which are most common in dental porcelain.

1) **Wake hackle**:

These lines are the most frequent fractographic features in dental porcelain. They start from an irregularity in the material being for example a void or an inclusion and run in the local direction of the crack. Wake hackle lines evolve when the crack front strikes an ir-

regularity and has to go around it. Usually, as the crack propagates along both sides of the irregularity, it slightly changes the fracture plane on both sides. Hence, a step is created between them when they get back together behind it. This step can be observed as wake hackle which is sometimes compared to a "weather vane".[253] Wake hackles can hardly be found in dense core materials since they contain very few inclusions or voids.[254]

2) Twist hackle:

Those very revealing features of the fractured surface are approximately parallel lines which all start to branch at one point. They are also called "delta patterns" or "river deltas".[253] Twist hackle occur in response to a rotation of the axis of principle stress as for example on corners, geometric irregularities or as the stress conditions change. The crack plane cannot turn all at once; instead it branches into small segments until the new crack plane is adjusted. The local direction of crack propagation can be determined, as it is known to originate at the branches and proceed towards the line.[253]

2.4.1.3 WALLNER LINES

Wallner lines are "rib shaped marks with a wavelike contour"[255] which were first explained by Helmut Wallner. The Wallner line forms on the interface of the crack front and the elastic wave arising from an elastic impulse. The elastic impulse can be generated by various occurrences such as a discontinuity inside or on the surface of the material or a discontinuity in the propagation of the crack front as it happens by the time the crack approaches its terminal velocity. Further, the elastic wave can be created by sources from outside of the material. As the elastic wave exerts an opposing force on the crack, it causes the entire crack front to twist out of the main fracture plane. This twist results in Wallner lines which are usually curved in the direction of the propagating crack even though they do not resemble the exact shape of the crack front.[253]

2.4.1.4 ARREST LINES

An arrest line is defined as "a sharp line on the fracture surface defining the crack front shape of an arrested or momentarily hesitated crack prior to resumption of crack propa-

gation under a more or less altered stress configuration". In contrast to Wallner lines, arrest lines are sharp and depict a replica of the crack front. In dental ceramic crowns, arrest lines evolve particularly under fatigue due to slow crack growth leading to a phased crack propagation.[253]

2.4.2 FRACTURE ORIGINS

The geometry of the subsurface crack zone of ceramic materials during indentation prior to fracture cannot be generalized as it is reliant to various factors. First, it depends on the shape of the indenter used which can either be sharp or blunt.[237, 259] Second, single load to failure tests result in different crack geometries than multi-cycle testing methods such as SSALT.[237, 241] Third, the damage maps depend on the ceramic system tested. Different kinds of cracks arise in bilayered specimens (monolithic ceramic and cement) and ceramic trilayers (ceramic bilayer and cement).[212, 260] The geometry of the subsurface crack zone also varies with the thickness and stiffness of the ceramic layers and their ratio.[261-263]

Furthermore, different crack geometries evolve depending on the direction of the applied load. In this case, one can distinguish between an axial loading direction (indenter contacts at 0° perpendicular to the specimen surface, applies the load and lifts off), a mouth-motion biaxial loading direction (indenter contacts at 0° perpendicular to the specimen surface, applies the load, slides 0.5 mm and lifts off), and an off-axis loading direction (indenter contacts at 30° perpendicular to the specimen surface, applies the load, slides and lifts).[193]

In axial loading, classical cone cracks are observed (I_c and O_c) (figure 1). Surrounding the compressive field below the indenter, they form in an area where high tensile stresses arise. There are two types of classical cone cracks. At low cycles, outer cone cracks originating from surface flaws form shallow ring cracks which pop in within a few cycles. As outer cone cracks grow at a low angle and a steady rate which is consistent with the slow crack growth rate, they usually do not cause much damage inside the material. After several hundreds of cycles, inner cone cracks evolve. Inner cone cracks are more aggressive than outer cone cracks since they grow more quickly and in a steeper angle towards the cementation surface where they become the source of failure. A mechanism called hy-

draulic pumping is considered to contribute to the driving force for inner cone cracks.[264, 265]
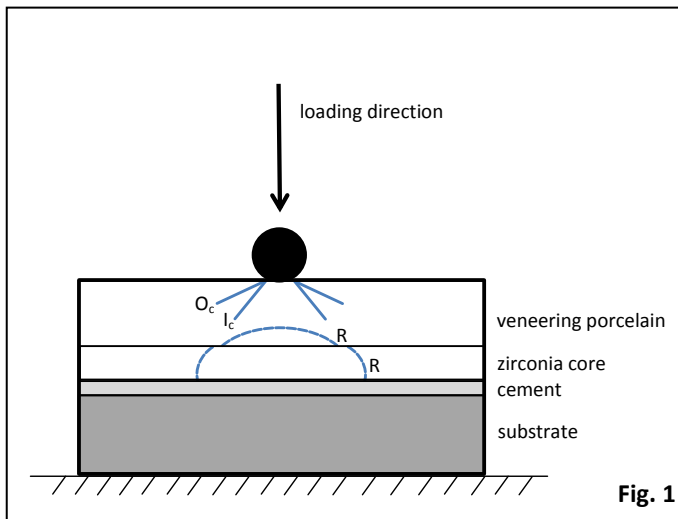
(Figure 1) Blunt, multi-cycle axial loading in water (not shown) of a flat, zirconia-based trilayer results mainly in outer (O_c) and inner cone cracks (I_c) on the top surface of the specimen.[248, 263] Radial cracks (R) on the bottom surface of the core and the veneering porcelain are shown as dashed lines since they are not typical for zirconia-based trilayers.[261, 266]

In trilayered all-ceramic specimens with a zirconia coping under blunt, multi-cycle and off-axis loading in water, failure generally emanates from partial cone cracks at the top surface (P_c) (figure 2).[251] Partial cone cracks are twisted cone cracks.[250] In off-axis loading, a sliding component is added to the indenter contact, equivalent to a coefficient of friction. Especially on rough surfaces, the coefficient of friction creates additional compressive stresses in front of the indenter whereas additional tensile stresses evolve behind it.[253, 264, 266, 267] Due to the stress field alteration, partial cone cracks are more aggressive than classical cone cracks. They propagate faster and in a steeper angle towards the cementation surface.[193, 251] The clinically relevant damage induced by cone cracks and partial cone cracks is chipping.[268]
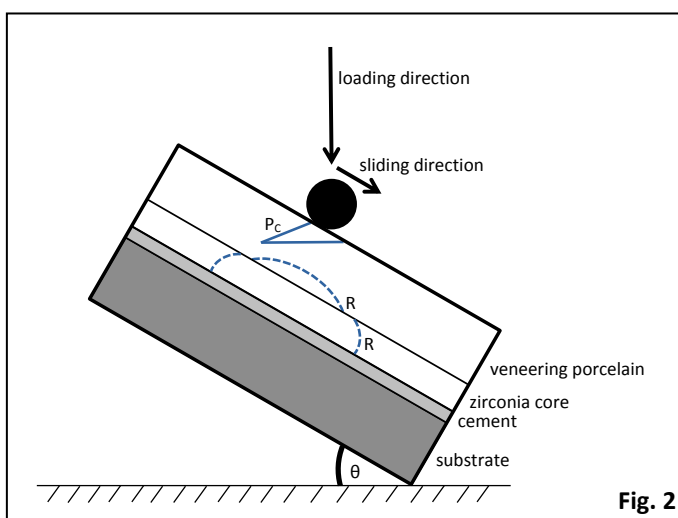
(Figure 2) Blunt, multi-cycle off-axis loading ($\theta=30°$) in water (not shown) of a flat, zirconia-based trilayer results mainly in partial cone cracks (P_c) on the top surface of the specimen.[249] Radial cracks (R) on the bottom surface of the core and the veneering porcelain are shown as dashed lines since they are not typical for zirconia-based trilayers.[261, 266]

Radial cracks at the cementation surface, so as observed in alumina-based trilayers or bilayered specimens (R) (figure 1+2), are usually absent in zirconia-based trilayers due to the extraordinary high strength of the zirconia.[263, 268-270] They arise in response to high tensile stresses at the ceramic undersurface induced by the load of the indenter applied on the opposite side of the ceramic layer.[212] This becomes particularly important when the ceramic layers are thin.[265] Radial cracks are highly deleterious to the restoration as they result in catastrophic bulk fractures.[271]

3 OBJECTIVES

The objective of this thesis is to compare two different zirconia coping designs regarding their effect on the fatigue resistance and the fracture propagation of anterior crowns, veneered with a nanofluorapatite glass-ceramic. The study is conducted using step-stress accelerated life testing (SSALT).

One out of two groups consists of 18 zirconia copings (NobelProcera; Nobel Biocare, Gothenburg, Sweden) with a standard coping design, implying a constant coping layer thickness of 0.5 mm. The other group includes 18 anatomically designed zirconia copings (NobelProcera; Nobel Biocare, Gothenburg, Sweden), which provide a constant layer thickness of the veneering porcelain as the incisal and interproximal coping thickness is increased (figure 3). In both groups (n=36), the veneering porcelain is applied using the hand-layering technique (e.max Ceram; Ivoclar Vivadent, Schaan, Liechtenstein).

Based on the results of previous studies on coping designs[39, 42-44], the research hypothesis is as following:

- The zirconia-based all-ceramic crowns with the anatomically designed coping are characterized by higher failure loads and less fracture propagation relative to the standard copings with a constant layer thickness of 0.5 mm.

Hence, the null hypothesis of this thesis is as following:

- There is no difference between the two groups regarding the failure loads and the fracture propagation.

Failure is defined as chipping, delamination or bulk fracture.

4 MATERIALS & METHODS

4.1 SPECIMEN PREPARATION

An extracted central incisor (tooth number 8) was prepared by a dentist according to the standard guidelines for all-ceramic restorations which include an incisal reduction of 2.0 mm, a 1.0 mm shoulder finish line, a preparation angle of 6° and rounded internal edges.[272]

The prepared natural tooth (including the root) was scanned by a scanner connected to a CAD/CAM unit (InLab MC XL; Sirona, Bensheim, Germany). The CAD/CAM unit produced 36 zirconium dioxide replicas of the entire prepared tooth (IPS e.max ZirCAD MO 0; Ivoclar Vivadent, Schaan, Liechtenstein) (figure 4).

Based on a plaster replica of the prepared natural tooth and a wax-up defining the final shape of the crown (Marotta Dental Studio, Huntington, NY, USA), two resin copings were shaped (GC Pattern resin; GC Corporation, Tokyo, Japan). One resin coping was modeled according to a standard design which comprises a constant layer thickness of 0.5 mm. The other resin coping was designed providing an increased incisal and interproximal coping thickness (anatomical design). Thus, the anatomical design includes a more constant layer thickness of the veneering porcelain (figure 3).

Corresponding to the manufacturer's recommendation (personal contact to Thomas Hill, Ivoclar Vivadent, Amherst, NY, USA), a minimum veneering porcelain thickness of 0.3 mm was respected. The veneering porcelain thickness of the crowns with the standard coping design ranged from 0.46 - 3.13 mm. For the crowns with the anatomically designed coping, a veneering porcelain thickness of 0.35 - 1.79 mm was attained. The veneering porce-
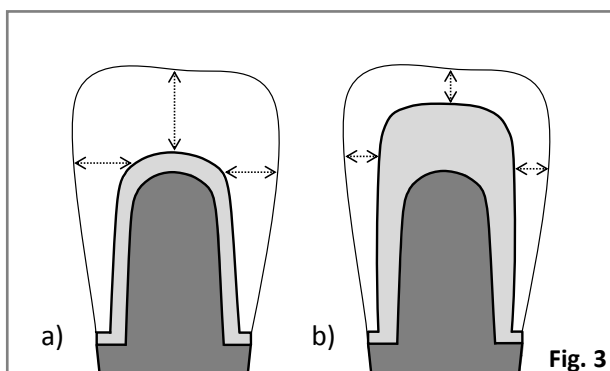
(Figure 3) Schematic of the two different crowns from labial (dark gray = prepared tooth, light gray = coping, white = veneering porcelain). The arrows indicate the thickness of the veneering porcelain on the incisal and interproximal parts of the crowns. The crown on the left (a) includes a standard coping design with a constant layer thickness of 0.5mm. The crown on the right (b) comprises an anatomically designed coping providing a constant layer thickness of the veneering porcelain as the incisal and interproximal portions of the coping are increased.

Fig. 3

lain thickness was measured using a cross-section of the impression of the final wax-up, in which the die with the respective coping was positioned.

Afterward, both resin copings were scanned (NobelProcera Scanner; Nobel Biocare, Gothenburg, Sweden) by a dental technician (Marotta Dental Studio, Huntington, NY, USA). The digital images of the two copings were transferred to a production center where 18 replicas of each coping were milled out of zirconia ingots (NobelProcera Zirconia; Nobel Biocare, Gothenburg, Sweden) in a presintered stage (figure 5). All 36 zirconium dioxide copings were then steam cleaned and air dried. Subsequently, they were veneered using the hand-layering technique (e.max Ceram (nanofluorapatite glass-ceramic); Ivoclar Vivadent, Schaan, Liechtenstein) (figure 5). The shape of the crowns corresponded to the shape of the wax-up in order to
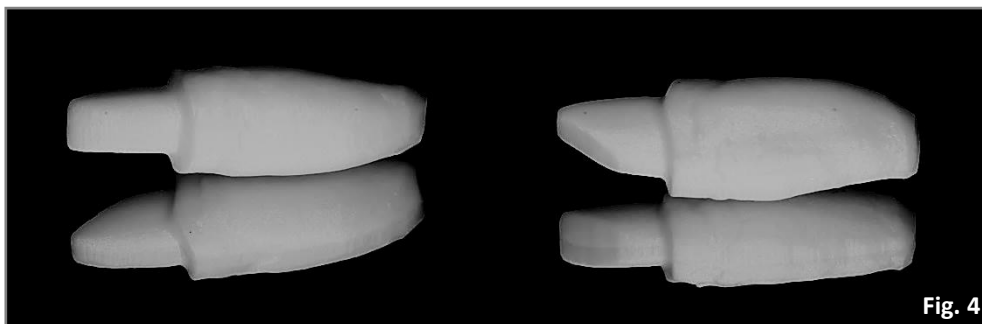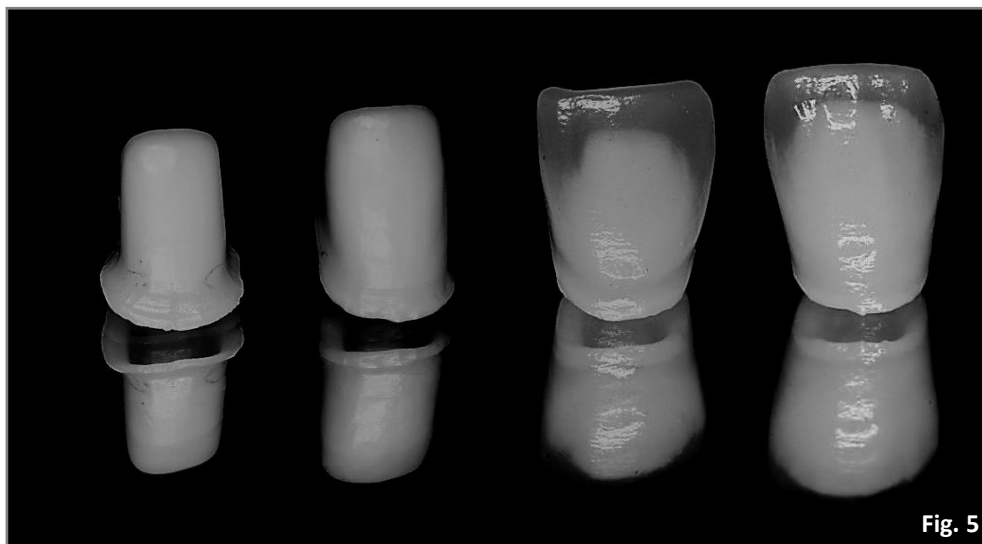
(Figure 4) Zirconia dies used as substructure material from labial (left) and mesio-palatal (right). The preparation implies an incisal reduction of 2 mm, a 1 mm shoulder finish line, a preparation angle of 6° and rounded internal edges.

(Figure 5) Zirconia copings before (first and second from left) and after (first and second from right) being hand-veneered with a translucent nanofluorapatite veneering porcelain. From left to right: zirconia coping with standard design (group S), zirconia coping with anatomical design (group A), hand-veneered crown with standard coping design (group S), hand-veneered crown with anatomical coping design (group A). Note the increased incisal and interproximal thickness of the anatomical coping relative to the standard coping.

achieve standardized conditions.

Consequently, the test groups were as following:

1. Group S: 18 hand-veneered crowns with a standard coping design
2. Group A: 18 hand-veneered crowns with an anatomical coping design

The veneering materials used for both groups were IPS e.max Ceram T clear (lot number: N74251 2; Ivoclar Vivadent, Schaan, Liechtenstein), IPS e.max Ceram build-up liquid (Ivoclar Vivadent, Schaan, Liechtenstein) and IPS e.max Ceram glaze paste (lot number: N74243; Ivoclar Vivadent, Schaan, Liechtenstein). The fabrication was done by a commercial dental laboratory (Marotta Dental Studio, Huntington, NY, USA).

Before the veneering porcelain was applied, a zirconia liner was used (lot number: L47191; Ivoclar Vivadent, Schaan, Liechtenstein). The firing temperatures of the zirconia liner were as following: After a 4 minute dry time, a base temperature of 403°C was hold for four minutes followed by a slow temperature ramp up of 40°C per minute. The oven started pulling vacuum at 450°C and stopped at 959°C. Afterward, a high temperature of 960°C was hold for one minute.

According to the manufacturer's information, all samples were built up in two bakes. The firing temperatures for the first and second bake were as following: After a 4 minute dry time, a base temperature of 403°C was hold for four minutes followed by a slow temperature ramp up of 40°C per minute. The oven started pulling vacuum at 450°C and stopped at 749°C. Afterwards, a high temperature of 750°C was hold for one minute. The firing temperatures for the glaze were as following: A base temperature of 403°C was hold for six minutes followed by a temperature ramp up of 60°C per minute. The oven started pulling vacuum at 450°C and stopped at 724°C. Afterward, a high temperature of 725°C was hold for one minute.[273] The furnace (Programat P500; Ivoclar Vivadent, Schaan, Liechtenstein) does not include a cooling device. Therefore, the cooling rate could not be determined for all firings. In the last firing cycle for the glaze, the furnace was opened after the temperature fell below 450°C.[273]

All 36 crowns and dies were sandblasted at 0.05 MPa using 50 µm Al_2O_3.[274] After washing and air drying, all crowns were adhesively cemented on the dies with a dual-curing resin cement (Multilink Implant; Ivoclar Vivadent, Schaan, Liechtenstein) applying a constant load of 20 N (figure 6).[275]

One of the cemented crowns was placed in a wax model (resin tube, diameter: 25.4 mm, filled with wax) at an angulation of 30° (figure 7).[250, 251, 264] Taking into consideration the biological width, the crown margins were placed 2.0 mm above the surface of the wax. An impression including the crown and the tube was taken using a vinyl polysiloxane impression material (Reprosil medium body; Dentsply, York, PA, USA). By means of this impression, all dies were embedded in resin tubes (diameter: 25.4 mm) and acrylic resin (Caulk Orthodontic Resin; Dentsply, York, PA, USA) at the same angulation. Prior to the mechanical testing, all specimens were stored in distilled water at 37°C for at least 14 days to assure full hydration of the cement and the acrylic resin.[276, 277]

(Figure 6) Crown (group A) cemented on the zirconia die with resin cement after low-pressure sandblasting (0.05 MPa).
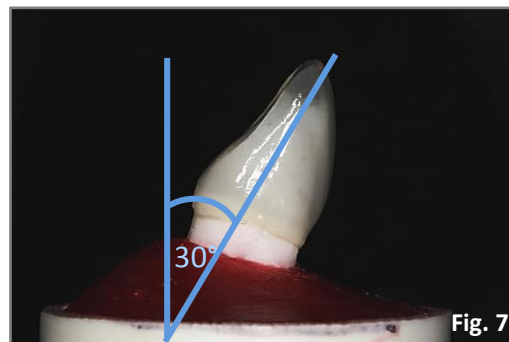
(Figure 7) Cemented crown (group S) placed in the wax model (red) at an angulation of 30° relative to the axis of the resin tube (white) which is similar to the loading axis. The crown margins were kept 2 mm above the surface of the wax. By means of a silicone impression, the model was duplicated and used to embed the crowns in resin-filled tubes (see Fig.8).

4.2   SINGLE LOAD TO FAILURE TEST

The static single load to failure test was performed on two crowns of each group. Therefore, the crown was mounted in a universal servo-hydraulic testing machine (Series 5566; Instron Corporation, Canton, MA, USA). The load was applied vertically by a spherical tungsten carbide indenter (diameter: 6.25 mm). The crosshead speed of 1.0 mm per minute was controlled by computer software (Merlin; Instron Corporation, Canton, MA, USA). Failure was defined as chipping, delamination or bulk fracture. The angle between the loading direction and the specimens' axis was 30° due to the angulation of the crowns relative to the axis of the tube (figure 8). The load was applied 2.0 - 2.5 mm

below the incisal edge[278] on the palatal face of the specimens (figure 9). The location of the indentation area was chosen in order to simulate the antagonizing incisal edge of the lower incisors. After testing, the mean failure load of all four samples was used to create the three profiles for the SSALT testing.
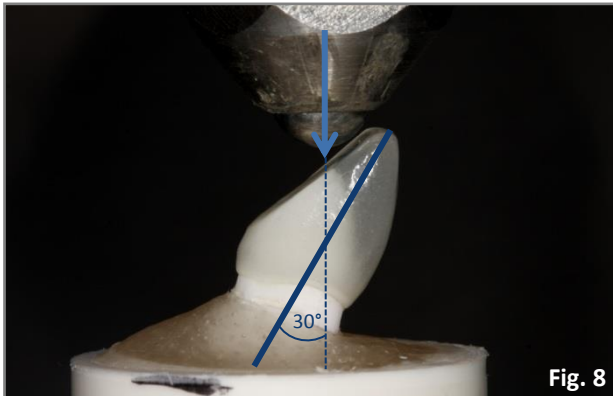
(Figure 8) Cemented crown (group S) embedded in resin and mounted in the universal testing machine. The load was applied at 30° to the specimen's axis by a spherical tungsten carbide indenter (above) and a cross speed of 1mm/min.

(Figure 9) Cemented crown (group S) embedded in resin and mounted in the universal testing machine. The load was applied 2.0-2.5 mm below the incisal edge.

4.3 FATIGUE TESTING

The fatigue testing was performed using sliding-contact step-stress accelerated life testing in distilled water at room temperature (SSALT, see chapter 2.3.2). Therefore, each sample was mounted in a mechanical testing machine (ELF 3300; EnduraTec Division, BOSE Corporation, Minnetonka, MN, USA) (figure 10+11) and subjected to one out of three testing profiles (figure 12) by means of a computer software (WinTest; Electro-Force systems group, BOSE Corporation, Eden Prairie, MN, USA). 16 samples of each group were tested. Failure was defined as chipping, delamination or bulk fracture. The SSALT profiles were developed considering the results of the single load to failure test and the range of clinically relevant loads.[235] They started at a step load of 5-15% of the mean static failure load. A load of 25 N was defined as the absolute minimum. Below the minimum load, the precision of the testing machine was limited. The upper load limit was estimated 700 N for all profiles. Expecting the influence of fatigue testing, the upper load limit was chosen being approximately ¾ of the mean statistic failure load of the static loading test. The SSALT profiles were divided into a mild (profile 1), a moderate (profile 2)

(Figure 10+11) Specimen mounted in the mechanical testing machine. The picture in Fig.10 is obtained from the side. Fig.11 shows a close-up from a top-side view. The basin provided the presence of water during fatigue testing. The holder guaranteed the immobility of the specimen. As the water basin is filled with water, the crown is hardly visible in Fig.10.

and an aggressive profile (profile 3), presenting a sample distribution of 8:4:4 for group S, and 9:4:2 for group A (see chapter 2.3.2) (figure 12).

Accordingly, the load values ranged from 50-700 N, 75-700 N and 125-700 N, respectively. Corresponding to the average amount of chewing cycles per year[279], the maximum amount of loading cycles was defined 165000, 130000 and 90000, respectively. The first specimen of group A ran in profile 0 (figure 13, appendices). This is due to the fact, that profile 0 turned out to be highly time-consuming since it started at a load of 25 N and went up to 200000 loading cycles. Therefore, it was replaced by profile 1.

The load was applied vertically by a spherical tungsten carbide indenter (diameter: 6.25 mm) 2.0 - 2.5 mm below the incisal edge on the palatal face of the specimens (similar to the set-up shown in figure 9). The location of the indentation area was chosen in order to simulate the antagonizing incisal edge of the lower incisors. As the specimens were embedded at an angulation of 30° relative to the loading axis, the load was applied from an off-axis direction (similar to the angulations shown in figure 8). Simulating articulation, the indenter touched the specimens' surface, applied the load, slid down approximately 1 mm and lifted up. The frequency was 2 Hz. The loading and unloading rate employed was 1000 N/sec. If a sample had not failed by the time the maximum amount of loading cycles was accomplished, it was considered as survival.

After mechanical testing, a statistical software (SPSS version 19; IBM Corporation, New York, NY, USA) was used to perform an ANOVA-test ($\alpha = 0.05$), in order to compare the samples of both testing groups regarding their failure loads and failure cycles. Moreover, accelerated life testing software (Alta Pro 7; Reliasoft, Tucson, AZ, USA) was used to conduct a Weibull reliability analysis which allows calculations for a small amount of samples. Weibull plots at a stress of 200 N with two-sided 90% confidence bounds were generated. The reliability for the completion of a mission of a minimum of 50000 cycles at 200 N was calculated.
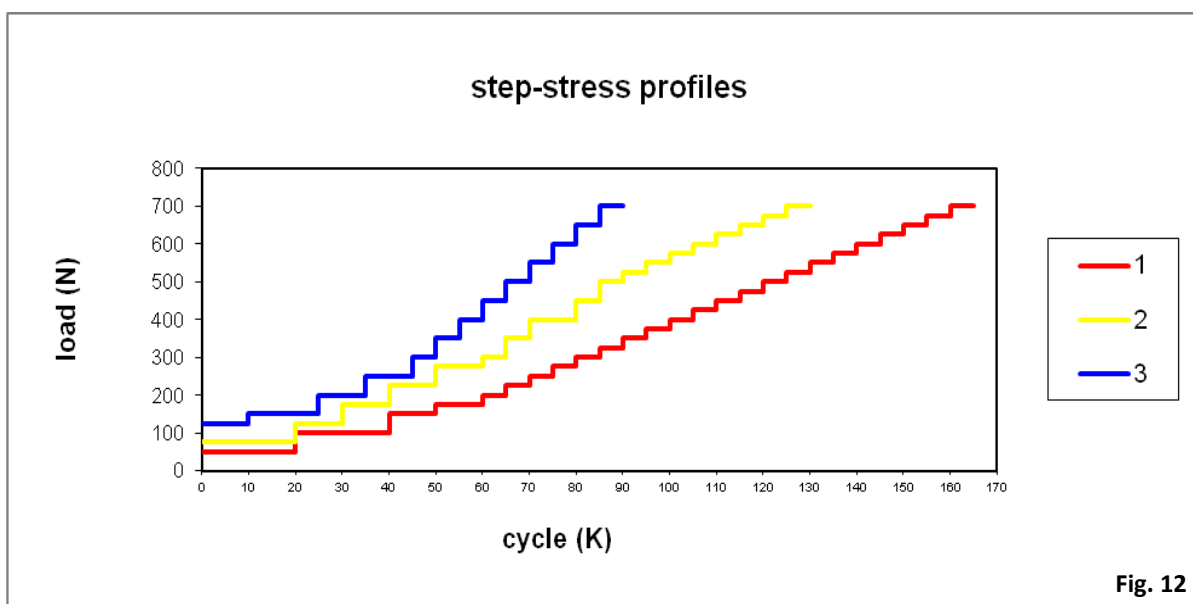
(Figure 12) SSALT profiles. Eight specimens of group S and nine specimens of group A were tested in the mild profile 1 (red line). Four of each group were tested in the moderate profile 2 (yellow line). Four specimens of group S and two specimens of group A were subjected to the aggressive profile 3 (blue line). Notice the differences amongst the three profiles regarding the initial load value and the slope of the curve. N=Newton, K=kilo.

4.4 FRACTOGRAPHIC ANALYSIS

At the end of each load-cycle step, each specimen was inspected for cracks and damage under the polarized light stereomicroscope (Leica MZ APO; Leica, Bensheim, Germany). Pictures were obtained from a top and side view at resolutions of 1.0x, 12.5x, 32.0x and 63.0x. Afterward, the specimen was appropriately repositioned into the mouth-motion fatigue machine so as to continue the next step of the SSALT fatigue testing.

The failed crowns and fractured segments were inspected under the polarized light stereomicroscope from the same views and resolutions as above. Representative samples

were gold-sputtered (Emitech K650; Emitech Products Incorporation, Houston, TX, USA) in order to evaluate the fractured surface using a scanning electron microscope (SEM) (Model 3500S; Hitachi, Osaka, Japan). The failure modes were microscopically categorized as inner cone cracks, outer cone cracks, partial cone cracks and radial cracks. The SEM was operating at 5 kV and the images were taken at resolutions of 35x, 70x, 150x, 350x, 500x, 1000x and 2500x.

Moreover, representative samples were embedded in epoxy resin (EpoFix; Struers GmbH, Copenhagen, Denmark). After that, they were serially sectioned perpendicular to the main crack plane in the presence of water (Isomet1000; Buehler, Lake Bluff, IL, USA). After polishing under copious water irrigation (Ecomet 4; Buehler, Lake Bluff, IL, USA), the samples were examined under the stereomicroscope and the SEM in order to detect possible subsurface damage and to confirm the failure mode. The stereooptical pictures were obtained from a top and side view at resolutions of 1.0x, 12.5x, 32.0x and 63.0x. The SEM was operating at 5 kV and the images were taken at resolutions of 25x, 50x, 70x and 150x.

5 RESULTS

5.1 SINGLE LOAD TO FAILURE TEST

The mean loads at failure, obtained from the static load test, were higher in group S (945 ± 151 N (n=2)) than in group A (706 ± 25 N (n=2)) (table 4; figure 14, appendices). The mean load of all samples (825 ± 142 N (n=4)) was used to determine the step-stress profiles for the fatigue testing. This resulted in load values from 25 N to 700 N (see chapter 4.3).

During the course of all four single load tests, the indenter slid down 3-5 mm on the palatal side of the specimen until failure occurred (figure 15). The failure modes will be presented in chapter 5.3.

	Load At Failure [N]	Mean Load [N]	Standard Deviation [N]
Group S n=2	838 1051	945	151
Group A n=2	688 724	706	25

(Table 4) Results of the static single load to failure test. The mean failure load and the standard deviation were calculated for each group. Group S=standard coping design, Group A=anatomical coping design, N=Newton.
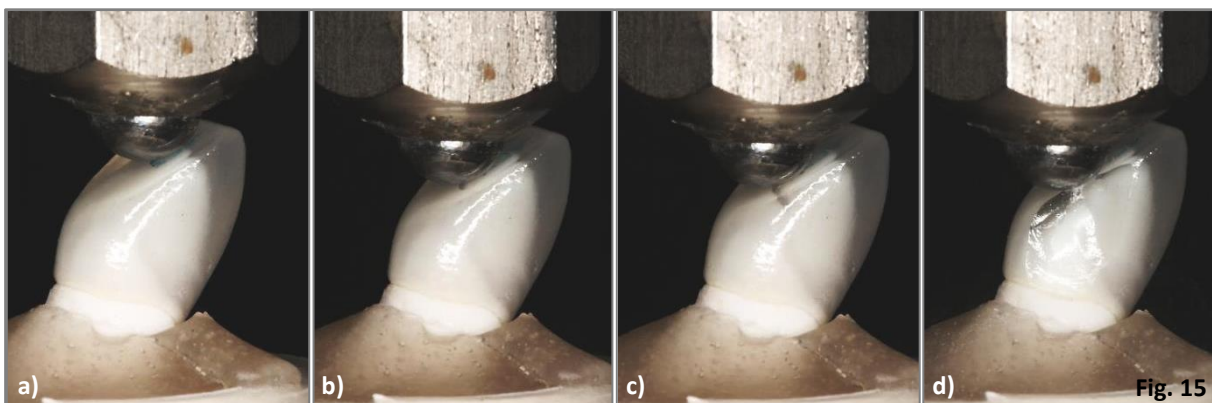
(Figure 15) Sequence of the single load to failure test. The pictures show a specimen of group A. From the starting point at 2.0-2.5 mm below the incisal edge (a), the indenter slid down the palatal face of the specimen (b-d). With increasing load, a crack arose below the indentation area (b) and propagated towards the interproximal area (c). The test was stopped after the specimen had failed (d).

5.2 FATIGUE TESTING

The failure modes, amount of cycles and loads to failure, obtained from the mouth-motion step-stress accelerated life testing, are listed in table 5. In total, 16 specimens of each group were tested. Five samples (n=2 in group S; n=3 in group A) were considered as survivals since they failed from precontacts of the indenter outside the actual indentation area (figure 16, appendices). A low test profile 0 was used to verify the estimated range of loads to failure under fatigue. Based on the first result, the test profiles 1, 2 and 3 were adjusted accordingly. The failure modes will be presented in chapter 5.3.

	Step-stress Profile	Failure (F) / Survival (S)	Load To Failure [N]	Cycles	Failure Mode
Group S	1	S	150	22520	Incisal chipping
n=16	1	S	250	70003	Incisal chipping
	1	F	250	70013	Incisal chipping
	1	F	275	78364	Incisal chipping
	1	F	275	79999	Incisal chipping
	1	F	300	80004	Incisal chipping
	1	F	300	80005	Incisal chipping
	1	F	475	116940	Incisal delamination
	2	F	275	59999	Incisal chipping
	2	F	350	65196	Incisal chipping
	2	F	350	66305	Incisal delamination
	2	F	550	99999	Incisal delamination
	3	F	150	20000	Incisal chipping
	3	F	150	18199	Incisal chipping
	3	F	350	54071	Incisal chipping
	3	F	400	59990	Incisal chipping
Group A	0	F	275	115027	Incisal chipping
n=16	1	S	100	39999	Incisal chipping
	1	S	250	70008	Incisal chipping
	1	F	275	79640	Incisal chipping
	1	F	275	79999	Incisal chipping
	1	S	300	80022	Incisal delamination
	1	F	300	80354	Incisal chipping
	1	F	300	83913	Incisal delamination
	1	F	525	130334	Incisal delamination
	1	F	525	125014	Incisal delamination
	2	F	350	69999	Incisal chipping
	2	F	450	84999	Incisal chipping
	2	F	500	89999	Incisal chipping
	2	F	525	90522	Incisal delamination
	3	F	450	64999	Incisal delamination
	3	F	600	77909	Incisal chipping

(Table 5) Results of the step-stress accelerated life testing. 16 specimens of each group were tested. Group S=standard coping design, Group A=anatomical coping design, F=failure, S=survival, N=Newton.

The results of the ANOVA-test ($\alpha = 0.05$), performed on failed specimens of profile 1 (n=6 for each group), showed no statistically significant difference between the failure loads of specimens of group S and group A. The mean loads to failure obtained from the ANOVA-test were 313 ± 82 N for group S, and 367 ± 123 N for group A (table 6). Considering the failed specimens of all profiles (n=14 for group S; n=13 for group A), the minimum load at which chipping occurred was 150 N for the crowns with the standard coping design, and 250 N for the crowns with the anatomical coping design.

	Mean Load To Failure [N]	Standard Deviation [N]	95% Confidence Interval for Mean	
			Lower Bound [N]	Upper Bound [N]
Group S Profile 1, n=6	313	82	227	398
Group A Profile 1, n=6	367	123	237	496

(Table 6) Results of the ANOVA-test, performed on failed specimens of profile 1. Six specimens of each group were included. There was no statistic difference between the two groups, since the 95% confidence intervals overlapped. Group S=standard coping design, Group A=anatomical coping design, N=Newton.

The use level probability Weibull plots (2-sided 90% confidence bounds) at a use stress of 200 N were compiled considering all failed specimens (n=14 for group S, n=13 for group A) (figure 17). A significant difference between the two groups was computed for 50000 loading cycles, the number of cycles associated with early failures. At 50000 loading cycles, the unreliability of specimens of group S was significantly higher. At 75000 and 100000 loading cycles, the results showed a clear trend towards higher reliability of the crowns with the anatomical coping design. However, the significance remained uncertain due to an overlap of the confidence bounds.

Figure 17 shows that there was a difference in the β-values between both groups (1.59 for group S and 2.66 for group A). Firstly, these values imply that fatigue was an acceleration factor for failure in both groups. Secondly, they show that there was a clear trend towards early failures in group S since the slope of the curve of group S was flatter than the slope of the group-A curve.
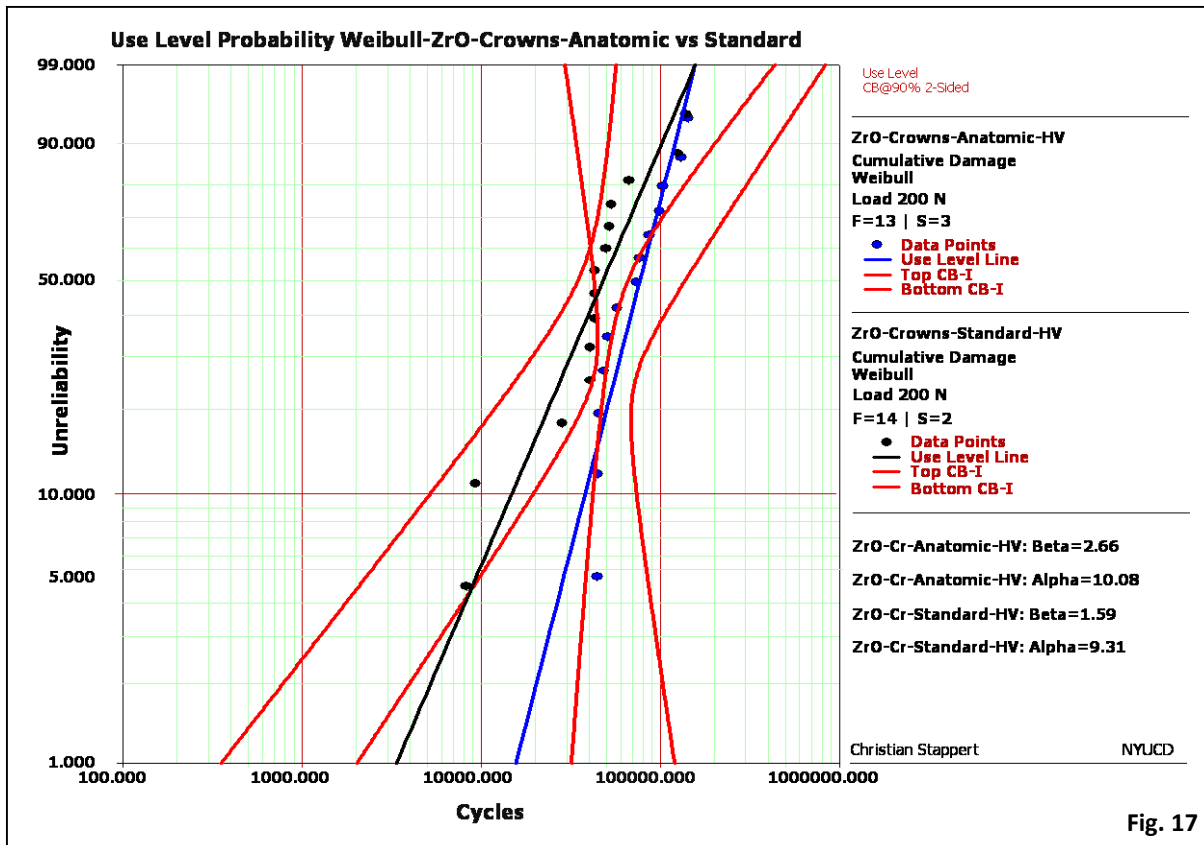
(Figure 17) Use level probability plot of the crowns with the standard coping design (black data points and line), and the crowns with the anatomical coping design (blue data points and line). The 2-sided 90% confidence bounds of both groups are represented by the red lines. There was a trend towards early failures in group S, since the slope of the curve is flatter than the slope of the curve of group A. In both groups the β-values were > 1 (1.59 for group S, 2.66 for group A). This indicates that fatigue was an acceleration factor for both groups. F=failed specimens, S=suspended specimens, CB=confidence bound.

The SSALT permits the estimation of reliability of the specimens at a given load level. This analysis includes failed specimens and suspended specimens. Reliability calculations for a cumulative damage of loads up to 200 N (2-sided 90% confidence bounds) are shown in figure 18+19 (appendices). The calculation resulted in 48% (29% - 64%) reliability for group S, and 80% (60% - 91%) reliability for group A at 50000 loading cycles. At 75000 cycles, the reliability of the crowns with the standard coping design decreased to 24% (5% - 51%) and to 53% (6% - 86%) for the crowns with the anatomically designed coping. At 100000 cycles, the calculated reliability was 11% (0% - 46%) for group S, and 25% (0% - 90%) for group A (table 7). The crowns with the anatomical coping design demonstrated higher mean survival probability at all cycle levels. Due to the fact that the confidence bounds of both groups overlapped, the significance between the two groups remained uncertain at 75000 and 100000 loading cycles. At 50000 loading cycles, the

crowns with the anatomical coping design showed significantly higher reliability compared to the crowns with the standard coping design. The Weibull analysis at a fatigue load of 200 N thus resulted in a clear trend towards higher reliability of the crowns with the anatomical coping design.

| | 200 N, 2-sided 90% Confidence Bounds | | | | | |
| | 50000 Cycles | | 75000 Cycles | | 100000 Cycles | |
	S	A	S	A	S	A
Upper CB	0.642	0.911	0.515	0.860	0.464	0.900
Reliability	**0.477**	**0.803**	**0.244**	**0.525**	**0.108**	**0.251**
Lower CB	0.292	0.595	0.050	0.064	1.50E-03	1.24E-08

(Table 7) Results of the reliability calculation for a cumulative damage of loads up to 200 N (2-sided 90% confidence bounds). The corresponding graphs are shown in Fig.18+19 (appendices). If a sample of group S had completed 50000 cycles with loads up to 200 N, the probability of survival was 48% (29%-64%). At the same time, the survival probability for a specimen of group A was 80% (60%-91%). The reliability was generally higher for specimens of group A. However, the significance of the results remained uncertain at 75000 and 100000 loading cycles since the confidence bounds of the two groups overlapped. S=group S (standard coping design), A=group A (anatomical coping design), N=Newton, CB=confidence bound.

5.3   FRACTOGRAPHIC ANALYSIS

The failure mode observed for all 36 specimens, independent of testing method, was cohesive fracture within the veneering porcelain. No bulk fracture or fracture of the zirconia die was observed.

In the static loading test, the cohesive fracture of the veneering porcelain occurred in the palatal or interproximal areas. In one specimen of group S the fracture also included the incisal edge (figure 20+21, appendices). One out of four samples failed from veneer chipping, the other three specimens failed from partial veneer delamination.

In samples subjected to fatigue testing, the fracture of the veneering porcelain was located on the incisal portion of the crowns (figure 22+23). In the majority of cases, the fracture included the entire incisal edge, extending to the incisal level of the coping. 13 out of 16 samples in group S failed from veneer chipping, the other three failed from partial veneer delamination (profile 1: n=1, profile 2: n=2). In group A (n=16), ten crowns failed from veneer chipping, and six from partial veneer delamination (profile 1: n=4, profile 2: n=1, profile 3: n=1).
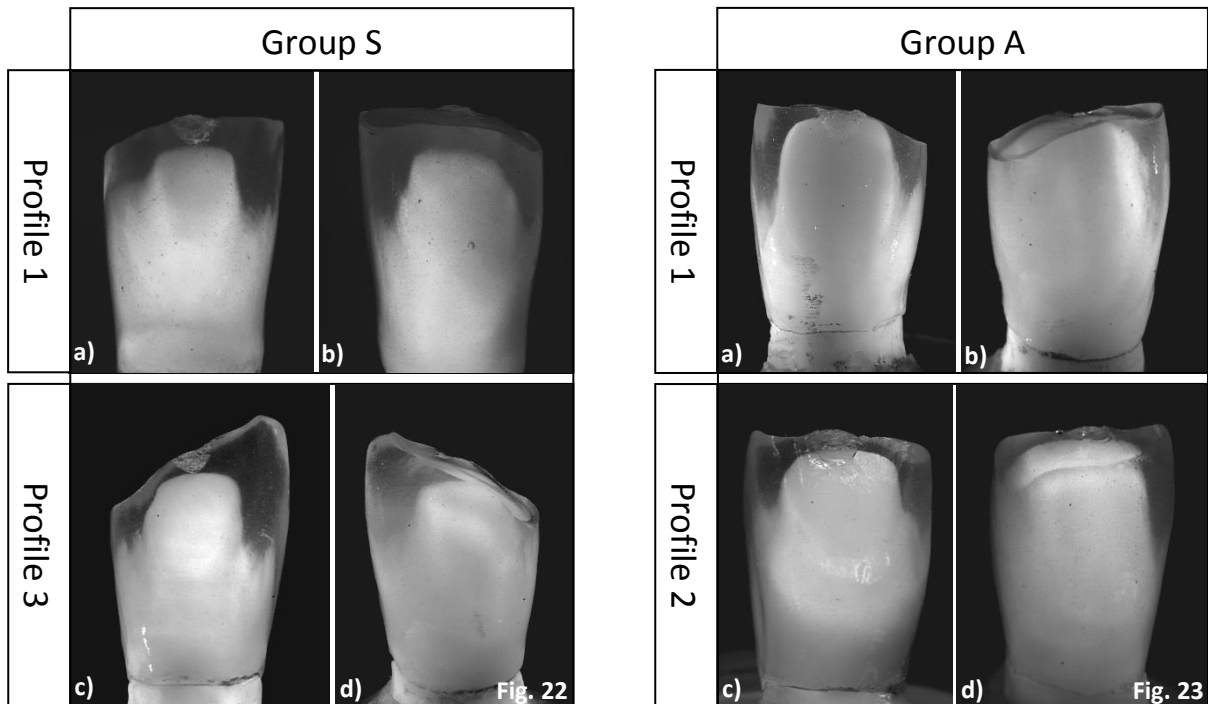
(Figure 22+23) Representative failure modes after fatigue testing (Fig.22: group S, Fig.23: group A). The pictures were obtained with the stereomicroscope (magnification: 1x), from a palatal (Fig.22a+c, Fig.23a+c) and a labial perspective (Fig.22b+d, Fig.23b+d), respectively. The upper row shows specimens subjected to the long-running profile 1 (Fig.22a+b, Fig.23a+b). Fig.22c+d show a specimen which had been running in the aggressive profile 3. Fig.23c+d show a specimen which had been subjected to the moderate profile 2. There were no differences in failure mode, neither between both groups nor between the different profiles. All specimens failed from incisal chipping or delamination.

Close examination of the fractured surface and the sectioned crowns (along the palatal-labial plane) revealed, that the cohesive fracture evolved from damage regions directly below the indenter slide path. The crack propagated radially throughout the material and finally led to failure as it reached the labial or interproximal outer surface of the veneering porcelain. This was concluded based on the location and direction of inner, outer and partial cone cracks (figure 24-26), wake hackles, twist hackles, arrest lines (figure 27+28) and fracture mirrors (figure 29). Those fracture patterns were observed in the veneering porcelain under the stereomicroscope and the SEM. The large radius of the arrest lines indicates that crack propagation was slow (figure 30). No cracks were observed in the zirconia coping or abutment.
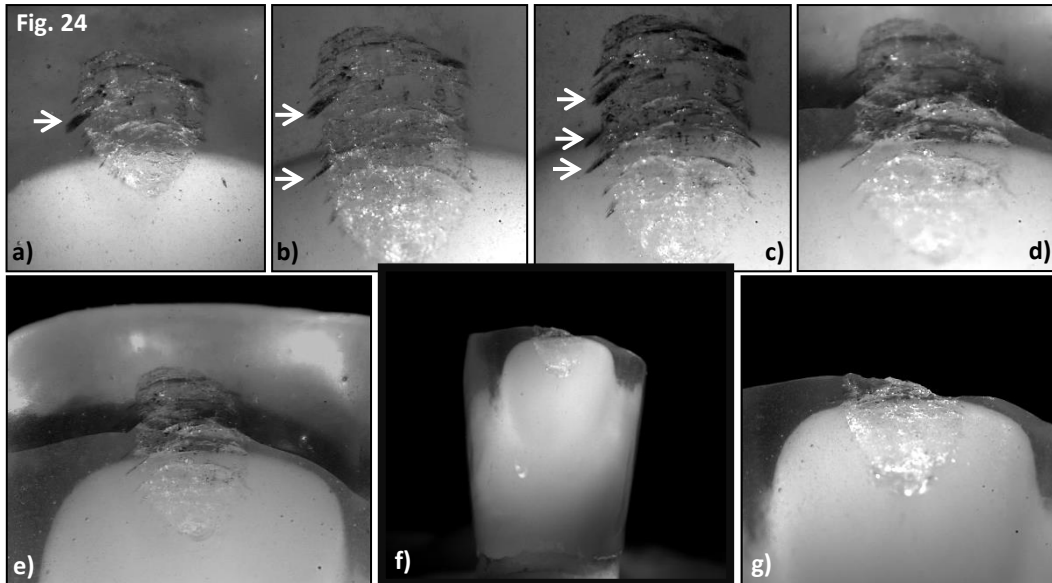
(Figure 24) Indentation area of a specimen of group A at different loading cycles (profile 2). The pictures were taken with the stereomicroscope (magnifications: 32x (a-d), 12.5x (e+g), 1x (f)), after 50000 (a), 60000 (b), 65000 (c) and 70000 cycles (d+e). (f)+(g) show the failed specimen (89999 cycles). Partial cone cracks formed below the indentation area and increased progressively in number and size (exemplary arrows in a-c). After 70000 cycles, a large crack became apparent (d+e). This crack finally led to failure (f+g).
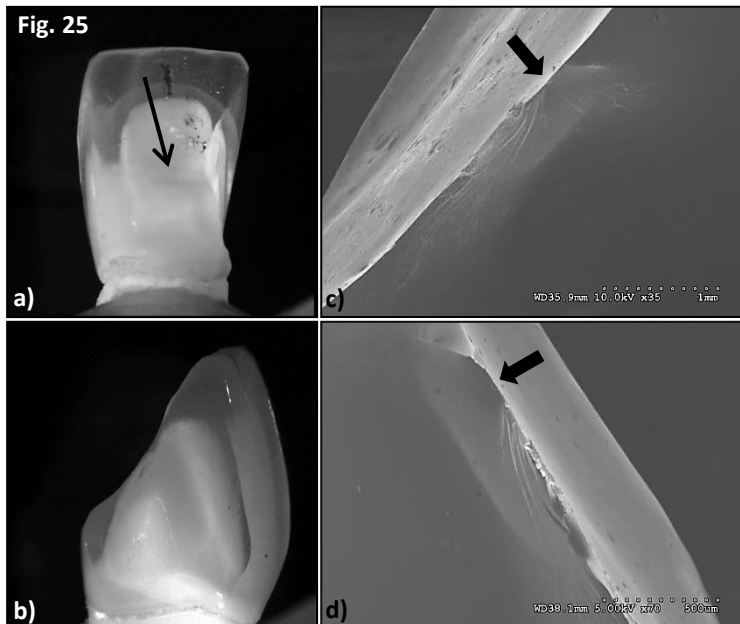
(Figure 25) Inner cone cracks below the indentation area of a failed specimen of group S after being subjected to static loading. The pictures in (a)+(b) were taken with the stereomicroscope (magnification: 1x), (c)+(d) with SEM (magnification: 35x (c), 70x (d)). (a) is obtained from a palatal, (b) from a mesial perspective. The arrow in (a) points out the sliding direction of the indenter during testing. (c) shows the failed crown from a mesial view. Inner cone cracks are visible below the indentation area, which is indicated by the arrow. (d) shows the chipped piece from a distal view. The arrow points on the indentation area. Inner cone cracks are visible below this area.
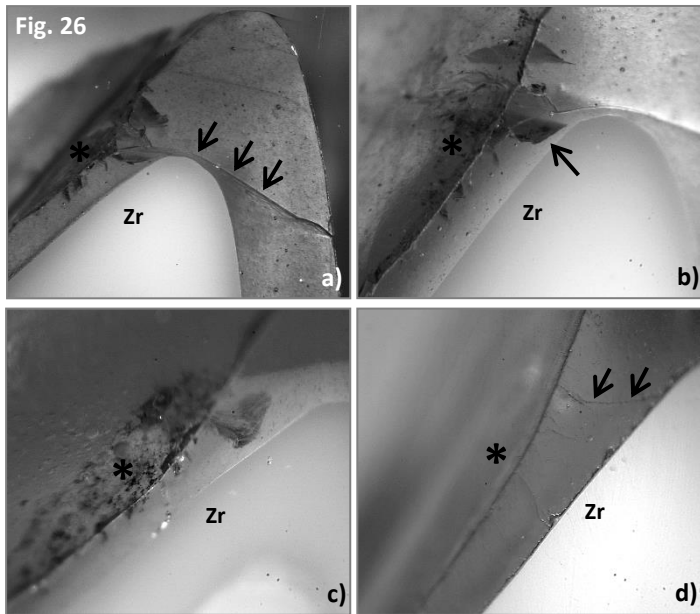
(Figure 26) Indentation area (✱) of sectioned crowns (palatal-labial plane) under the stereomicroscope (magnification: 32x). (a)+(b) show the same specimen (group A) at different perspectives. It had failed from chipping, the chipped piece was repositioned. The arrows in (a) point on the crack leading to failure. Note that below the crack, a thin layer of porcelain remained on the zirconia coping. The arrow in (b) points on a large partial cone crack which propagated from the indentation area onto the zirconia coping. (c) (group S), and (d) (group A) show specimens which were suspended. Since they had not failed from the indentation area, it was possible to examine the subsurface damage before failure. Both show partial cone cracks in the veneering porcelain, evolving from the indentation area and propagating towards the zirconia coping. Zr=zirconia coping.
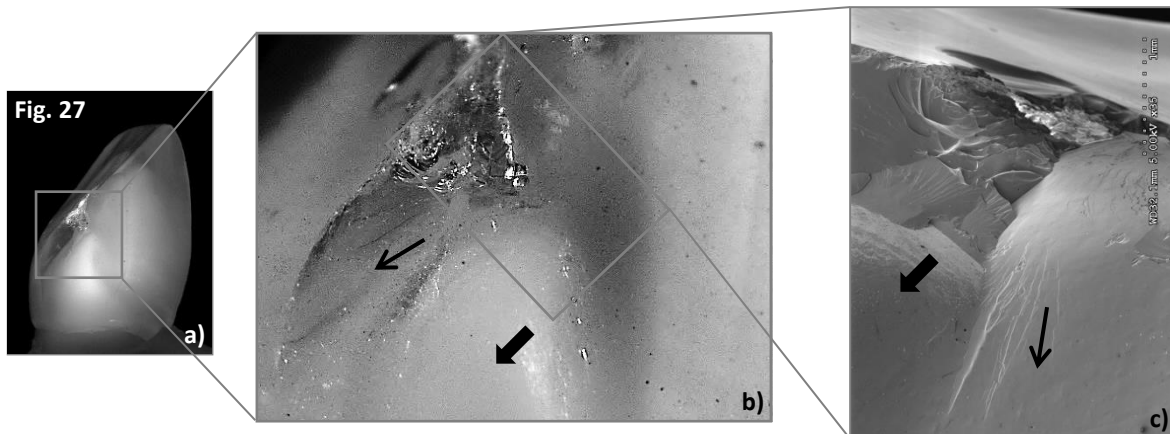
(Figure 27) Failed specimen after being subjected to static loading (group A). The pictures were obtained with stereomicroscope (magnification: 1x (a); 32x (b)) and SEM (c, magnification: 35x). The specimen failed from delamination. (a) shows the entire specimen from a mesial view. (b)+(c) are close-ups of the fractured area. The thick arrow points on the exposed zirconia surface. The thin arrows are parallel to the direction of hackle lines on the fractured veneering porcelain surface. They evolved from the indentation area and ran in the local direction of the crack.
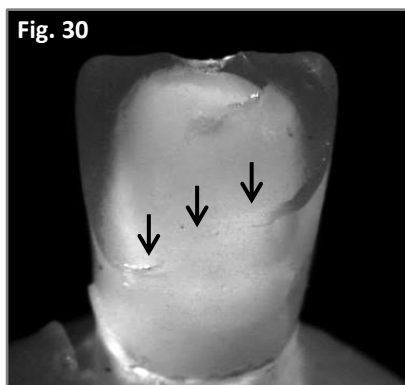
(Figure 30) Arrest line (arrows) in a failed crown of group S. The picture was obtained with the stereomicroscope from a labial view (magnification: 1x). The distance from the origin of the fracture (indentation area, not visible from this perspective) to the arrest line was large, taking up almost the entire fractured surface. This indicates that crack propagation was slow.
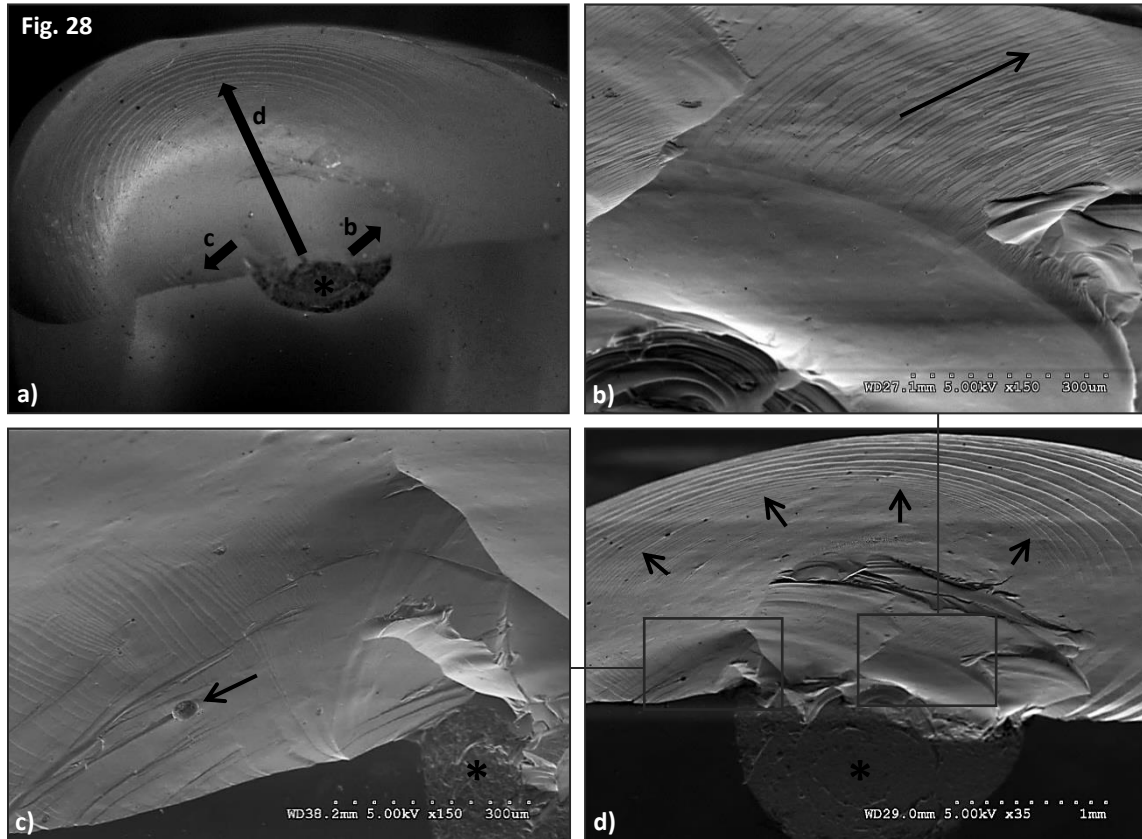
(Figure 28) Crack patterns on the surface of a failed specimen of group S. The pictures were obtained from a top view by means of the stereomicroscope (a, magnification: 16x) and the SEM (magnification: 150x (b+c), 35x (d)). (a)+(d) show an overview of the fractured porcelain surface. (b)+(c) are close-ups of the regions indicated in (d) (squares). The arrow in (b) is parallel to twist hackle lines running in the local direction of the crack. A wake hackle line is shown in (c). It evolved from a void in the veneering porcelain, indicated by the arrow which points in the direction of crack propagation. In (d), the arrows point at arrest lines. They are curved in the shape of the crack front, forming circles around the indentation area. The thick arrows in (a) summarize the findings of the surface examination (b-d). The thick arrows point in the direction of local crack propagation. This shows that the crack leading to fracture originated from the indentation area and propagated radially throughout the material. *=indentation area.
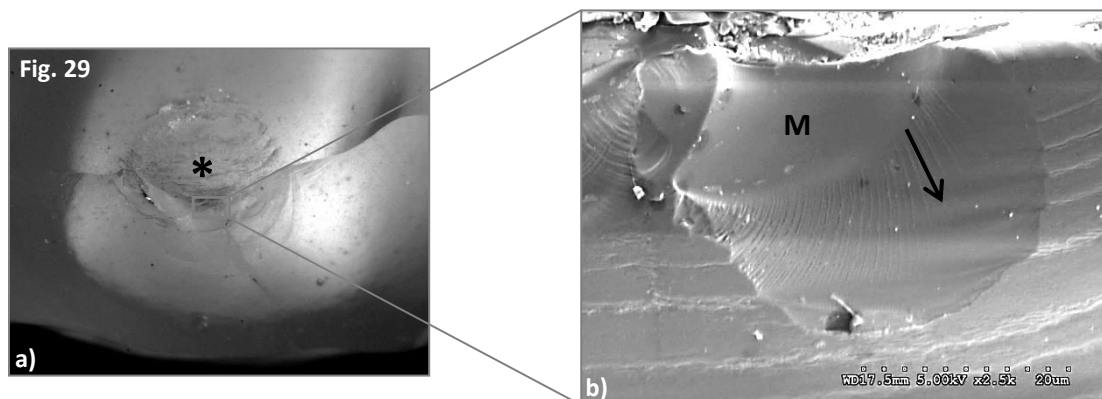
(Figure 29) Fracture mirror (M) on the surface of a failed crown of group S. The picture in (a) was obtained with the stereomicroscope (magnification: 12.5x) from a top view. (b) is a close-up (SEM, magnification: 2500x) of the fractured surface directly below the indentation area (*). It shows a fracture mirror (M), surrounded by radial hackle lines (arrow pointing in the direction of the hackles). These fracture patterns reveal that the origin of the fracture was located directly below the indentation area, and that the crack propagated radially into the depth of the material.

6 DISCUSSION

This thesis investigated the effect of two different zirconia coping designs on the fatigue resistance and the fracture propagation of hand-veneered, anterior all-ceramic crowns. One group consisted of 18 crowns with a constant coping thickness of 0.5 mm. The other group included 18 crowns with an anatomical coping design, in which the incisal and interproximal coping thickness was increased.

The results showed a statistically significant difference in fatigue resistance at low loading cycles. No significant difference in failure probability was found between the two groups at longer loading cycles. Fracture propagation was similar in both groups. Therefore, the research hypothesis was partially accepted, and the null hypothesis was rejected.

There was a clear trend towards higher fatigue resistance of the crowns with the anatomically designed zirconia copings, whereas the crowns with the standard coping design seemed to be more susceptible to early failures. All crowns failed from chipping or delamination.

In an extensive literature search on "PubMed" and "Google scholar", no study was found that had already tested the mechanical properties of anatomically designed zirconia copings on anterior crowns. Four in vitro studies were found investigating the anatomical zirconia coping design on molar crowns. Kokubo et al.[42] and Sundh & Sjögren et al.[39] showed that zirconia-based molar crowns with an even thickness of the veneering porcelain achieved significantly higher fracture loads under static loading than those with an uneven veneering porcelain thickness. Rosentritt et al.[43], and Larsson et al.[44] subjected molar all-ceramic crowns with the two different coping designs to cyclic loading (not to step-stress accelerated life testing (SSALT)). In both studies, the crowns with the anatomically designed zirconia coping performed significantly better than the crowns with standard coping design. In all four studies, the crowns failed from fracture within the veneering porcelain. Fracture of the zirconia copings was not observed.

The results of the present thesis are thus in accordance with previous in vitro studies on all-ceramic crowns with anatomically designed zirconia copings. Moreover, the results of the thesis provide evidence to several short-term clinical studies that recommend zirconia copings with an increased occlusal and interproximal veneering porcelain support.[32, 35]

In order to improve the mechanical stability of posterior zirconia-based all-ceramic crowns, another coping design has been suggested recently. It includes a cervical zirconia collar on the oral face of the crown, which conduces to the support of the veneering porcelain. It is based on a design that was originally developed for metal-based restorations. The outcomes of the corresponding in vitro studies (using SSALT) are ambivalent. One study showed that crowns with the modified coping design are more reliable in comparison to crowns with a standard coping design.[226] Another study found no statistically significant difference between copings with and without the cervical collar.[225] Clinically, this modified coping design is used with good outcome, but there are no long-term studies yet.[227, 228]

In the present study, an ANOVA-test was performed on the failure loads generated in profile 1 (n=6 for each group), as the amount of samples in the other three profiles was too small to justify it (profile 0: n=1 or 0, respectively; profile 2: n=4; profile 3: n=2 or 4, respectively). This analysis showed, that the mean fatigue failure loads of both groups (group S: 313 ± 82 N (n=6); group A: 367 ± 123 N (n=6)) were above the average clinical load range in the anterior dentition (140-200 N).[235]

As expected, the mean failure loads of the ANOVA-test were lower than the mean failure loads obtained from the static loading test (group S: 945 ± 151 N (n=2); group A: 706 ± 25 N (n=2)). This was due to the fact that the fatigue loading accumulated damage inside the material and, as a result, weakened it before higher loads were applied.[237, 238] Furthermore, the fatigue loading involved water as surrounding medium, which is an important factor assisting slow crack growth.[195] In order to estimate the clinical reliability of the tested crowns, this scenario is more realistic than the static loading test.

The static loading test showed higher failure loads in group S compared to group A, whereas in fatigue testing the failure loads of group A were generally higher. Taking into consideration the small amount of samples subjected to static loading, the results obtained from this test are not representative. They should not be referred to as values of ultimate strength for the tested crowns. The only objective of the static loading test was to evaluate the approximate strength of the specimens in order to generate the profiles for the SSALT.

The specimens of both groups withstood fatigue loads up to 150 N with limited failures. According to the highest value of the mean masticatory loading forces[235], the use stress for the Weibull analysis was determined 200 N. The confidence bounds were set 90%. This means that the frequency with which they contain the true value is 0.90.[280]

The master Weibull plot of unreliability versus number of cycles clearly showed more early failures in group S. Additionally, group S showed lower predictability (more failures at lower numbers of cycles) compared to group A. From a patient satisfaction viewpoint, early failures are unacceptable. Yet, a statistically significant difference remained uncertain for loading cycles higher than 50000 due to overlapping confidence bounds and the potential small sample size.

The β-value (Weibull shape factor) describes failure rate changes over time. In both groups, it was higher than 1 (β=1.59 in group S, β=2.66 in group A). This indicates that the failure rate is increasing over time. Therefore it is associated with failures caused by damage accumulation. If β=1, the failure rate would not vary over time, which would imply that the failures were not time dependent. A β-value < 1 would insinuate early failures, since the failure rate would decrease over time.[280] Clinical β-values usually range from 1-2 (personal contact to Van P. Thompson, Department of Biomaterials and Biomimetics, NYUCD, NY, USA).

The Weibull reliability calculations for the completion of a mission of 50000, 75000 and 100000 cycles at 200 N clearly showed higher values in group A. The mean survival probability was constantly lower, and decreased more rapidly in group S than in group A. Considering the absence of overlapping confidence bounds between the two groups as reference for significance, the Weibull analysis suggested that there was no statistically significant difference between the two groups at 75000 and 100000 loading cycles. For a mission of 50000 loading cycles at loads up to 200 N, the overlap was only minor (0.047). Taking into consideration that the mean reliability level of group A (0.80) was higher than the upper confidence bound of group S (0.64), it was concluded that there was a statistically significant difference between the two groups at 50000 loading cycles. At 75000 loading cycles, the mean reliability value of group A (0.56) was not within the upper confidence bound of group S (0.52). It is hence assumed that there was no statistically significant difference but sign for significance at 75000 loading cycles. The significance remained uncertain for 100000 loading cycles due to a wide range of the confidence

bounds. As mentioned before, a larger sample size would be required to further define the confidence bounds; and thus to verify or decline the present trend.

In comparison to the use level probability plot, the reliability calculations also included suspended specimens. Suspended specimens do account for reliability calculations since they are considered as survivals until they are taken out of the testing process. Suspensions usually have little effect on the slope (β-value). Even though statisticians always prefer complete samples (no suspensions), in research suspensions are very common. Three out of five suspensions in this study were suspended earlier than the first specimen failed. The effect of these "early suspensions" on the Weibull reliability analysis is negligible.[280]

Both statistical methods used in this study, the ANOVA-test and the Weibull analysis, showed no certainty in significance between both groups due to high standard deviations and overlapping confidence bounds. To increase the level of statistical confidence, a substantial amount of additional specimens would need to be tested.

The material of the dies used in this study was zirconium dioxide, which has a high Young's modulus compared to dentine (zirconium dioxide: 21 GPa, dentine: 13-15 GPa)[210, 214]. It was chosen expecting the tensile stresses in the high-stress areas (cervical-palatal) to eventually exceed the strength of a dentine-like resin material. Preliminary testing for this investigation pointed out early failures of dies made of Z100 composite (3M ESPE; St. Paul, MN, USA), a material with similar mechanical properties to dentine.[281] In this preliminary study, two samples fractured in the cervical area of the die before the tested crowns failed from fatigue. It has to be noted that the rigidity of the dies might have led to higher failure loads in comparison to tooth-supported restorations.[237] The results of this study are, however, relevant for implant-supported restorations; especially since chipping is more likely to occur if the restoration is supported by implants.[28, 282, 283]

The zirconia dies were embedded in resin (Caulk Orthodontic Resin; Dentsply, York, PA, USA). In comparison to the zirconia (21 GPa)[210], the resin has a low Young's modulus (3 GPa)[284] and provides only little mobility for the dies. With regard to tooth-supported restorations with a periodontal ligament, the micromobility will lead to lower failure loads compared to a rigid test model.[285] For implant-supported restorations, the

usage of resin is appropriate as its elastic modulus (3 GPa)[284] resembles the jaw bone's elastic modulus (trabecular bone: 1370 MPa, cortical bone: 13700 MPa)[286].

Crowns with zirconia copings can be used for the restoration of anterior and posterior teeth.[287] In the anterior dentition they constitute an alternative to monolithic, lithium disilicate glass-ceramic materials.[20] In comparison to zirconium dioxide, glass-ceramics contain an amorphous phase and a fine crystallite size which enable the transmission of light.[19, 58] At the same time, these materials provide sufficient mechanical strength to withstand the mean masticatory forces in the anterior dentition.[288] Conversely, zirconia-based anterior restorations are critical as part of all-ceramic full-arch restorations and for patients with parafunctional activities as they withstand high masticatory forces.[235, 289] They can also be used to mask a dark background such as a dark tooth or core buildup material.[18]

The fractographic results of this study are consistent with previous observations of studies on zirconia-porcelain trilayers or crowns in off-axis fatigue loading.[43, 226, 244, 245, 251, 262, 268, 290] The crowns subjected to fatigue testing (n=32) all failed from cohesive fracture within the veneering porcelain on the incisal edge of the crown. In most of the cases, the fracture included the entire incisal edge of the specimen. This would imply the replacement of the restoration in the clinical situation.

The fracture origin was always located within the indentation area. From there, partial cone cracks propagated into the depth of the veneering porcelain bypassing the zirconia coping. Fracture of the zirconia copings or dies were not observed. Even a close examination of the sectioned crowns and fractured surfaces at magnifications up to 2500x did not reveal cracks in the zirconia coping or abutment.

During the examination, special attention was paid to the cervical-palatal area of the dies, copings and veneering porcelain, where the highest tensile stresses were concentrated. Cracks in the zirconia coping are of major clinical importance. They are usually undetected and can lead to spontaneous, catastrophic failure of the restoration. All crowns subjected to fatigue fractured on the incisal edge. The location of the fracture was different in the static loading test in which specimens mainly failed from interproximal chipping or partial delamination. This was due to the fact that, during the course of the static load test, the indenter slid far down the palatal face of the specimen. With increasing load, the indentation area was moved cervical.

A forecast on the expected clinical performance of a restoration tested in the laboratory is restricted, since there are many variables which influence the intraoral behavior of a material.[291] In vitro studies can, however, be a time- and cost-effective method to study and compare standardized models in a controlled environment. The step-stress accelerated life testing method has been reported to reproduce clinical failure modes[244, 245], even though the loads are lower and the loading cycles are longer in the clinical situation. The crowns used in this study were produced by the same milling devices in a dental laboratory. They were cemented on the dies identical to the clinical application. There may have been minor differences in the dimension of the multiplied zirconia dies, and also in the cement thickness, since the zirconia dies and copings were milled in a presintered stage. The dimensions of the ceramic layers (zirconia coping and veneering porcelain) in each group were similar. Furthermore, the specimens were loaded on a reproducible position and direction with a standardized magnitude (dependent on the profile) in an aqueous environment.

In this context, special attention has to be paid to the loading position. The application of the load can hardly be controlled in the clinical situation. As a result, the stress is more allocated compared to the conditions in the laboratory, where the load is concentrated on a particular, defined area.[291] Therefore, the in vitro indentation represents a more reproducible but also a more catastrophic scenario.[202] In this study, the load was applied 2.0 – 2.5 mm below the incisal edge on the palatal surface of the specimens.[278] Considering the diameter of the indenter (6.25 mm), this position was mainly located above the bulk of the coping in group A (incisal veneering porcelain thickness: 1.79 mm). In group S (incisal veneering porcelain thickness: 3.13 mm), the load was mainly applied on the unsupported veneering porcelain. The improved support of the veneering porcelain can be considered as one reason that the crowns with the anatomically designed copings generally performed better than the ones with the standard coping design. During indentation, each component of the specimen was subjected to tensile and compressive stresses. The stiff zirconia coping (Young's modulus: 210 GPa)[210] minimized the flexure of the veneering porcelain (Young's modulus: 65 GPa).[210, 292] Tensile stresses inside the veneering porcelain during loading were therefore reduced and compressive stresses increased. These compressive stresses decelerated the propagation of partial cone cracks evolving from the indentation area towards the zirconia coping.[251, 265]

The reduction of veneering porcelain flexure also prevented the generation of radial cracks (none of the cohesive fractures originated from radial cracks). These cracks arise in response to high tensile stresses at the ceramic undersurface, below the indentation area.[212, 265, 293] Additionally, the high tensile strength of the zirconium dioxide (1200 MPa)[71] prevented the formation of radial cracks on the cement interface.[263, 268] In the clinical situation, radial cracks on the cement-ceramic interface are highly detrimental. They lead to spontaneous, catastrophic bulk fractures.[271] The results of this study are thus in accordance with various clinical studies reporting that bulk fractures are rare in zirconia-based restorations.[25, 26, 33, 217] Conversely, bulk fractures remain the major mechanical failure mode in alumina-based and monolithic glass-ceramic FDPs.[22-24, 217]

During fatigue testing, the specimens failed from chipping or partial delamination. Delamination is characterized as a complete detachment of the veneering porcelain from the coping. Chipping is defined as a cohesive fracture solely located within the veneering porcelain.

The mean failure loads of the specimens failed from partial delamination were higher than the mean failure loads of the corresponding group. Once a crack had reached the zirconia-porcelain interface, it probably required additional energy to deflect it back into the veneering porcelain.[294, 295] Furthermore, partial delamination occurred more often in specimens of group A (6 out of 16), compared to specimens of group S (3 out of 16). A possible explanation may be the different position of the indentation area in the two groups, relative to the coping. The indentation area in group A was mainly located directly above the coping. Due to the thinner (incisal) layer thickness of the zirconia coping in group S, the incisal level of the coping was located cervical from the indentation area. Partial cone cracks, originating from the indentation area, were therefore more likely to bypass the zirconia-porcelain interface in group S. Since all specimens failed from cohesive fracture within the veneering porcelain, it was concluded that there were no differences between both groups with regard to the failure mode. Moreover, there were no differences in failure mode between the different SSALT-profiles.

As already mentioned in the introduction of this thesis, chipping and delamination seem to be a problem specific to zirconia.[21, 210] Changes in the design of the restoration (such as increasing the coping thickness) might improve the apparent strength but won't solve the material-specific problem of zirconia-based all-ceramic restorations.

Various possible reasons for the high chipping/delamination rate in zirconia-based restorations have been suggested in the literature, yet without decisive solution. These are mismatching coefficients of thermal expansion (CTE) between the veneering porcelain and the core material, the surface property changes of the zirconia induced by the veneering porcelain, the manufacturing method of the veneering porcelain and the low thermal conductivity of the zirconia.

It is unlikely, that a mismatch in CTE was the reason for chipping or delamination in this study. The CTE of the veneering porcelain ($9.5*10^{-6}$ K^{-1})[91] was matched to the CTE of the zirconia coping ($10.4*10^{-6}$ K^{-1})[210]. The CTE of the veneering porcelain should be ~10% lower than the CTE of the core material in order to avoid the generation of tensile stresses inside the veneering porcelain.[38] These would occur, if the CTE of the veneering porcelain was higher than the CTE of the core material. However, the same principle is used for every ceramic system, for zirconia-based restorations as well as for alumina-based restorations or porcelain-fused-to-metal (PFM).

Another possible explanation for the high chipping rate in zirconia-based restorations is a chemical interaction between the veneering porcelain and the zirconia coping during firing. Firstly, the (melting) veneering porcelain could have induced changes in the geometry of surface zirconia crystals. This process is assumed to occur analogous to the water penetration of zirconia grain boundaries at moderately elevated temperatures known from low temperature degradation (LTD).[133] Secondly, stabilizing dopants in the zirconia (e.g. Yttria) could have dissolved in the silicate ceramic material at high temperatures. Both scenarios would have led to an increase in volume in surface zirconia crystals, resulting in tensile stresses on the bottom side of the veneering porcelain.[37] In this study, the zirconia surface was treated with a zirconia liner before the veneering porcelain was applied. Zirconia liners help to reduce possible interactions of the silicate and the zirconia ceramic material and can improve the bond strength at the porcelain-zirconia interface.[37, 296]

The firing protocol of the veneering porcelain might be another explanation that chipping was the most common failure mode in this study. Zirconia has a low thermal conductivity, compared to other coping materials.[36] After the final firing of the veneering porcelain, the heat on the bottom side of the veneering porcelain was not released as quickly as on the top surface adjoining the air. Due to a temperature gradient, this could have resulted in

tensile prestresses inside the veneering porcelain.[36] Differences in veneering porcelain thickness might have created additional residual stresses.[297]

The manufacturing process of the crowns tested in this study followed the manufacturer's recommendations. The furnace (Programat P500; Ivoclar Vivadent, Schaan, Liechtenstein) does not include a cooling device. Therefore, the cooling rate could not be determined for all firings. In the last firing cycle (glaze), the furnace was opened after the temperature fell below 450°C. In order to reduce chipping, it might, however, be helpful to elongate the cooling time after the last firing cycle (unpublished data; Fabio Lorenzoni, Department of Biomaterials and Biomimetics, NYUCD, NY, USA).

In this context, special attention needs to be paid to the manufacturing method of the veneering porcelain. Previous in vitro fatigue studies on zirconia- and alumina-based all-ceramic FDPs point out that specimens veneered with the hand-layering technique perform better than over-pressed specimens.[231, 298] This is interesting because press-ceramics usually exhibit greater strength and fracture toughness than feldspathic ceramics.[12, 13, 101, 142] An approach based on the layer thickness of the veneering porcelain during firing might explain these paradox findings. Residual stresses evolve in the veneering porcelain during cooling due to thermal contraction. The hand-layering technique provides small shrinkage volumes during cooling since the material is applied in multiple (thin) layers.[231, 299] With increasing layer thickness (over-pressed restorations) these residual stresses multiply. As mentioned above, residual stresses evolve in the veneering porcelain during cooling due to a temperature gradient between the outer and the inner surface. With respect to the low thermal conductivity of zirconia, this becomes even worse.[36] It would thus be interesting to compare the fatigue reliability and fracture modes of different veneering techniques applied on the two different zirconia copings used in this study (unpublished data; Christian Stappert, Department of Biomaterials and Biomimetics, NYUCD, NY, USA).

7 CONCLUSION

Within the limitations of this study, the following conclusions can be drawn:

- The crowns with the standard coping design and the ones with the anatomical coping design resist the average masticatory forces in the anterior dentition. It is hence assumed that they are suitable for clinical application in the anterior region.

- Both zirconia-based crown systems predominantly failed from incisal chipping.

- There was a clear trend towards higher reliability of the crowns with the anatomical coping design. The anatomical coping design should have the potential to reduce the probability of early clinical crown failures by veneer chipping.

8 ABSTRACT

Objectives: The objective of this thesis was to determine the effect of two different zirconia coping designs on the fatigue strength and fracture propagation of the corresponding anterior all-ceramic crown. **Materials and methods:** One group consisted of 18 crowns with a constant zirconia coping thickness of 0.5 mm (group S). The other group included 18 crowns with an anatomically designed zirconia coping (increased incisal and interproximal coping thickness) (group A). The crowns were hand-veneered (IPS e.max Ceram, Ivoclar) and adhesively cemented (Multilink Implant, Ivoclar) on zirconia dies. The zirconia copings and dies were CAD/CAM produced (copings: NobelProcera, Nobel Biocare; dies: IPS e.max ZirCAD, Ivoclar Vivadent). A single load to failure test was performed to estimate the initial ultimate strength (n=4). 32 specimens were subjected to one out of three stress-time varying profiles using mouth motion (2Hz) step-stress accelerated life testing (ELF-3300, Bose). After mechanical testing, a fractographic analysis was performed by means of the stereomicroscope and the SEM. The reliability of the crowns was computed using a cumulative-damage step-stress analysis (Alta-7-Pro, Reliasoft).

Results: Chipping of the veneering porcelain was the main failure mode in both groups. Nine specimens showed areas of delamination. The mean loads at failure were 313 ± 82 N (n=6) for group S and 367 ± 123 N (n=6) for group A (profile 1). The use level probability Weibull plot at 200 N and 50k loading cycles showed a statistically significant difference between the two groups, associated with early failures, in group S. For longer loading cycles, the significance remained uncertain, but showed a clear trend towards higher reliability of the crowns with the anatomical coping design. The reliability calculations at 200 N and 50k cycles (2-sided at 90.0 % confidence bounds) resulted in 0.48 (0.64/0.29) reliability for group S, and 0.8 (0.91/0.6) reliability for group A. In general, group A generated higher mean reliability values than group S. Cracks leading to failure evolved from the area directly below the indenter slide path. No cracks were observed in the zirconia coping or die. **Conclusion:** The tested crowns are suitable for clinical application in the anterior region. There was a clear trend towards higher reliability of the crowns with the anatomical coping design. The anatomical coping design should have the potential to reduce the probability of early clinical failures by veneer chipping. The failure modes in both crown systems were similar.

9 ZUSAMMENFASSUNG (GERMAN)

Zielsetzung: Die Auswirkung zweier verschiedener Zirkoniumdioxid-Gerüstdesigns (NobelProcera, Nobel Biocare) auf die Dauerbelastbarkeit und das Bruchverhalten von vollkeramischen Frontzahnkronen festzustellen. **Material&Methode**: Gruppe S bestand aus 18 Kronen, deren Gerüst eine konstante Schichtstärke von 0,5 mm aufwies. Die Gerüste der Gruppe A (n=18) waren anatomisch geformt (erhöhte Schichtstärke im inzisalen und approximalen Bereich). Die Kronen beider Gruppen wurden mit einer Glaskeramik (IPS e.max Ceram, Ivoclar) in der Schichttechnik verblendet und adhäsiv auf Zirkoniumdioxidzahnstümpfe (IPS e.max ZirCAD, Ivoclar) zementiert (Multilink Implant, Ivoclar). Die Gerüste und Zahnstümpfe wurden mit CAD/CAM hergestellt. Zuerst wurde die statische Bruchfestigkeit mit Hilfe eines Bruchbelastungstests ermittelt (n=4). Die restlichen 32 Kronen wurden dann mit Hilfe eines Kausimulators (ELF-3300, BOSE) und drei verschiedenen Belastungsprofilen auf Ihre Dauerbelastungsfähigkeit getestet (SSALT). Alle Kronen wurden unter dem Lichtmikroskop und dem REM fraktographisch untersucht. **Ergebnisse**: Chipping im inzisalen Bereich war die Ursache, die am häufigsten zum Versagen führte. Neun Kronen wiesen delaminierte Bereiche auf. Die mittleren Bruchlastwerte unter Dauerbelastung waren 313 ± 82 N (n=6) in Gruppe S, und 367 ± 123 N (n=6) in Gruppe A (Profil 1). Der Weibullgraph ergab einen statistisch signifikanten Unterschied für eine Belastung von 200 N und 50k Kauzyklen, wobei Gruppe S häufiger zu frühen Fehlern neigten als Gruppe A. Für längere Belastungszyklen verblieb die Signifikanz unsicher, zeigte aber einen deutlichen Trend in Richtung höherer Zuverlässigkeit von Gruppe A. Für eine Belastung von 200 N und 50k Belastungszyklen ergab sich eine Zuverlässigkeit von 0,48 (0,64/0,29) für Gruppe S, und 0,8 (0,91/0,6) für Gruppe A. Im Allgemeinen wies Gruppe A höhere mittlere Zuverlässigkeitswerte auf als Gruppe S. Die Risse, die zum Versagen der Kronen führten, gingen von der Region direkt unter dem Belastungspunkt aus. Es konnten keine Risse im Zirkoniumdioxidgerüst oder den Zahnstümpfen festgestellt werden. **Schlussfolgerung**: Die getesteten Kronen sind für die klinische Anwendung im Frontzahnbereich geeignet. Es ergab sich ein deutlicher Trend in Richtung höherer Zuverlässigkeit der Kronen mit anatomischem Gerüstdesign. Das anatomische Gerüstdesign kann die Wahrscheinlichkeit von vorzeitigen Verblendkeramikbrüchen reduzieren. Die Fehlerquellen beider Kronensysteme waren ähnlich.

10 APPENDICES
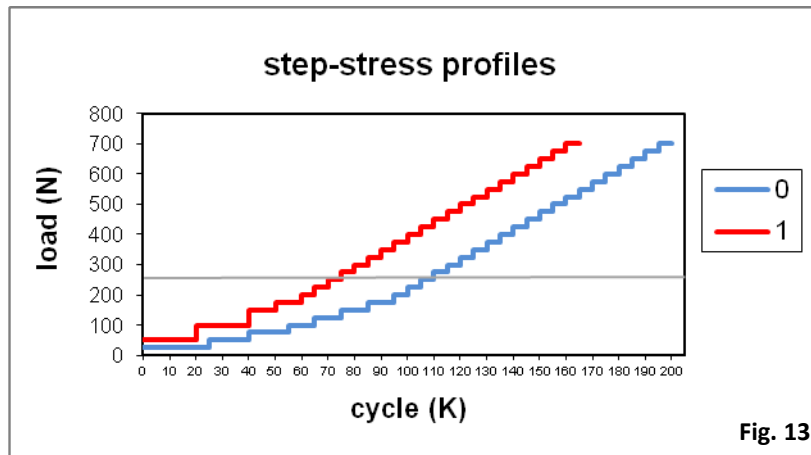
(Figure 13) SSALT profiles. In the beginning, profile 0 (blue line) was considered the mild profile. After subjecting one sample of group A to profile 0, it was replaced by profile 1 (red line). All other samples ran in profile 1 since it was more time-efficient. For example (grey line), by the time the sample reached the load level of 250 N, it took 4 h and 51 min longer if profile 0 was used instead of profile 1. N=Newton, K=kilo.
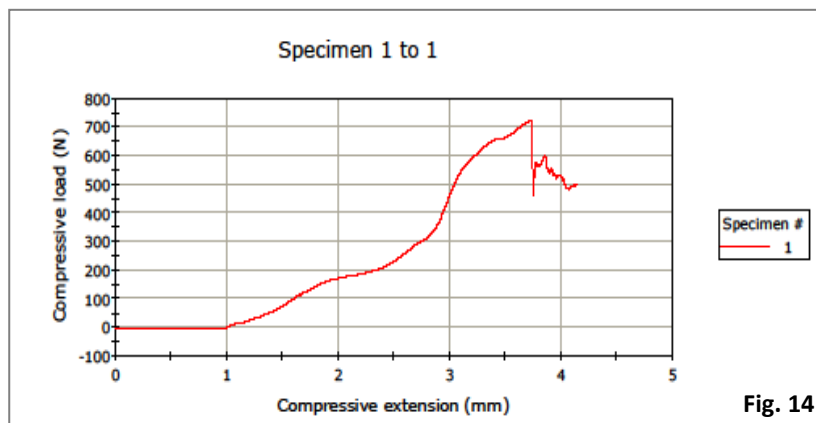
(Figure 14) Graph recorded by the Instron machine during the course of the static load test on a specimen of group A. The red line shows the compressive load plotted against the compressive extension caused by the indenter. The specimen failed at 724 N. N=Newton.
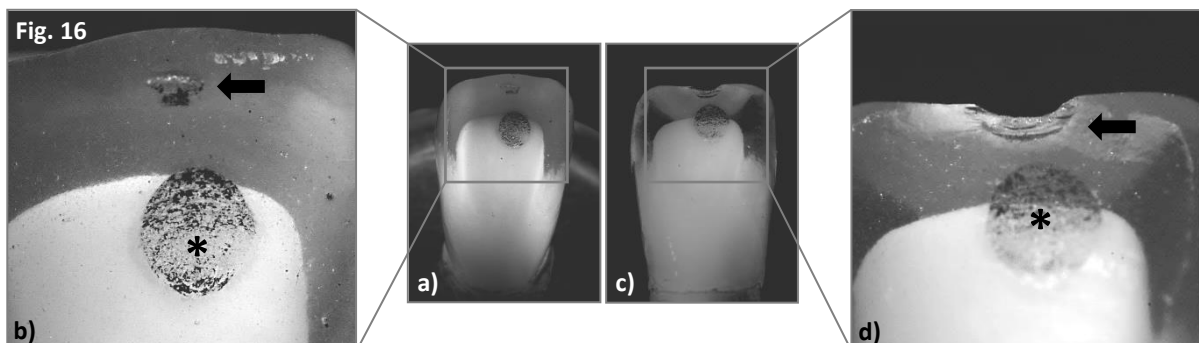
(Figure 16) Stereomicroscope pictures of a representative sample which was considered as survival (magnifications: 1x (a+c), 12.5x (b+d). (a)+(b) show the sample before, and (c)+(d) after it had failed from a precontact on the incisal edge. The arrow in (b) points on the precontact point located above the contact point of the tungsten carbide sphere (*). This precontact had led to fracture (arrow in (d)), before the specimen failed from the actual indentation area. For the statistical analysis, it was assumed that, by the time the fracture occurred, those samples had not failed yet.
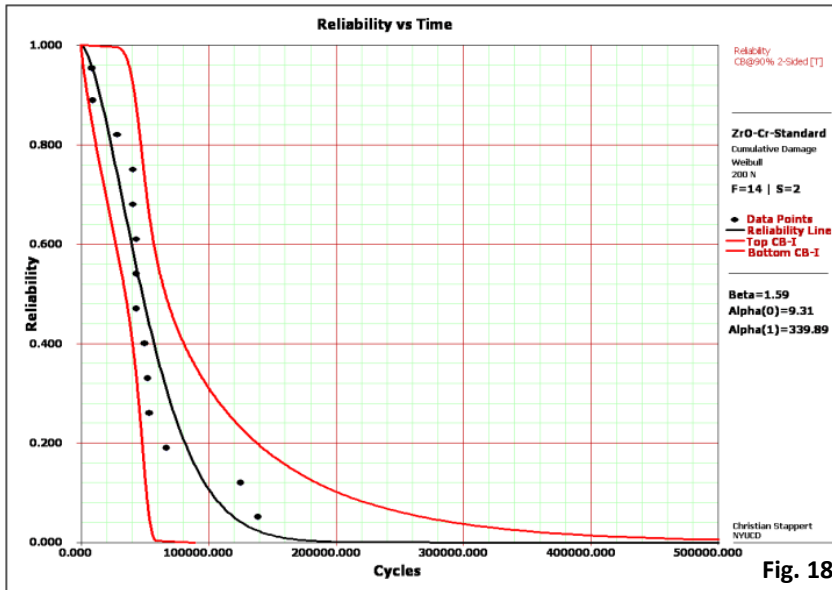
Fig. 18

(Figure 18+19) Reliability at a use stress of 200 N plotted against loading cycles at 2-sided 90% confidence bounds. Fig.18 shows the graph of the reliability analysis of group S (black points and line). Fig.19 shows the graph of the reliability analysis of group A (blue points and line). The confidence bounds of both groups are represented by the red lines. A detailed description of the reliability calculation is given in table 7.

Fig. 19

Fig. 20

Fig. 21
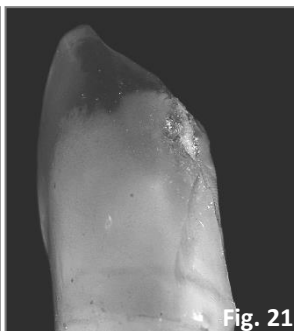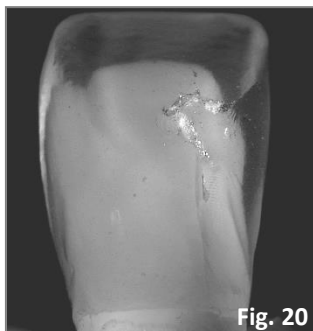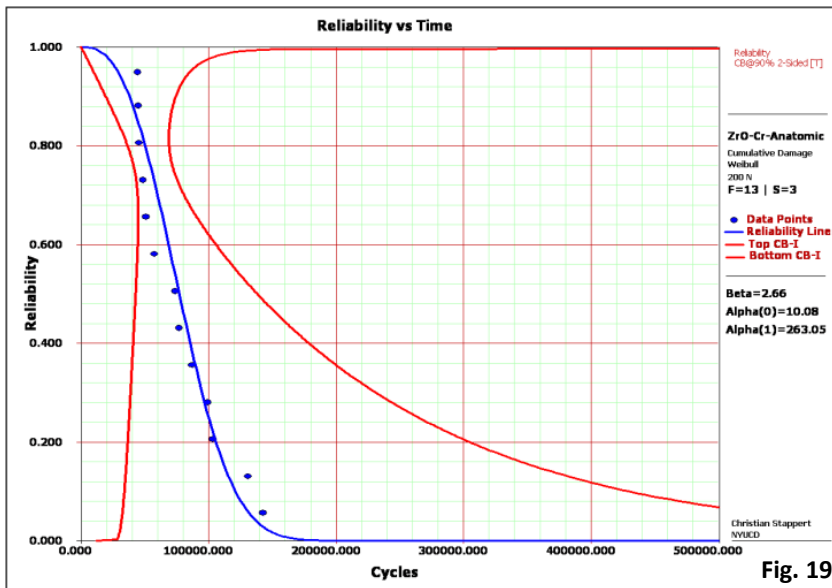
(Figure 20+21) Failed specimens from the single load to failure test under the stereomicroscope obtained from a palatal view (magnification: 1x). Fig.20 shows a representative specimen (group A) which failed from delamination in the interproximal area. Fig.21 shows exceptionally large chipping, including the incisal edge (group S). No bulk fracture or fracture of the zirconia die was observed.

11 REFERENCES

1. Piconi C, Maccauro G (1999) Zirconia as a ceramic biomaterial. Biomaterials 20(1):1-25

2. Anusavice KJ (1992) Degradability of dental ceramics. Adv Dent Res 6:82-9

3. Covacci V, Bruzzese N, Maccauro G, Andreassi C, Ricci GA, Piconi C (1999) In vitro evaluation of the mutagenic and carcinogenic power of high purity zirconia ceramic. Biomaterials 20(4):371-6

4. Mackert JR (1992) Side-effects of dental ceramics. Adv Dent Res 6:90-3

5. Kelly JR, Rose TC (1983) Nonprecious alloys for use in fixed prosthodontics: a literature review. J Prosthet Dent 49(3):363-70

6. Baricevic M, Mravak-Stipetic M, Stanimirovic A, Blanusa M, Kern J, Loncar B (2011) Salivary concentrations of nickel and chromium in patients with burning mouth syndrome. Acta Dermatovenerol Croat 19(1):2-5

7. Elshahawy WM, Watanabe I, Kramer P (2009) In vitro cytotoxicity evaluation of elemental ions released from different prosthodontic materials. Dent Mater 25(12):1551-5

8. Kelly JR (2004) Dental ceramics: current thinking and trends. Dent Clin North Am 48(2):viii, 513-30

9. Raptis NV, Michalakis KX, Hirayama H (2006) Optical behavior of current ceramic systems. Int J Periodontics Restorative Dent 26(1):31-41

10. Omar H, Atta O, El-Mowafy O (2008) Difference between selected and obtained shade for metal-ceramic crown systems. Oper Dent 33(5):502-7

11. Tan PL, Dunne JT (2004) An esthetic comparison of a metal ceramic crown and cast metal abutment with an all-ceramic crown and zirconia abutment: a clinical report. J Prosthet Dent 91(3):215-8

12. Seghi RR, Sorensen JA (1995) Relative flexural strength of six new ceramic materials. Int J Prosthodont 8(3):239-46

13. Seghi RR, Denry IL, Rosenstiel SF (1995) Relative fracture toughness and hardness of new dental ceramics. J Prosthet Dent 74(2):145-50

14. Morena R, Lockwood PE, Fairhurst CW (1986) Fracture toughness of commercial dental porcelains. Dent Mater 2(2):58-62

15. Zarone F, Russo S, Sorrentino R (2011) From porcelain-fused-to-metal to zirconia: clinical and experimental considerations. Dent Mater 27(1):83-96

16. Garvie RC, Hannink RH, Pascoe RT (1975) Ceramic steel? Nature 258(5537):703-04

17. Hannink RHJ, Kelly PM, Muddle BC (2000) Transformation Toughening in Zirconia-Containing Ceramics. J Am Ceram Soc 83(3):461-87

18. Aboushelib MN, Dozic A, Liem JK (2010) Influence of framework color and layering technique on the final color of zirconia veneered restorations. Quintessence Int 41(5):e84-9

19. Heffernan MJ, Aquilino SA, Diaz-Arnold AM, Haselton DR, Stanford CM, Vargas MA (2002) Relative translucency of six all-ceramic systems. Part I: core materials. J Prosthet Dent 88(1):4-9

20. Heffernan MJ, Aquilino SA, Diaz-Arnold AM, Haselton DR, Stanford CM, Vargas MA (2002) Relative translucency of six all-ceramic systems. Part II: core and veneer materials. J Prosthet Dent 88(1):10-5

21.   Sailer I, Pjetursson BE, Zwahlen M, Hammerle CH (2007) A systematic review of the survival and complication rates of all-ceramic and metal-ceramic reconstructions after an observation period of at least 3 years. Part II: Fixed dental prostheses. Clin Oral Implants Res 18 Suppl 3:86-96

22.   Christensen RP, Ploeger BJ (2010) A Clinical Comparison of Zirconia, Metal and Alumina Fixed-Prosthesis Frameworks Veneered With Layered or Pressed Ceramic. J Am Dent Assoc 141(11):1317-29

23.   Wolfart S, Eschbach S, Scherrer S, Kern M (2009) Clinical outcome of three-unit lithium-disilicate glass-ceramic fixed dental prostheses: up to 8 years results. Dent Mater 25(9):e63-71

24.   Vult von Steyern P (2005) All-ceramic fixed partial dentures. Studies on aluminum oxide- and zirconium dioxide-based ceramic systems. Swed Dent J Suppl 173:1-69

25.   Beuer F, Edelhoff D, Gernet W, Sorensen JA (2009) Three-year clinical prospective evaluation of zirconia-based posterior fixed dental prostheses (FDPs). Clin Oral Investig 13(4):445-51

26.   Ohlmann B, Rammelsberg P, Schmitter M, Schwarz S, Gabbert O (2008) All-ceramic inlay-retained fixed partial dentures: preliminary results from a clinical study. J Dent 36(9):692-6

27.   Larsson C, Vult von Steyern P (2010) Five-year follow-up of implant-supported Y-TZP and ZTA fixed dental prostheses. A randomized, prospective clinical trial comparing two different material systems. Int J Prosthodont 23(6):555-61

28.   Larsson C, Vult von Steyern P, Sunzel B, Nilner K (2006) All-ceramic two- to five-unit implant-supported reconstructions. A randomized, prospective clinical trial. Swed Dent J 30(2):45-53

29.   Kollar A, Huber S, Mericske E, Mericske-Stern R (2008) Zirconia for teeth and implants: a case series. Int J Periodontics Restorative Dent 28(5):479-87

30.   Raigrodski AJ, Chiche GJ, Potiket N, Hochstedler JL, Mohamed SE, Billiot S, et al (2006) The efficacy of posterior three-unit zirconium-oxide-based ceramic fixed partial dental prostheses: a prospective clinical pilot study. J Prosthet Dent 96(4):237-44

31.   Vult von Steyern P, Carlson P, Nilner K (2005) All-ceramic fixed partial dentures designed according to the DC-Zirkon technique. A 2-year clinical study. J Oral Rehabil 32(3):180-7

32.   Tinschert J, Schulze KA, Natt G, Latzke P, Heussen N, Spiekermann H (2008) Clinical behavior of zirconia-based fixed partial dentures made of DC-Zirkon: 3-year results. Int J Prosthodont 21(3):217-22

33.   Sailer I, Feher A, Filser F, Gauckler LJ, Luthy H, Hammerle CH (2007) Five-year clinical results of zirconia frameworks for posterior fixed partial dentures. Int J Prosthodont 20(4):383-8

34.   Sailer I, Gottnerb J, Kanelb S, Hammerle CH (2009) Randomized controlled clinical trial of zirconia-ceramic and metal-ceramic posterior fixed dental prostheses: a 3-year follow-up. Int J Prosthodont 22(6):553-60

35.   Molin MK, Karlsson SL (2008) Five-year clinical prospective evaluation of zirconia-based Denzir 3-unit FPDs. Int J Prosthodont 21(3):223-7

36.   Swain MV (2009) Unstable cracking (chipping) of veneering porcelain on all-ceramic dental crowns and fixed partial dentures. Acta Biomater 5(5):1668-77

37. Denry I, Kelly JR (2008) State of the art of zirconia for dental applications. Dent Mater 24(3):299-307

38. Fischer J, Stawarczyk B, Tomic M, Strub JR, Hammerle CH (2007) Effect of thermal misfit between different veneering ceramics and zirconia frameworks on in vitro fracture load of single crowns. Dent Mater 26(6):766-72

39. Sundh A, Sjogren G (2004) A comparison of fracture strength of yttrium-oxide- partially-stabilized zirconia ceramic crowns with varying core thickness, shapes and veneer ceramics. J Oral Rehabil 31(7):682-8

40. Wakabayashi N, Anusavice KJ (2000) Crack initiation modes in bilayered alumina/porcelain disks as a function of core/veneer thickness ratio and supporting substrate stiffness. J Dent Res 79(6):1398-404

41. Proos KA, Swain MV, Ironside J, Steven GP (2003) Influence of core thickness on a restored crown of a first premolar using finite element analysis. Int J Prosthodont 16(5):474-80

42. Kokubo Y, Tsumita M, Kano T, Fukushima S (2011) The influence of zirconia coping designs on the fracture load of all-ceramic molar crowns. Dent Mater 30(3):281-5

43. Rosentritt M, Steiger D, Behr M, Handel G, Kolbeck C (2009) Influence of substructure design and spacer settings on the in vitro performance of molar zirconia crowns. J Dent 37(12):978-83

44. Larsson C, Madhoun SE, Wennerberg A, Vult von Steyern P (2012) Fracture strength of yttria-stabilized tetragonal zirconia polycrystals crowns with different design: an in vitro study. Clin Oral Implants Res 23(7):820-6

45. Kingery WD, Bowen HK, Uhlmann DR (1976) Introduction to Ceramics. John Wiley & Sons, New York, NY, USA

46. Giordano R, McLaren EA (2010) Ceramics overview: classification by microstructure and processing methods. Compend Contin Educ Dent 31(9):682-4, 86, 88 passim; quiz 98, 700

47. Kelly JR (2008) Dental ceramics: what is this stuff anyway? J Am Dent Assoc 139Suppl: 4S-7S

48. Park S, Quinn JB, Romberg E, Arola D (2008) On the brittleness of enamel and selected dental materials. Dent Mater 24(11):1477-85

49. Hurlbut CS, Klein C (1985) Manual of Mineralogy. 20 ed John Wiley & Sons, New York, NY, USA

50. Knight CTG, Balec RJ, Kinrade SD (2007) The structure of silicate anions in aqueous alkaline solutions. Angew Chem Int Ed 46(43):8148-52

51. Chaudhuri SP (1982) Crystallization of glass of the system $K_2O(Na_2O)$---Al_2O_3---SiO_2. Ceram Int 8(1):27-33

52. Cattell MJ, Chadwick TC, Knowles JC, Clarke RL, Samarawickrama DY (2006) The nucleation and crystallization of fine grained leucite glass-ceramics for dental applications. Dent Mater 22(10):925-33

53. Stookey SD (1959) Catalyzed crystallisation of glass in theory and practice. Ind Eng Chem 51(7):805–808

54. Denry IL, Holloway JA, Rosenstiel SF (1998) Crystallization kinetics of a low-expansion feldspar glass for dental applications. J Biomed Mater Res 41(3):398-404

55. Mackert JR, Evans AL (1991) Effect of cooling rate on leucite volume fraction in dental porcelains. J Dent Res 70(2):137-9

56. Mackert JR, Evans AL (1991) Quantitative X-Ray-Diffraction Determination of Leucite Thermal-Instability in Dental Porcelain. J Am Ceram Soc 74(2):450-53

57. Morena R, Lockwood PE, Mackert JR, Fairhurst CW (1984) Fracture-Toughness and Crack-Microstructure Interaction of a Dental Porcelain. J Dent Res 63:234-34

58. Beall GH, Duke DA (1969) Transparent Glass-Ceramics. J Mater Sci 4:340-52

59. Mackert JR, Butts MB, Fairhurst CW (1986) The Effect of the Leucite Transformation on Dental Porcelain Expansion. Dent Mater 2(1):32-36

60. Weinstein LK, Weinstein AB., inventor; Weinstein LK.,Weinstein AB., assignee (1962) Fused porcelain-to-metal teeth

61. Shareef MY, Noort R, Messer PF, Piddock V (1994) The effect of microstructural features on the biaxial flexural strength of leucite reinforced glass-ceramics. J Mater Sci Mater Med 5(2):113-18

62. Cattell MJ, Chadwick TC, Knowles JC, Clarke RL, Lynch E (2001) Flexural strength optimisation of a leucite reinforced glass ceramic. Dent Mater 17(1):21-33

63. Mackert JR, Jr., Twiggs SW, Russell CM, Williams AL (2001) Evidence of a critical leucite particle size for microcracking in dental porcelains. J Dent Res 80(6):1574-9

64. Wyckoff RWG (1960) Crystal structures. 5 ed Interscience Publishers, New York, NY, USA

65. Cattell MJ, Chadwick TC, Knowles JC, Clarke RL (2005) The crystallization of an aluminosilicate glass in the K2O-Al2O3-SiO2 system. Dent Mater 21(9):811-22

66. Ban S, Matsuo K, Iwase H, Kaikawa K, Hasegawa J (1999) Lattice parameter changes of leucite by incorporation of various cations substituted for potassium. Dent Mater 18(4):385-94

67. Kon M, Kawano F, Asaoka K, Matsumoto N (1994) Effect of leucite crystals on the strength of glassy porcelain. Dent Mater 13(2):138-47

68. Hermansson L, Carlsson R (1978) On the crystallization of the glassy phase in whitewares. Trans J Brit Ceram Soc 77(2):32-35

69. Mackert JR, Butts MB, Morena R, Fairhurst CW (1986) Phase Changes in a Leucite-Containing Dental Porcelain Frit. J Am Ceram Soc 69(4):C-69-C-72

70. Taylor D, Henderson CM (1968) Thermal expansion of leucite group of minerals. Am Mineral 53(9-10):1476

71. Fischer J, Kappert H (2011) Keramik als zahnärztlicher Werkstoff. In: Strub JR, editor. Curriculum Prothetik Band II. Quintessenz Verlag, Berlin, Germany, p. 485-501

72. Denry IL (1996) Recent advances in ceramics for dentistry. Crit Rev Oral Biol Med 7(2):134-43

73. Mackert JR (1988) Effect of thermally induced changes on porcelain-metal compatibility. In: Preston JD, editor. Perspectives in Dental Ceramics, Proceedings of the Fourth International Symposium on Ceramics. Quintessence Publishing, Chicago, IL,USA, p. 53-64

74. Davidge RW, Green TJ (1968) The strength of two-phase ceramic/glass materials. J Mater Sci 3(6):629-34

75. Primus CM, Chu CC, Shelby JE, Buldrini E, Heckle CE (2002) Opalescence of dental porcelain enamels. Quintessence Int 33(6):439-49

76. Yen T-W, Blackman RB, Baez RJ (1993) Effect of acid etching on the flexural strength of a feldspathic porcelain and a castable glass ceramic. J Prosthet Dent 70(3):224-33

77. Della Bona A, van Noort R (1998) Ceramic surface preparations for resin bonding. Am J Dent 11(6):276-80

78. Della Bona A, Anusavice KJ (2002) Microstructure, composition, and etching topography of dental ceramics. Int J Prosthodont 15(2):159-67

79. Höland W, Rheinberger V, Apel E, van't Hoen C (2007) Principles and phenomena of bio-engineering with glass-ceramics for dental restoration. J Eur Ceram Soc 27(2-3):1521-26

80. Höland W, Beall G (2002) Glass-ceramic technology. 1 ed American Ceramic Society, Westerville, OH, USA

81. Denry I, Holloway J (2010) Ceramics for Dental Applications: A Review. Materials 3(1):351-68

82. Borom MP, Turkalo AM, Doremus RH (1975) Strength and Microstructure in Lithium Disilicate Glass-Ceramics. J Am Ceram Soc 58(9-10):385-91

83. Culp L, McLaren EA (2010) Lithium disilicate: the restorative material of multiple options. Compend Contin Educ Dent 31(9):716-20, 22, 24-5

84. Höland W, Apel E, van t Hoen C, Rheinberger V (2006) Studies of crystal phase formations in high-strength lithium disilicate glass-ceramics. J Non-Cryst Solids 352(38-39):4041-50

85. Deubener J, Brückner R, Sternitzke M (1993) Induction time analysis of nucleation and crystal growth in di- and metasilicate glasses. J Non-Cryst Solids 163(1):1-12

86. Zanotto ED (1997) Metastable phases in lithium disilicate glasses. J Non-Cryst Solids 219:42-48

87. Höland W, Rheinberger V, Frank M (1999) Mechanisms of nucleation and controlled crystallization of needle-like apatite in glass-ceramics of the SiO2-Al2O3-K2O-CaO-P2O5 system. J Non-Cryst Solids 253(1-3):170-77

88. Thompson JY, Anusavice KJ, Balasubramaniam B, Mecholsky JJ (1995) Effect of Microcracking on the Fracture Toughness and Fracture Surface Fractal Dimension of Lithia-Based Glass-Ceramics. J Am Ceram Soc 78(11):3045-49

89. Höland W, Schweiger M, Frank M, Rheinberger V (2000) A comparison of the microstructure and properties of the IPS Empress®2 and the IPS Empress® glass-ceramics. J Biomed Mater Res 53(4):297-303

90. Luo XP, Silikas N, Allaf M, Wilson NHF, Watts DC (2001) AFM and SEM study of the effects of etching on IPS-Empress 2TM dental ceramic. Surf Sci 491(3):388-94

91. IPS e.max Ceram - Scientific Documentation (2011) www.ivoclarvivadent.us. Schaan, Liechtenstein: Ivoclar Vivadent AG

92. IPS e.max ZirPress - Scientific Documentation (2005) www.ivoclarvivadent.com. Schaan, Liechtenstein: Ivoclar Vivadent AG

93. Corfu F, Hanchar JM, Hoskin PWO, Kinny P (2003) Atlas of Zircon Textures. Rev Mineral Geochem 53(1):469-500

94. Hornberger H, Marquis PM (1995) Mechanical properties and microstructure of in-Ceram, a ceramic-glass composite for dental crowns. Glas Sci Technol 68(6):188-94

95. Probster L, Diehl J (1992) Slip-casting alumina ceramics for crown and bridge restorations. Quintessence Int 23(1):25-31

96. Sadoun M (1989) Slip Cast Alumina Ceramics. Paper presented at: GC International Conference on Dental Ceramics; September 13; Leeds Castle, England.

97. Clarke DR (1992) Interpenetrating Phase Composites. J Am Ceram Soc 75(4):739-58

98. Xiao-ping L, Jie-mo T, Yun-long Z, Ling W (2002) Strength and fracture toughness of MgO-modified glass infiltrated alumina for CAD/CAM. Dent Mater 18(3):216-20

99. Kelly JR, Nishimura I, Campbell SD (1996) Ceramics in dentistry: historical roots and current perspectives. J Prosthet Dent 75(1):18-32

100. Wolf WD, Vaidya KJ, Francis LF (1996) Mechanical Properties and Failure Analysis of Alumina-Glass Dental Composites. J Am Ceram Soc 79(7):1769-76

101. Guazzato M, Albakry M, Ringer SP, Swain MV (2004) Strength, fracture toughness and microstructure of a selection of all-ceramic materials. Part I. Pressable and alumina glass-infiltrated ceramics. Dent Mater 20(5):441-48

102. van Dijken JW (1999) All-ceramic restorations: classification and clinical evaluations. Compend Contin Educ Dent 20(12):1115-24, 26 passim; quiz 36

103. Cales B (2000) Zirconia as a sliding material: histologic, laboratory, and clinical data. Clin Orthop Relat Res 379:94-112

104. Drouin JM, Cales B, Chevalier J, Fantozzi G (1997) Fatigue behavior of zirconia hip joint heads: experimental results and finite element analysis. J Biomed Mater Res 34(2):149-55

105. Ruff O, Ebert F, Stephan E (1929) Beiträge zur Keramik hochfeuerfester Stoffe II. Das System $ZrO2$ - CaO. Z Anorg Allg Chem 180(1):215-24

106. Evans AG (1990) Perspective on the Development of High-Toughness Ceramics. J Am Ceram Soc 73(2):187-206

107. Kelly JR, Denry I (2008) Stabilized zirconia as a structural ceramic: An overview. Dent Mater 24(3):289-98

108. Kisi EH, Howard CJ (1998) Crystal structures of zirconia phases and their interrelation. Key Eng Mater 153-154:1-36

109. Garvie RC, Nicholson PS (1972) Phase Analysis in Zirconia Systems. J Am Ceram Soc 55(6):303-05

110. Subbarao EC (1981) Zirconia-an overview. In: Heuer AH, Hobbs LW, editors. Advances in Ceramics, Science and Technology of Zirconia. The American Ceramic Society, Columbus , OH, USA, p. 1-24

111. Bansal GK, Heuer AH (1972) On a martensitic phase transformation in zirconia ($ZrO2$)--I. Metallographic evidence. Acta Metall 20(11):1281-89

112. Bansal GK, Heuer AH (1974) On a martensitic phase transformation in zirconia ($ZrO2$)--II. Crystallographic aspects. Acta Metall 22(4):409-17

113. Goff JP, Hayes W, Hull S, Hutchings MT, Clausen KN (1999) Defect structure of yttria-stabilized zirconia and its influence on the ionic conductivity at elevated temperatures. Phys Rev B 59(22):14202

114. Garvie RC, Nicholson PS (1972) Structure and Thermomechanical Properties of Partially Stabilized Zirconia in the $CaO-ZrO2$ System. J Am Ceram Soc 55(3):152-57

115. Conrad HJ, Seong WJ, Pesun IJ (2007) Current ceramic materials and systems with clinical recommendations: a systematic review. J Prosthet Dent 98(5):389-404

116. Porter DL, Heuer AH (1977) Mechanisms of Toughening Partially Stabilized Zirconia (PSZ). J Am Ceram Soc 60(3-4):183-84

117. Heuer AH, Lange FF, Swain MV, Evans AG (1986) Transformation Toughening: An Overview. J Am Ceram Soc 69(3):i-iv

118. Christel P, Meunier A, Heller M, Torre JP, Peille CN (1989) Mechanical properties and short-term in-vivo evaluation of yttrium-oxide-partially-stabilized zirconia. J Biomed Mater Res 23(1):45-61

119. Evans AG, Cannon RM (1986) Overview no. 48: Toughening of brittle solids by martensitic transformations. Acta Metall 34(5):761-800

120. Evans AG, Heuer AH (1980) Review - Transformation Toughening in Ceramics: Martensitic Transformations in Crack-Tip Stress Fields. J Am Ceram Soc 63(5-6):241-48

121. Reed JS, Lejus A-M (1977) Affect of grinding and polishing on near-surface phase transformations in zirconia. Mater Res Bull 12(10):949-54

122. Guazzato M, Albakry M, Quach L, Swain MV (2004) Influence of grinding, sandblasting, polishing and heat treatment on the flexural strength of a glass-infiltrated alumina-reinforced dental ceramic. Biomaterials 25(11):2153-60

123. Lange FF (1982) Transformation toughening. J Mater Sci 17(1):247-54

124. Heuer AH (1987) Transformation Toughening in ZrO2-Containing Ceramics. J Am Ceram Soc 70(10):689-98

125. Fabris S, Paxton AT, Finnis MW (2002) A stabilization mechanism of zirconia based on oxygen vacancies only. Acta Mater 50(20):5171-78

126. Gupta TK, Bechtold JH, Kuznicki RC, Cadoff LH, Rossing BR (1977) Stabilization of tetragonal phase in polycrystalline zirconia. J Mater Sci 12(12):2421-26

127. Rieth PH, Reed JS, Naumann AW (1976) Fabrication and flexural strength of ultra-fine grained yttria-stabilized zirconia. Am Ceram Soc Bull 55:717

128. Guazzato M, Albakry M, Ringer SP, Swain MV (2004) Strength, fracture toughness and microstructure of a selection of all-ceramic materials. Part II. Zirconia-based dental ceramics. Dent Mater 20(5):449-56

129. Theunissen GSAM, Bouma JS, Winnubst AJA, Burggraaf AJ (1992) Mechanical properties of ultra-fine grained zirconia ceramics. J Mater Sci 27(16):4429-38

130. Bravo-Leon A, Morikawa Y, Kawahara M, Mayo MJ (2002) Fracture toughness of nanocrystalline tetragonal zirconia with low yttria content. Acta Mater 50(18):4555-62

131. Heuer AH, Claussen N, Kriven WM, Ruhle M (1982) Stability of Tetragonal ZrO2 Particles in Ceramic Matrices. J Am Ceram Soc 65(12):642-50

132. Chevalier J (2006) What future for zirconia as a biomaterial? Biomaterials 27(4):535-43

133. Chevalier J, Gremillard L, Virkar AV, Clarke DR (2009) The Tetragonal-Monoclinic Transformation in Zirconia: Lessons Learned and Future Trends. J Am Ceram Soc 92(9):1901-20

134. Coble RL (1961) Sintering Crystalline Solids. I. Intermediate and Final State Diffusion Models. J Appl Phys 32(5):787-92

135. Coble RL (1961) Sintering Crystalline Solids. II. Experimental Test of Diffusion Models in Powder Compacts. J Appl Phys 32(5):793-99

136. Meyer JM, O'Brien WJ, Yu CU (1976) Sintering of Dental Porcelain Enamels. J Dent Res 55(4):696-99

137. Claus H (1989) The structure and microstructure of dental porcelain in relationship to the firing conditions. Int J Prosthodont 2(4):376-84

138. Rice RW (1996) Grain size and porosity dependence of ceramic fracture energy and toughness at 22 °C. J Mater Sci 31(8):1969-83

139. Jones DW, Wilson HJ (1975) Porosity in dental ceramics. Br Dent J 138(1):16-21

140. Cheung KC, Darvell BW (2002) Sintering of dental porcelain: effect of time and temperature on appearance and porosity. Dent Mater 18(2):163-73

141. Wohlwend A, Strub JR (1990) Metal ceramic and full ceramic restorations (2). Quintessenz 41(7):1161-75

142. Albakry M, Guazzato M, Swain MV (2004) Influence of hot pressing on the microstructure and fracture toughness of two pressable dental glass-ceramics. J Biomed Mater Res B Appl Biomater 71(1):99-107

143. Dong JK, Luthy H, Wohlwend A, Scharer P (1992) Heat-pressed ceramics: technology and strength. Int J Prosthodont 5(1):9-16

144. Oh SC, Dong JK, Luthy H, Scharer P (2000) Strength and microstructure of IPS Empress 2 glass-ceramic after different treatments. Int J Prosthodont 13(6):468-72

145. Giordano R (1999) A comparison of all-ceramic restorative systems, Part 1. Gen Dent 47(6):566-70

146. Cattell MJ, Knowles JC, Clarke RL, Lynch E (1999) The biaxial flexural strength of two pressable ceramic systems. J Dent 27(3):183-96

147. Mackert JR, Jr., Williams AL (1996) Microcracks in dental porcelain and their behavior during multiple firing. J Dent Res 75(7):1484-90

148. Eidenbenz S, Lehner CR, Scharer P (1994) Copy milling ceramic inlays from resin analogs: a practicable approach with the CELAY system. Int J Prosthodont 7(2):134-42

149. Tinschert J, Zwez D, Marx R, Anusavice KJ (2000) Structural reliability of alumina-, feldspar-, leucite-, mica- and zirconia-based ceramics. J Dent 28(7):529-35

150. Beuer F, Schweiger J, Eichberger M, Kappert HF, Gernet W, Edelhoff D (2009) High-strength CAD/CAM-fabricated veneering material sintered to zirconia copings--a new fabrication mode for all-ceramic restorations. Dent Mater 25(1):121-8

151. Beuer F, Schweiger J, Edelhoff D (2008) Digital dentistry: an overview of recent developments for CAD/CAM generated restorations. Br Dent J 204(9):505-11

152. Strub JR, Rekow ED, Witkowski S (2006) Computer-aided design and fabrication of dental restorations: Current systems and future possibilities. J Am Dent Assoc 137(9):1289-96

153. Witkowski S (2005) (CAD)/CAM in Dental Technology. Quintessence Dent Technol 28:169-84

154. Duret F (1988) Computers in dentistry. Part two. Francois Duret--a man with vision. J Can Dent Assoc 54(9):664

155. Duret F, Blouin JL, Duret B (1988) CAD-CAM in dentistry. J Am Dent Assoc 117(6):715-20

156. Filser F (2001) Direct ceramic machining of ceramic dental restorations [PhD]. Zürich, Switzerland: ETH Zürich

157. Filser F, Kocher P, Gauckler LJ (2003) Net-shaping of ceramic components by direct ceramic machining. Assembly Autom 23(4):382-90

158. Grossman DG (1972) Machinable Glass-Ceramics Based on Tetrasilicic Mica. J Am Ceram Soc 55(9):446-49

159. Tinschert J, Natt G, Hassenpflug S, Spiekermann H (2004) Status of current CAD/CAM technology in dental medicine. Int J Comput Dent 7(1):25-45

160. Luthardt RG, Holzhüter MS, Rudolph H, Herold V, Walter MH (2004) CAD/CAM-machining effects on Y-TZP zirconia. Dent Mater 20(7):655-62

161. Denry IL, Holloway JA, Tarr LA (1999) Effect of heat treatment on microcrack healing behavior of a machinable dental ceramic. J Biomed Mater Res 48(6):791-6

162. Sundh A, Molin M, Sjogren G (2005) Fracture resistance of yttrium oxide partially-stabilized zirconia all-ceramic bridges after veneering and mechanical fatigue testing. Dent Mater 21(5):476-82

163. Manicone PF, Rossi Iommetti P, Raffaelli L (2007) An overview of zirconia ceramics: basic properties and clinical applications. J Dent 35(11):819-26

164. Yin L, Huang H (2004) Ceramic Response to High Speed Grinding. Mach Sci Technol 8(1):21-37

165. Blue DS, Griggs JA, Woody RD, Miller BH (2003) Effects of bur abrasive particle size and abutment composition on preparation of ceramic implant abutments. J Prosthet Dent 90(3):247-54

166. Kosmac T, Oblak C, Jevnikar P, Funduk N, Marion L (1999) The effect of surface grinding and sandblasting on flexural strength and reliability of Y-TZP zirconia ceramic. Dent Mater 15(6):426-33

167. Piwowarczyk A, Ottl P, Lauer HC, Kuretzky T (2005) A clinical report and overview of scientific studies and clinical procedures conducted on the 3M ESPE Lava All-Ceramic System. J Prosthodont 14(1):39-45

168. Komine F, Gerds T, Witkowski S, Strub JR (2005) Influence of framework configuration on the marginal adaptation of zirconium dioxide ceramic anterior four-unit frameworks. Acta Odontol Scand 63(6):361-66

169. Raigrodski AJ (2003) Clinical and laboratory considerations for the use of CAD/CAM Y-TZP-based restorations. Pract Proced Aesthet Dent 15(6):469-76; quiz 77

170. Matsui K, Horikoshi H, Ohmichi N, Ohgai M, Yoshida H, Ikuhara Y (2003) Cubic-Formation and Grain-Growth Mechanisms in Tetragonal Zirconia Polycrystal. J Am Ceram Soc 86(8):1401-08

171. Chevalier JJ, Deville S, Münch E, Jullian R, Lair F (2004) Critical effect of cubic phase on aging in 3 mol% yttria-stabilized zirconia ceramics for hip replacement prosthesis. Biomaterials 25(24):5539-45

172. Luthardt RG, Holzhuter M, Sandkuhl O, Herold V, Schnapp JD, Kuhlisch E, et al (2002) Reliability and properties of ground Y-TZP-zirconia ceramics. J Dent Res 81(7):487-91

173. Suttor DS, Hauptmann H, Schnagl R, Frank S, inventor; 3M ESPE AG (Seefeld, DE), assignee (2004) Coloring ceramics by way of ionic or complex-containing solutions.

174. Tinschert J, Natt G, Mautsch W, Spiekermann H, Anusavice KJ (2001) Marginal fit of alumina-and zirconia-based fixed partial dentures produced by a CAD/CAM system. Oper Dent 26(4):367-74

175. Bindl A, Mormann WH (2005) Marginal and internal fit of all-ceramic CAD/CAM crown-copings on chamfer preparations. J Oral Rehabil 32(6):441-7

176. Andersson M, Odén A (1993) A new all-ceramic crown: A dense-sintered, high-purity alumina coping with porcelain. Acta Odontol Scand 51(1):59-64

177. Haag P, Andersson M, Steyern P, Odén A (2004) 15 years of clincal experience with Procera alumina. A review. Appl Osseointegration Res 4:7-12

178. Stappert CF, Baldassarri M, Zhang Y, Hanssler F, Rekow ED, Thompson VP (2012) Reliability and fatigue failure modes of implant-supported aluminum-oxide fixed dental prostheses. Clin Oral Implants Res 23(10):1173-80

179. Rinke S, Hüls A (1996) Copy-milled aluminous core ceramic crowns: A clinical report. J Prosthet Dent 76(4):343-46

180. Rinke S, Margraf G, Jahn L, Hüls A (1994) Qualitätsbeurteilung von kopiergefrästen vollkeramischen Kronengerüsten (Celay/In-Ceram). Schweiz Monatsschr Zahnmed 104(12):1495-99

181. McLean JW (1991) The science and art of dental ceramics. Oper Dent 16(4):149-56

182. Brodbelt RH, O'Brien WJ, Fan PL, Frazer-Dib JG, Yu R (1981) Translucency of human dental enamel. J Dent Res 60(10):1749-53

183. Antonson SA, Anusavice KJ (2001) Contrast ratio of veneering and core ceramics as a function of thickness. Int J Prosthodont 14(4):316-20

184. Dozic A, Tsagkari M, Khashayar G, Aboushelib M (2010) Color management of porcelain veneers: influence of dentin and resin cement colors. Quintessence Int 41(7):567-73

185. Paul SJ, Pliska P, Pietrobon N, Scharer P (1996) Light transmission of composite luting resins. Int J Periodontics Restorative Dent 16(2):164-73

186. Touati B, Miara P (1993) Light transmission in bonded ceramic restorations. J Esthet Dent 5(1):11-8

187. Anusavice KJ, Zhang N-Z (1997) Chemical durability of Dicor and lithia-based glass-ceramics. Dent Mater 13(1):13-19

188. Kirkpatrick JJR, Enion DS, Burd DAR (1995) Hydrofluoric acid burns: a review. Burns 21(7):483-93

189. Chaiyabutr Y, McGowan S, Phillips KM, Kois JC, Giordano RA (2008) The effect of hydrofluoric acid surface treatment and bond strength of a zirconia veneering ceramic. J Prosthet Dent 100(3):194-202

190. Meng XF, Yoshida K, Gu N (2010) Chemical adhesion rather than mechanical retention enhances resin bond durability of a dental glass-ceramic with leucite crystallites. Biomed Mater 5(4):044101

191. Benetti P, Della Bona A, Kelly JR (2010) Evaluation of thermal compatibility between core and veneer dental ceramics using shear bond strength test and contact angle measurement. Dent Mater 26(8):743-50

192. Dorsch P (1986) Harmony of ceramic and alloy. Comparison of thermal behavior. Dent Lab (Munch) 34(9):1343-8

193. Bonfante EA, Coelho PG, Guess PC, Thompson VP, Silva NR (2010) Fatigue and damage accumulation of veneer porcelain pressed on Y-TZP. J Dent 38(4):318-24

194. Griffith AA (1921) The Phenomena of Rupture and Flow in Solids. Philosophical Transactions of the Royal Society of London. Series A, Containing Papers of a Mathematical or Physical Character 221:163-98

195. Gonzaga CC, Cesar PF, Miranda WG, Jr., Yoshimura HN (2011) Slow crack growth and reliability of dental ceramics. Dent Mater 27(4):394-406

196. Wiederhorn SM (1968) Moisture assisted crack growth in ceramics. Int J Fract 4(2):171-77

197. Rekow ED, Harsono M, Janal M, Thompson VP, Zhang G (2006) Factorial analysis of variables influencing stress in all-ceramic crowns. Dent Mater 22(2):125-32

198. Giannakopoulos AE, Larsson PL, Vestergaard R (1994) Analysis of Vickers indentation. Int J Solids Struct 31(19):2679-708

199. Vander Voort GF, Lucas GM (1998) Microindentation hardness testing. Adv Mater Process 154(3):21-2+

200. Quinn J, Quinn G (1997) Indentation brittleness of ceramics: a fresh approach. J Mater Sci 32(16):4331-46

201. Fischer H, Marx R (2000) Festigkeit von Dentalkeramik. ZWR 109(5):240-44

202. Kelly JR (1995) Perspectives on strength. Dent Mater 11(2):103-10

203. Schwickerath H (1986) Dauerfestigkeit von Keramik. Dtsch zahnarztl Z 41:264-66

204. ISO 6872 (2008) Dentistry - Ceramic materials. Geneva, Switzerland: International Organisation for Standardisation

205. ISO 9693 (1999) Dentistry - Metal-ceramic dental restorative systems. Geneva, Switzerland: International Organisation for Standardisation

206. Weibull W (1951) Statistical distribution function of wide applicability. J Appl Mech 18:293-7

207. Quinn JB, Quinn GD (2010) A practical and systematic review of Weibull statistics for reporting strengths of dental materials. Dent Mater 26(2):135-47

208. Guazzato M, Quach L, Albakry M, Swain MV (2005) Influence of surface and heat treatments on the flexural strength of Y-TZP dental ceramic. J Dent 33(1):9-18

209. IPS e.max CAD - Scientific Documentation (2005) www.ivoclarvivadent.us. Schaan, Liechtenstein: Ivoclar Vivadent AG

210. Guess PC, Schultheis S, Bonfante EA, Coelho PG, Ferencz JL, Silva NR (2011) All-ceramic systems: laboratory and clinical performance. Dent Clin North Am 55(2):333-52, ix

211. Şakar-Deliormanli A, Güden M (2006) Microhardness and fracture toughness of dental materials by indentation method. J Biomed Mater Res B Appl Biomater 76B(2):257-64

212. Lawn BR, Deng Y, Miranda P, Pajares A, Chai H, Kim DK (2002) Overview: Damage in brittle layer structures from concentrated loads. J Mater Res 17:3019-36

213. Hengchang X, Wenyi L, Tong W (1989) Measurement of thermal expansion coefficient of human teeth. Aust Dent J 34(6):530-35

214. Sano H, Ciucchi B, Matthews WG, Pashley DH (1994) Tensile properties of mineralized and demineralized human and bovine dentin. J Dent Res 73(6):1205-11

215. Wataha JC, Messer RL (2004) Casting alloys. Dent Clin North Am 48(2):vii-viii, 499-512

216. IPS e.max Press - Scientific documentation (2009) www.ivoclarvivadent.us. Schaan, Liechtenstein: Ivoclar Vivadent AG

217. Pjetursson BE, Sailer I, Zwahlen M, Hammerle CH (2007) A systematic review of the survival and complication rates of all-ceramic and metal-ceramic reconstructions after an observation period of at least 3 years. Part I: Single crowns. Clin Oral Implants Res 18 Suppl 3:73-85

218. Odman P, Andersson B (2001) Procera AllCeram crowns followed for 5 to 10.5 years: a prospective clinical study. Int J Prosthodont 14(6):504-9

219. Fradeani M, Redemagni M (2002) An 11-year clinical evaluation of leucite-reinforced glass-ceramic crowns: a retrospective study. Quintessence Int 33(7):503-10

220. Ortorp A, Kihl ML, Carlsson GE (2012) A 5-year retrospective study of survival of zirconia single crowns fitted in a private clinical setting. J Dent 40(6):527-30

221. Cehreli MC, Kokat AM, Akca K (2009) CAD/CAM Zirconia vs. slip-cast glass-infiltrated Alumina/Zirconia all-ceramic crowns: 2-year results of a randomized controlled clinical trial. J Appl Oral Sci. 17(1):49-55

222. Groten M, Huttig F (2010) The performance of zirconium dioxide crowns: a clinical follow-up. Int J Prosthodont 23(5):429-31

223. Ortorp A, Kihl ML, Carlsson GE (2009) A 3-year retrospective and clinical follow-up study of zirconia single crowns performed in a private practice. J Dent 37(9):731-6

224. Bonfante EA, da Silva NR, Coelho PG, Bayardo-Gonzalez DE, Thompson VP, Bonfante G (2009) Effect of framework design on crown failure. Eur J Oral Sci 117(2):194-9

225. Lorenzoni FC, Martins LM, Silva NR, Coelho PG, Guess PC, Bonfante EA, et al (2010) Fatigue life and failure modes of crowns systems with a modified framework design. J Dent 38(8):626-34

226. Silva NR, Bonfante EA, Rafferty BT, Zavanelli RA, Rekow ED, Thompson VP, et al (2011) Modified Y-TZP core design improves all-ceramic crown reliability. J Dent Res 90(1):104-8

227. Pogoncheff CM, Duff RE (2010) Use of zirconia collar to prevent interproximal porcelain fracture: a clinical report. J Prosthet Dent 104(2):77-9

228. Marchack BW, Futatsuki Y, Marchack CB, White SN (2008) Customization of milled zirconia copings for all-ceramic crowns: a clinical report. J Prosthet Dent 99(3):169-73

229. Tsalouchou E, Cattell MJ, Knowles JC, Pittayachawan P, McDonald A (2008) Fatigue and fracture properties of yttria partially stabilized zirconia crown systems. Dent Mater 24(3):308-18

230. Guess PC, Zhang Y, Thompson VP (2009) Effect of veneering techniques on damage and reliability of Y-TZP trilayers. Eur J Esthet Dent 4(3):262-76

231. Baldassarri M, Zhang Y, Thompson VP, Rekow ED, Stappert CFJ (2011) Reliability and failure modes of implant-supported zirconium-oxide fixed dental prostheses related to veneering techniques. J Dent 39(7):489-98

232. Wolfart S, Harder S, Eschbach S, Lehmann F, Kern M (2009) Four-year clinical results of fixed dental prostheses with zirconia substructures (Cercon): end abutments vs. cantilever design. Eur J Oral Sci 117(6):741-9

233. Guazzato M, Walton TR, Franklin W, Davis G, Bohl C, Klineberg I (2010) Influence of thickness and cooling rate on development of spontaneous cracks in porcelain/zirconia structures. Aust Dent J 55(3):306-10

234. Hickel R, Roulet JF, Bayne S, Heintze SD, Mjor IA, Peters M, et al (2007) Recommendations for conducting controlled clinical studies of dental restorative materials. Clin Oral Investig 11(1):5-33

235. Körber KH, Ludwig K (1983) Maximale Kaukraft als Berechnungsfaktor zahntechnischer Konstruktionen. Dent Lab 31:55-60

236. Studart AR, Filser F, Kocher P, Gauckler LJ (2007) In vitro lifetime of dental ceramics under cyclic loading in water. Biomaterials 28(17):2695-705

237. Kelly JR (1999) Clinically relevant approach to failure testing of all-ceramic restorations. J Prosthet Dent 81(6):652-61

238. Jung YG, Peterson IM, Kim DK, Lawn BR (2000) Lifetime-limiting strength degradation from contact fatigue in dental ceramics. J Dent Res 79(2):722-31

239. White SN, Zhao XY, Zhaokun Y, Li ZC (1995) Cyclic mechanical fatigue of a feldspathic dental porcelain. Int J Prosthodont 8(5):413-20

240. Kim DK, Jung YG, Peterson IM, Lawn BR (1999) Cyclic fatigue of intrinsically brittle ceramics in contact with spheres. Acta Mater 47(18):4711-25

241. Zhang Y, Kim JW, Bhowmick S, Thompson VP, Rekow ED (2009) Competition of fracture mechanisms in monolithic dental ceramics: flat model systems. J Biomed Mater Res B Appl Biomater 88(2):402-11

242. Clifford M, Brooks R, Howe A, Kennedy A, McWilliam S, Pickering S, et al (2009) An Introduction to Mechanical Engineering - Part 1. Taylor & Francis Group, LLC, Boca Raton, FL, USA

243. Lee YL, Pan J, Hathaway R, Barkey M (2005) Fatigue Testing and Analysis: Theory and Practice. Elsevier Butterworth-Heinemann, Burlington, MA, USA

244. Coelho PG, Bonfante EA, Silva NR, Rekow ED, Thompson VP (2009) Laboratory simulation of Y-TZP all-ceramic crown clinical failures. J Dent Res 88(4):382-6

245. Coelho PG, Silva NR, Bonfante EA, Guess PC, Rekow ED, Thompson VP (2009) Fatigue testing of two porcelain-zirconia all-ceramic crown systems. Dent Mater 25(9):1122-7

246. Nelson WB (1990) Accelerated Testing - statistical models, test plans and data analysis. 1 ed. John Wiley & Sons, New York, NY, USA

247. Fard N, Li C (2009) Optimal simple step stress accelerated life test design for reliability prediction. J Stat Plan Infer 139(5):1799-808

248. Bhowmick S, Melendez-Martinez JJ, Hermann I, Zhang Y, Lawn BR (2007) Role of indenter material and size in veneer failure of brittle layer structures. J Biomed Mater Res B Appl Biomater 82(1):253-9

249. Zhang Y, Chai H, Lawn BR (2010) Graded structures for all-ceramic restorations. J Dent Res 89(4):417-21

250. Kim JH, Kim JW, Myoung SW, Pines M, Zhang Y (2008) Damage maps for layered ceramics under simulated mastication. J Dent Res 87(7):671-5

251. Kim JW, Kim JH, Janal MN, Zhang Y (2008) Damage maps of veneered zirconia under simulated mastication. J Dent Res 87(12):1127-32

252. ANSI (2010) Standard Practice for Fractography and Characterization of Fracture Origins in Advanced Ceramics. ASTM C 1322 - 05B. Washington DC, USA: American National Standards Institute

253. Quinn G (2007) Special Publication 960-17: Fractography of Ceramics and Glasses. National Institute of Standards and Technology, Washington DC, USA

254. Quinn JB, Quinn GD, Kelly JR, Scherrer SS (2005) Fractographic analyses of three ceramic whole crown restoration failures. Dent Mater 21(10):920-9

255. Frechette VD (1990) Failure analysis of brittle materials. Westerville, OH, USA: American Ceramic Society

256. ANSI (2010) Standard Practice for Fractographic Analysis of Fracture Mirror Sizes in Ceramics and Glasses. ASTM C 1678 – 10. Washington DC, USA: American National Standards Institute

257. Scherrer SS, Quinn GD, Quinn JB (2008) Fractographic failure analysis of a Procera® AllCeram crown using stereo and scanning electron microscopy. Dent Mater 24(8):1107-13

258. Scherrer SS, Quinn JB, Quinn GD, Kelly JR (2006) Failure analysis of ceramic clinical cases using qualitative fractography. Int J Prosthodont 19(2):185-92

259. Peterson IM, Pajares A, Lawn BR, Thompson VP, Rekow ED (1998) Mechanical characterization of dental ceramics by hertzian contacts. J Dent Res 77(4):589-602

260. Jung YG, Wuttiphan S, Peterson IM, Lawn BR (1999) Damage modes in dental layer structures. J Dent Res 78(4):887-97

261. Deng Y, Miranda P, Pajares A, Guiberteau F, Lawn BR (2003) Fracture of ceramic/ceramic/polymer trilayers for biomechanical applications. J Biomed Mater Res A 67(3):828-33

262. Kim B, Zhang Y, Pines M, Thompson VP (2007) Fracture of porcelain-veneered structures in fatigue. J Dent Res 86(2):142-6

263. Rhee Y-W, Kim H-W, Deng Y, Lawn BR (2001) Contact-induced Damage in Ceramic Coatings on Compliant Substrates: Fracture Mechanics and Design. J Am Ceram Soc 84(5):1066-72

264. Zhang Y, Kim J-W, Kim J-H, Lawn BR (2008) Fatigue Damage in Ceramic Coatings From Cyclic Contact Loading With a Tangential Component. J Am Ceram Soc 91(1):198-202

265. Zhang Y, Song J-K, Lawn BR (2005) Deep-penetrating conical cracks in brittle layers from hydraulic cyclic contact. J Biomed Mater Res B Appl Biomater 73B(1):186-93

266. Lawn BR, Wiederhorn SM, Roberts DE (1984) Effect of sliding friction forces on the strength of brittle materials. J Mater Sci 19(8):2561-69

267. Kim JW, Kim JH, Thompson VP, Zhang Y (2007) Sliding contact fatigue damage in layered ceramic structures. J Dent Res 86(11):1046-50

268. Santana T, Zhang Y, Guess P, Thompson VP, Rekow ED, Silva NR (2009) Off-axis sliding contact reliability and failure modes of veneered alumina and zirconia. Dent Mater 25(7):892-8

269. Stappert CF, Baldassarri M, Zhang Y, Stappert D, Thompson VP (2012) Contact fatigue response of porcelain-veneered alumina model systems. J Biomed Mater Res B Appl Biomater 100B(2):508–515

270. Stappert C, Park D-W, Stappert D, Rekow E, Thompson V (2006) Damage modes and Reliability of Alumina and Zirconia Ceramic-Layer-Structures. J Dent Res 85(Spec Iss B):2092

271. Kelly JR, Giordano R, Pober R, Cima MJ (1990) Fracture surface analysis of dental ceramics: clinically failed restorations. Int J Prosthodont 3(5):430-40

272. Strub JR, Kern M, Türp JC, Witkowski S, Heydecke G, Wolfart S (2011) Curriculum Prothetik Band II. 4 ed. Quintessenz Verlag, Berlin, Germany

273. Programat – Firing program table (°C) (2011) www.ivoclarvivadent.com. 3 ed. Schaan, Liechtenstein: Ivoclar Vivadent AG

274. Kern M, Barloi A, Yang B (2009) Surface conditioning influences zirconia ceramic bonding. J Dent Res 88(9):817-22

275. Black S, Amoore JN (1993) Measurement of forces applied during the clinical cementation of dental crowns. Physiol Meas 14(3):387

276. Huang M, Thompson VP, Rekow ED, Soboyejo WO (2008) Modeling of water absorption induced cracks in resin-based composite supported ceramic layer structures. J Biomed Mater Res B Appl Biomater 84(1):124-30

277. Silva NRFA, de Souza GM, Coelho PG, Stappert CFJ, Clark EA, Rekow ED, et al (2008) Effect of water storage time and composite cement thickness on fatigue of a glass-ceramic trilayer system. J Biomed Mater Res B Appl Biomater 84B(1):117-23

278. Shirakura A, Lee H, Geminiani A, Ercoli C, Feng C (2009) The influence of veneering porcelain thickness of all-ceramic and metal ceramic crowns on failure resistance after cyclic loading. J Prosthet Dent 101(2):119-27

279. DeLong R, Sakaguchi RL, Douglas WH, Pintado MR (1985) The wear of dental amalgam in an artificial mouth: a clinical correlation. Dent Mater 1(6):238-42

280. Abernethy RB (2000) The New Weibull Handbook. 4 ed Abernethy RB, North Palm Beach, FL, USA

281. Stappert CF, Ozden U, Gerds T, Strub JR (2005) Longevity and failure load of ceramic veneers with different preparation designs after exposure to masticatory simulation. J Prosthet Dent 94(2):132-9

282. Nothdurft FP, Pospiech PR (2009) Zirconium dioxide implant abutments for posterior single-tooth replacement: first results. J Periodontol 80(12):2065-72

283. Vult von Steyern P, Kokubo Y, Nilner K (2005) Use of abutment-teeth vs. dental implants to support all-ceramic fixed partial dentures: an in-vitro study on fracture strength. Swed Dent J 29(2):53-60

284. Park SE, Chao M, Raj PA (2009) Mechanical Properties of Surface-Charged Poly(Methyl Methacrylate) as Denture Resins. Int J Dent 2009:841431

285. Rosentritt M, Behr M, Gebhard R, Handel G (2006) Influence of stress simulation parameters on the fracture strength of all-ceramic fixed-partial dentures. Dent Mater 22(2):176-82

286. Van Oosterwyck H, Duyck J, Vander Sloten J, Van der Perre G, De Coomans M, Lieven S, et al (1998) The influence of bone mechanical properties and implant fixation upon bone loading around oral implants. Clin Oral Implants Res 9(6):407-18

287. Spear F, Holloway J (2008) Which all-ceramic system is optimal for anterior esthetics? J Am Dent Assoc 139 Suppl:19S-24S

288. Silva NR, Thompson VP, Valverde GB, Coelho PG, Powers JM, Farah JW, et al (2011) Comparative reliability analyses of zirconium oxide and lithium disilicate restorations in vitro and in vivo. J Am Dent Assoc 142 Suppl 2:4S-9S

289. Larsson C, Vult von Steyern P, Nilner K (2010) A prospective study of implant-supported full-arch yttria-stabilized tetragonal zirconia polycrystal mandibular fixed dental prostheses: three-year results. Int J Prosthodont 23(4):364-9

290. Baldassarri M, Zhang Y, Thompson VP, Rekow ED, Stappert CF (2011) Reliability and failure modes of implant-supported zirconium-oxide fixed dental prostheses related to veneering techniques. J Dent 39(7):489-98

291. Rekow ED, Harsono M, Janal M, Thompson VP, Zhang G (2006) Factorial analysis of variables influencing stress in all-ceramic crowns. Dent Mater 22(2):125-32

292. Guazzato M, Proos K, Quach L, Swain MV (2004) Strength, reliability and mode of fracture of bilayered porcelain/zirconia (Y-TZP) dental ceramics. Biomaterials 25(20):5045-52

293. Lawn BR, Pajares A, Zhang Y, Deng Y, Polack MA, Lloyd IK, et al (2004) Materials design in the performance of all-ceramic crowns. Biomaterials 25(14):2885-92

294. Kim J, Park S, Jung Y, Lee H (2006) Evaluation and Control of Crack Propagation in Dense Porcelain/Porous Alumina Layered Structures for Dental Material Applications. Key Eng Mater 317-318:457-60

295. Kim JW, Bhowmick S, Hermann I, Lawn BR (2006) Transverse fracture of brittle bilayers: relevance to failure of all-ceramic dental crowns. J Biomed Mater Res B Appl Biomater 79(1):58-65

296. Aboushelib MN, Kleverlaan CJ, Feilzer AJ (2006) Microtensile bond strength of different components of core veneered all-ceramic restorations. Part II: Zirconia veneering ceramics. Dent Mater 22(9):857-63

297. Guess PC, Kulis A, Witkowski S, Wolkewitz M, Zhang Y, Strub JR (2008) Shear bond strengths between different zirconia cores and veneering ceramics and their susceptibility to thermocycling. Dent Mater 24(11):1556-67

298. Stappert CF, Baldassarri M, Zhang Y, Hanssler F, Rekow ED, Thompson VP (2012) Reliability and fatigue failure modes of implant-supported aluminum-oxide fixed dental prostheses. Clin Oral Implants Res 23(10):1173-80

299. Isgro G, Kleverlaan CJ, Wang H, Feilzer AJ (2005) The influence of multiple firing on thermal contraction of ceramic materials used for the fabrication of layered all-ceramic dental restorations. Dent Mater 21(6):557-64

12 ACKNOWLEDGEMENTS

13 LEBENSLAUF